

POLITECNICO DI TORINO

Master of Science in Mechanical Engineering

Master Thesis

**Benchmarking of the blended control strategy in Plug-in
Hybrid Electric Vehicles and energy efficiency analysis
in real-world conditions**



**Politecnico
di Torino**

Supervisors:

prof. Federico MILLO

prof. Luciano ROLANDO

Company tutor:

ing. Alessandro TANSINI

Candidate:

Luca CULTRARA

April 2023

Abstract

Nowadays the reduction of greenhouse gases (GHG) in the transport sector plays a crucial role in the European Union regulations. Plug-in Hybrid Electric Vehicles (PHEVs) represent a valid solution to immediately decrease vehicle tailpipe CO₂ emissions combining the advantages of conventional vehicles and battery electric ones. However the complexity of PHEVs is higher because of the presence of more on-board sources of power, so an appropriate Energy Management System (EMS) is needed. The standard control consists in implementing first the charge depleting (CD) strategy which uses electric energy from the battery to achieve pure electric driving and later the charge sustaining (CS) strategy which is mainly internal combustion engine (ICE) assisted. The aim of this thesis is to analyse the experimental data acquired from real-world trips of a C-segment PHEV in order to assess the operation and the possible advantages of a specific EMS control strategy: the blended mode. In this mode the electric motor (EM) and the ICE are used together along the trip with the aim of improving the overall fuel economy of the trip. The real-world approach is important because this strategy cannot be efficiently evaluated only within type approval scenarios.

This work has been conducted in cooperation with the Sustainable Transport Unit of the European Commission's Joint Research Centre (JRC) in Ispra (Italy). Different users have used the PHEV under consideration for a period of time carrying out several real-world trips according to their private schedule. The real-time data about the vehicle operation were registered during the trips using the On-board Diagnostics (OBD) and the Unified Diagnostic Services (UDS).

This thesis firstly proposes a literature review to examine fuel consumption (FC) in type approval tests and real-world trips, to figure out some examples about the operation of the blended control strategies and to assess the real-world CO₂ emissions in PHEVs. In the following parts, the real-world trips were categorised, the blended trips were compared with similar ones where the more classic charge depleting and charge sustaining (CD-CS) strategy was used and the two control strategies were analysed.

Sommario

Oggi giorno la riduzione dei gas serra nel settore dei trasporti ricopre un ruolo chiave nelle normative dell'Unione Europea. I veicoli ibridi plug-in (Plug-in Hybrid Electric Vehicles, PHEVs) rappresentano una valida soluzione per ridurre da subito le emissioni di CO₂ del veicolo tailpipe (ossia allo scarico) combinando i vantaggi dei veicoli convenzionali e di quelli elettrici. Tuttavia la complessità dei veicoli ibridi plug-in è maggiore a causa della presenza di più fonti di potenza a bordo, quindi è necessario un appropriato sistema di gestione dell'energia (Energy Management System, EMS). Il controllo ordinario consiste nell'utilizzare all'inizio la strategia charge depleting (CD) che usa l'energia elettrica della batteria per realizzare la guida in puro elettrico e successivamente la strategia charge sustaining (CS) dove vi è invece un sostanziale utilizzo del motore a combustione interna (Internal Combustion Engine, ICE).

Lo scopo di questa tesi è di analizzare i dati sperimentali acquisiti da viaggi effettuati su strada (real-world) con un veicolo ibrido plug-in di segmento C per valutare il funzionamento e i possibili vantaggi di una specifica strategia di controllo: la modalità blended. In questa modalità il motore elettrico (Electric Motor, EM) e il motore a combustione interna operano assieme lungo il viaggio con lo scopo di migliorare il risparmio di combustibile complessivo del viaggio. L'approccio real-world è importante perché tale strategia non può essere adeguatamente valutata solo in scenari di test omologativi in laboratorio.

Questo lavoro è stato svolto in cooperazione con l'Unità di trasporto sostenibile del Centro Comune di Ricerca (Joint Research Centre, JRC) di Ispra (Italia). Diversi utenti hanno utilizzato il veicolo ibrido plug-in considerato per un certo periodo di tempo effettuando diversi viaggi real-world secondo i loro programmi. I dati in tempo reale sono stati registrati durante i viaggi mediante la On-board Diagnostics (OBD) e la Unified Diagnostic Services (UDS).

Questa tesi propone inizialmente una recensione di alcuni articoli presenti in letteratura per esaminare il consumo di combustibile nei test omologativi in laboratorio e in viaggi real-world, per comprendere alcuni esempi sul funzionamento delle strategie blended e per valutare le emissioni di CO₂ real-world nei veicoli ibridi plug-in. Nelle parti successive, tutti i viaggi real-world sono stati categorizzati, i viaggi blended sono stati confrontati con quelli in cui è stata utilizzata la più tradizionale strategia charge depleting e charge sustaining (CD-CS) e le due strategie di controllo sono state analizzate.

Acknowledgments

I want to thank my supervisors, professor Federico Millo and professor Luciano Rolando, and my company tutor Alessandro Tansini who supported my Master's degree thesis activity and who helped me in this project with willingness and openness.

I express my gratitude to the Sustainable Transport Unit of the European Commission's Joint Research Centre (JRC) of Ispra for the work that permitted the development of this thesis and for the possibility to come to the JRC's site in Ispra and for the cordial welcome.

I want to thank my parents and my friends for all the support that gave me during my academic career and in these last months.

Contents

1	Introduction.....	16
1.1	Mobility and CO ₂ emissions trends	17
1.2	CO ₂ emission certification in Europe	21
1.3	Real world CO ₂ emissions	24
1.3.1	CO ₂ emissions GAP between certification and real-world.....	24
1.3.2	Real-world factors which affect fuel consumption	27
2	Hybrid Electric Vehicles (HEVs)	29
2.1	Architectures	29
2.2	HEVs and PHEVs	33
2.3	PHEVs operating strategies.....	33
2.4	Charge Depleting and Charge Sustaining mode.....	35
2.5	Blended mode.....	36
2.6	Advantages and disadvantages of the blended mode	37
3	CO ₂ emission certification for HEVs.....	53
3.1	NOVC-HEVs.....	56
3.1.1	Test procedure for NOVC-HEVs.....	56
3.1.2	Charge sustaining CO ₂ correction.....	59
3.2	OVC-HEVs	61
3.2.1	Test procedure for OVC-HEVs and CO ₂ correction.....	61
3.2.2	Utility factor-weighted CO ₂ emissions	64
3.3	Real-world CO ₂ emissions in PHEVs	67
4	Case study	69
4.1	Tested vehicle.....	69
4.2	Experimental campaign.....	70
5	Data Analysis	71
5.1	Real-world trips categorization	73
5.2	Comparison between blended trips and CD-CS trips.....	74
5.2.1	ICE switching ON.....	74
5.2.2	ICE switching OFF	82
5.2.3	Powersplit.....	87
5.2.4	Gear shifting.....	91

5.2.5 Fuel consumption.....	92
Conclusions.....	96
Appendix A.....	97
Appendix B.....	98
References.....	99

List of Tables

Table 1.1 - Differences between NEDC and WLTP (source [7]).....	23
Table 1.2 - Summary of the accuracy results of the OBD measurements (values from [10]).....	26
Table 1.3 - FC declared and measured from the laboratory and on road test (PEMS) (values from [8]).....	27
Table 2.1 – Operation limits of the ZEV mode and blended mode (data from [16])	39
Table 2.2 - Summary of the CO ₂ calculation in TA test using NEDC and WLTC	39
Table 2.3 - Results for the different four real-world trips in [17] (table from [17]).....	42
Table 2.4 - Comparison of the different control strategies in [18] (table from [18]).....	42
Table 2.5 - Blended mode fuel cost improvements compared to the CD-CS strategy for $\mu = 35 \text{ km}$ referred to the distance x (table from [20]).....	51
Table 2.6 - Blended mode fuel cost improvements compared to the CD-CS strategy for $\mu = 55 \text{ km}$ referred to the distance x (table from [20]).....	52
Table 3.1 - RCB correction criteria thresholds (table from [14])	59
Table 3.2 - Parameters for the determination of fractional utility factors (values from [14])	65
Table 3.3 - Results of the CO ₂ gap between real-world operation and TA values (values from [23])	68
Table 4.1 - PHEV main specifications.....	69
Table 5.1 - Some of the main data logged along the real-world trips.....	71
Table 5.2 - Powertrain status conditions	87
Table 5.4 - Average final battery SOC values in the two strategies	92

List of Figures

Figure 1.1 - Greenhouse gas emissions in the EU (figure from EEA [2]).....	17
Figure 1.2 - Evolution of CO ₂ emissions in the EU by sector from 1990 to 2019 (figure from [3]).	18
Figure 1.3 - Greenhouse gas emissions by aggregated sector in the EU from 1990 to 2018 (figure from EEA [4])	19
Figure 1.4 – Greenhouse gas emissions in the EU by transport mode (figure from [3]).....	20
Figure 1.5 - Schematic illustration (the percentage could vary due to possible developments in the regulations) showing how after 2021 the CO ₂ emissions target is a reduction percentage relative to the 2021 starting point (figure from [6]).....	21
Figure 1.6 - Simulation results for all three vehicle considered over six different scenarios. All values are expressed in g CO ₂ / km (figure from [9]).....	25
Figure 1.7 - Weighted average emissions for NEDC type approval, WLTP (High and Low) and realistic scenario with errors bars (figure from [9]).....	25
Figure 1.8 - The relative importance (% of contribution) of individual factors to the total FC gap variability (figure from [8]).....	28
Figure 2.1 - Scheme of a series hybrid architecture.....	29
Figure 2.2 - Scheme of a parallel hybrid architecture.....	30
Figure 2.3 - P0 to P5 parallel hybrid architectures, Cx: Clutch x, T: Transmission, Px: Position of the electric machine(s) in each configuration x (figure from [13]).....	30
Figure 2.4 - Scheme of a complex series-parallel hybrid architecture.....	32
Figure 2.5 - Scheme of a complex powersplit hybrid architecture	32
Figure 2.6 - The role of the EMS in a hybrid electric vehicle (figure from [11]).....	34
Figure 2.7 - Example of a SOC profile in a CD-CS trip.....	35
Figure 2.8 - Example of the SOC profile in a blended trip.....	36
Figure 2.9 - ICE ON/OFF status and battery SOC for the ZEV mode along the WLTP (top) and NEDC (bottom) (figure from [16])	37
Figure 2.10 - ICE ON/OFF status and battery SOC for the blended mode along the WLTP (top) and NEDC (bottom) (figure from [16])	38
Figure 2.11 - Vehicle operating modes along WLTC for blended (top) and ZEV (bottom) (figure from [16]).....	38
Figure 2.12 – CO ₂ emissions along the NEDC and the WLTC combining the blended mode with the sport mode (figure from [16])	40
Figure 2.13 – CO ₂ emissions along the NEDC and the WLTC combining the ZEV mode with the sport mode (figure from [16])	40
Figure 2.14 - Working principle of the EMS proposed in [17] (figure from [17]).....	41
Figure 2.15 - Results of the four control strategies in [18] simulation (figure from [18])	43
Figure 2.16 - Evolution of the results in the four EMSs of [18] (figure from [18])	43
Figure 2.17 - Frequency of the ICE operation points overlapping engine’s iso-efficiency lines, in red, in the four control strategies of [18] (figure from [18]).....	44

Figure 2.18 - Optimal SOC trajectory (in blue) and linear SOC trajectory (in red) without LEZ and road grade for 3xDUB driving cycle (a) and 2xHDUDDS driving cycle (b) with respect to distance s (figure from [19])	45
Figure 2.19 - Optimal SOC trajectory (in blue) and shortest-length (piecewise linear, in black) trajectory in case of LEZ presence and without road grade for 3xDUB and 3xHDUDDS with $SOC_i = 90\%$, $SOC_f = 30\%$ (a, c) and $SOC_i = 50\%$, $SOC_f = 50\%$ (b, d) (figure from [19])	45
Figure 2.20 - Optimal SOC trajectory (in blue) and shortest-length (piecewise linear, in black) trajectory in case of registered road grade, for 3xDUB also with LEZ (b, c), with different SOC_i and SOC_f (figure from [19])	46
Figure 2.21 - Optimal SOC trajectories and linear ones for 4xDUB driving cycle and recorded road grade (a), low frequency (b), mid frequency (c) and high frequency sinusoidal road grades (figure from [19]).....	46
Figure 2.22 - SOC time derivative with respect to power demand Pd (figure from [19])	47
Figure 2.23 - Optimal and synthesized SOC trajectories for recorded road grade (a) and for sinusoidal profiles (b, c, d) (figure from [19])	47
Figure 2.24 - Total fuel consumption for CD-CS and blended mode for different driving cycle without LEZ (figure from [19])	48
Figure 2.25 – Total fuel consumption for the 4xDUB driving cycle and for different reference trajectory synthesis, linear and non-linear (advanced) one, for 4xDUB driving cycle and for recorded road grade (a), low frequency (b), mid frequency (c) and high frequency sinusoidal road grades (figure from [19]).....	48
Figure 2.26 - Normal distribution of the probability density function when the predicted trip length is 35 km (figure from [20])	49
Figure 2.27 - Speed and SOC trajectories for profile A with predicted trip length $\mu = 55\text{ km}$ (figure from [20]).....	50
Figure 2.28 - Speed and SOC trajectories for profile B with predicted trip length $\mu = 55\text{ km}$ (figure from [20]).....	50
Figure 2.29 - Speed and SOC trajectories for profile C with predicted trip length $\mu = 55\text{ km}$ (figure from [20]).....	51
Figure 3.1 - Class 3 WLTC.....	55
Figure 3.2 - NOVC-HEVs charge-sustaining Type 1 test (figure from [14]).....	56
Figure 3.3 - Selection of a driver-selectable mode for OVC-HEVs, NOVC-HEVs and NOVC-FCHVs under charge-sustaining operating condition (figure from [14])	57
Figure 3.4 - Selection of a driver-selectable mode for OVC-HEVs, NOVC-HEVs and NOVC-FCHVs under charge-sustaining operating condition (figure from [14])	58
Figure 3.5 - Charge-depleting type 1 test for OVC-HEV (figure from [14])	61
Figure 3.6 - Subsequent charge-sustaining Type 1 test for OVC-HEV (figure from [14]).....	62
Figure 3.7 - Selection of driver-selectable mode for OVC-HEVs under charge-depleting operating condition (figure from [14]).....	63
Figure 3.8 - WLTP Utility Factor curve (figure from [22]).....	66
Figure 3.9 - Combined probability distribution used for obtaining the CO ₂ emissions under realistic use patterns (on the left the JRC average speed distribution, on the right Geco air average speed distribution (figure from [23]).....	67
Figure 5.1 - ICE switching ON points in the function of vehicle speed and acceleration	75

Figure 5.2 - ICE switching ON points in the function of vehicle speed and acceleration with the violin plots addition	75
Figure 5.3 - ICE switching ON points in the function of vehicle speed and wheels torque.....	76
Figure 5.4 - ICE switching ON points in the function of vehicle speed and wheels torque with violin plots.....	77
Figure 5.5 - ICE switching ON points of both strategies in the function of vehicle acceleration and wheels power.....	77
Figure 5.6 - ICE switching ON points of both strategies in the function of vehicle acceleration and wheels power with violins plots.....	78
Figure 5.7 - ICE switching ON points of blended strategy in the function of vehicle acceleration, wheels power and vehicle speed with colour bar.....	78
Figure 5.8 - ICE switching ON points of CD-CS strategy in the function of vehicle acceleration, wheels power and vehicle speed with colour bar.....	79
Figure 5.9 - ICE switching ON points of blended strategy in the function of vehicle acceleration, wheels power and vehicle speed	79
Figure 5.10 - ICE switching ON points of CD-CS strategy in the function of vehicle acceleration, wheels power and vehicle speed	80
Figure 5.11 - ICE switching ON interpolation surfaces of both strategies in the function of vehicle acceleration, wheels power and vehicle speed.....	81
Figure 5.12 - ICE switching ON interpolation surfaces of blended (left) and CD-CS (right) strategy contour plots in the function of vehicle acceleration, wheels power and vehicle speed.....	81
Figure 5.13 - ICE switching OFF points of both strategies in the function of vehicle acceleration and wheels power.....	82
Figure 5.14 - ICE switching OFF points of both strategies in the function of vehicle acceleration and wheels power with violins plots.....	83
Figure 5.15 - ICE switching OFF points of blended strategy in the function of vehicle acceleration, wheels power and vehicle speed with colour bar.....	83
Figure 5.16 - ICE switching OFF points of CD-CS strategy in the function of vehicle acceleration, wheels power and vehicle speed with colour bar.....	84
Figure 5.17 - ICE switching OFF points of blended strategy in the function of vehicle acceleration, wheels power and vehicle speed	84
Figure 5.18 - ICE switching OFF points of CD-CS strategy in the function of vehicle acceleration, wheels power and vehicle speed	85
Figure 5.19 - ICE switching OFF interpolation surfaces of both strategies in the function of vehicle acceleration, wheels power and vehicle speed.....	86
Figure 5.20 - ICE switching OFF interpolation surfaces of blended (left) and CD-CS (right) strategy contour plots in the function of vehicle acceleration, wheels power and vehicle speed.....	86
Figure 5.21 - ICE power represented in the function of the total power to the wheels for blended trips.....	88
Figure 5.22 - ICE power represented in the function of the total power to the wheels for CD-CS trips.....	88
Figure 5.23 - Operating points in the ICE power band for the blended strategy	89
Figure 5.24 - Operating points in the ICE power band for the CD-CS strategy.....	90
Figure 5.25 - Operating points in the ICE power band for both strategies with violin plots.....	90

Figure 5.26 - Probability density for the different gears in the function of the vehicle speed..... 91
Figure 5.27 - Single trips total fuel consumption plotted referring to the wheels energy rate 92
Figure 5.28 - Single trips final SOC plotted with the trip average vehicle speed..... 93
Figure 5.29 - Single trips final SOC plotted with the trip total distance..... 94
Figure 5.30 - Single trips final SOC plotted with the trip difference in altitude 94

Acronyms

AER	All-electric range
BAS	Belt alternator starter
BEV	Battery Electric Vehicle
BSG	Belt starter generator
CD	Charge Depleting
CS	Charge Sustaining
ECMS	Equivalent Consumption Minimization Strategy
EEA	European Environment Agency
EM	Electric Motor
EMS	Energy Management System
FC	Fuel Consumption
GHG	Green House Gases
GPS	Global Positioning System
HDUDDS	Heavy Duty Urban Dynamometer Driving Schedule
HDV	Heavy-duty vehicle
HEV	Hybrid Electric Vehicle
ICCT	The International Council on Clean Transportation
ICE	Internal Combustion Engine
ITS	Intelligent Transportation System
JRC	Joint Research Centre
LDV	Light-duty vehicle
LEZ	Low-emission zones
LPM	Load Point Moving
NA	Naturally aspirated
NEDC	New European Driving Cycle
NOVC- FCHV	Not Off-Vehicle Charging Fuel Cell Hybrid Vehicle
NOVC-HEV	Not Off-Vehicle Charging Hybrid Electric Vehicles
OBD	On-board Diagnostics
OBFCM	On-board Fuel Consumption Monitoring
OEM	Original equipment manufacturer
OOL	Optimal Operating Line
OVC-HEV	Off-Vehicle Charging Hybrid Electric Vehicles

PEMS	Portable Emissions Measurement System
PHEV	Plug-in Hybrid Electric Vehicle
RB	Rule Based
RB ICE OFF	Regenerative Braking ICE OFF
RB ICE ON	Regenerative Braking ICE ON
RDE	Real Driving Emissions
REESS	Rechargeable electric energy storage system
RPM	Revolutions per minute
RRC	Rolling resistance coefficient
RWD	Real-world driving
TA	Type Approval
TC	Turbo charged
UDS	Unified Diagnostic Services
UF	Utility factor
VELA	Vehicle Emissions Laboratory
WLTC	Worldwide Harmonized Light Vehicles Test Cycle
WLTP	Worldwide Harmonized Light Vehicles Test Procedure
ZEV	Zero Emission Vehicle

1 Introduction

The climate-altering emissions represent today a crucial issue. The European Union (EU) efforts to reduce the greenhouse gases (GHG) emissions, in particular the carbon dioxide (CO₂), are increasing. The European Council has set the goal for the EU to cut its greenhouse gas emissions by at least 55% by 2030, compared to 1990, and become climate neutral by 2050 [1]. Transport is the only sector where greenhouse gas emissions have increased in the past three decades, rising 33,5% between 1990 and 2019 [2].

In this framework, Hybrid Electric Vehicles (HEVs) and Plug-in Hybrid Electric Vehicles (PHEVs) represent a valid solution to immediately decrease vehicle tailpipe CO₂ emissions combining the advantages of conventional vehicles and battery electric ones. Nevertheless the complexity of this type of vehicles is higher due to the presence of more on-board power actuators, namely the electric motor (EM) and the internal combustion engine (ICE). Thus an appropriate powertrain control strategy is necessary to obtain an optimal fuel economy.

This thesis aims to analyse, using real-world trips data, the behaviour of two control strategies: the more classical charge depleting and charge sustaining (CD-CS) one and the blended one. This work was conducted in cooperation with the Sustainable Transport Unit of the European Commission's Joint Research Centre (JRC) in Ispra (Italy). Different users have used a 5 doors, C-Segment, parallel P2 PHEV, considered representative of the European market, for a period of time carrying out several real-world trips according to their private schedule. The real-time data about the vehicle operation were registered during the trips using the On-board Diagnostics (OBD) and the Unified Diagnostic Services (UDS).

The CD-CS control strategy establishes at the beginning the charge depleting (CD) phase, where pure electric driving is achieved. Then, when the battery state of charge (SOC) reaches the target reference value, the charge sustaining (CS) phase, which is mainly ICE assisted, begins.

Instead, the blended control strategy aims to improve the overall trip fuel economy using the electric motor and the internal combustion engine together along the whole trip exploiting their more efficient operative regions. However it requires more details about the trip, such as the destination and the energy demand. Therefore the real-world approach of this study is important because this strategy cannot be efficiently evaluated only within type approval scenarios.

This thesis firstly proposes a literature review to examine fuel consumption (FC) in type approval tests and real-world trips, to figure out some examples about the operation of the blended control strategies and to assess the real-world CO₂ emissions in PHEVs. Then an overview of hybrid electric vehicles and of the related European CO₂ emissions certifications is presented.

The following parts describe the case study and the procedure of the data analysis, conducted creating a specific Python script, regarding the real-world trips. Data were processed to calculate some metrics related to trips characteristic, powertrain operating conditions, fuel and energy efficiency. Some significant aggregated results were computed and all the trips were categorised in order to identify the ones in which the blended mode occurred. These latter trips were compared

with similar ones where the charge depleting and charge sustaining (CD-CS) strategy was used and were analysed considering different operative aspects.

At the end the obtained results and proposals for possible future works are presented.

1.1 Mobility and CO₂ emissions trends

In [2] the European Environment Agency (EEA) reports that greenhouse gas emission in the European Union decreased, as it's possible to see in Figure 1.1, by 32% between 1990 and 2020, a notable overachievement of the EU's 2020 reduction target of 20%. Preliminary estimates indicate that emissions rebounded in 2021 but remain below pre-COVID-19 levels. The 2021 emissions increase was driven by the recovery from the pandemic and a greater uptake of energy sources with higher emissions in the second half of 2021.

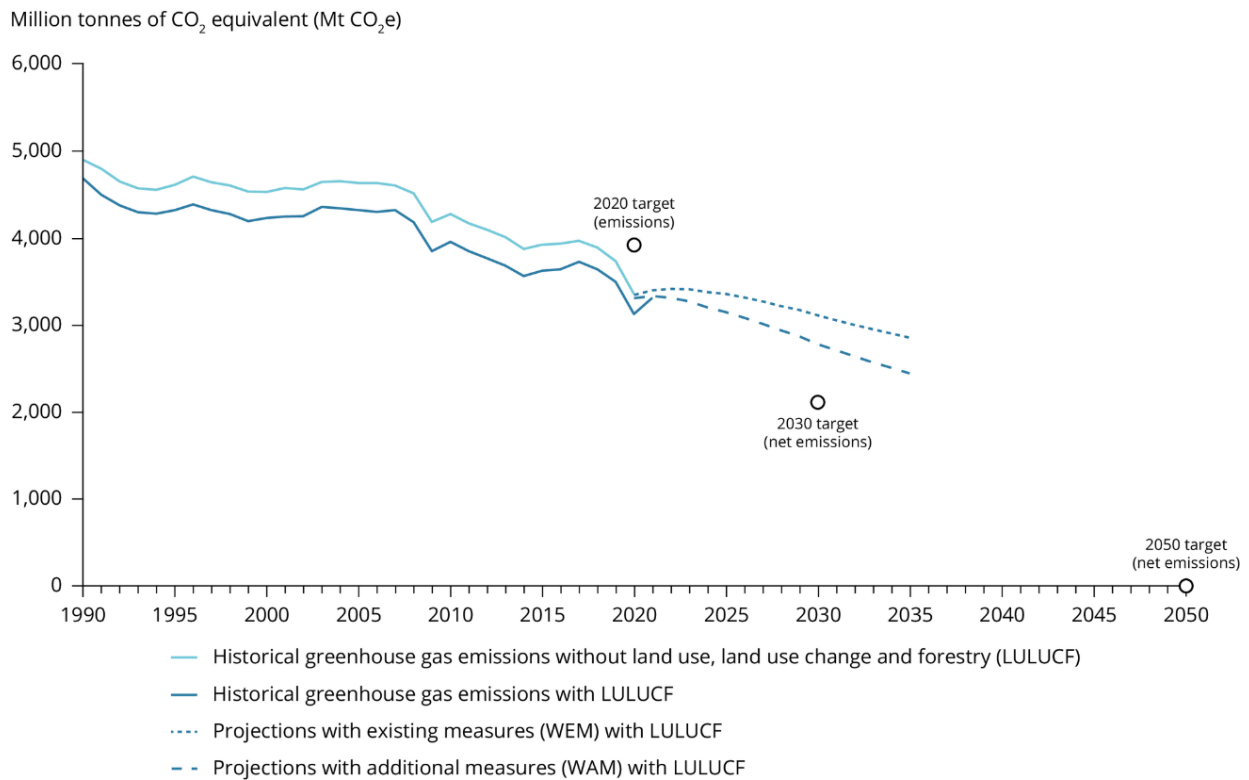


Figure 1.1 - Greenhouse gas emissions in the EU (figure from EEA [2])

Nevertheless, as it's possible to notice in Figure 1.3, transport is the only sector where greenhouse gas emissions have increased in the past three decades, rising 33,5% between 1990 and 2019. The same trend is illustrated more in detail in Figure 1.3 referring to the period from 1990 to 2018.

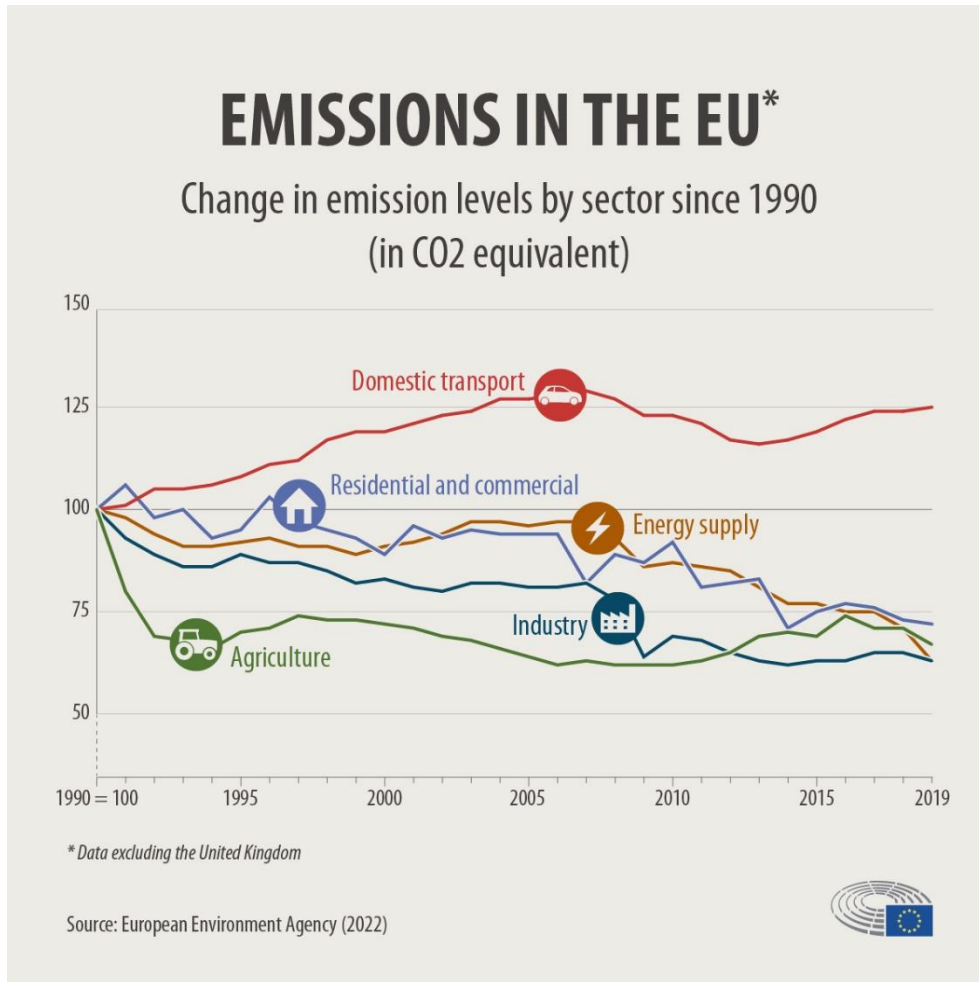


Figure 1.2 - Evolution of CO₂ emissions in the EU by sector from 1990 to 2019 (figure from [3])

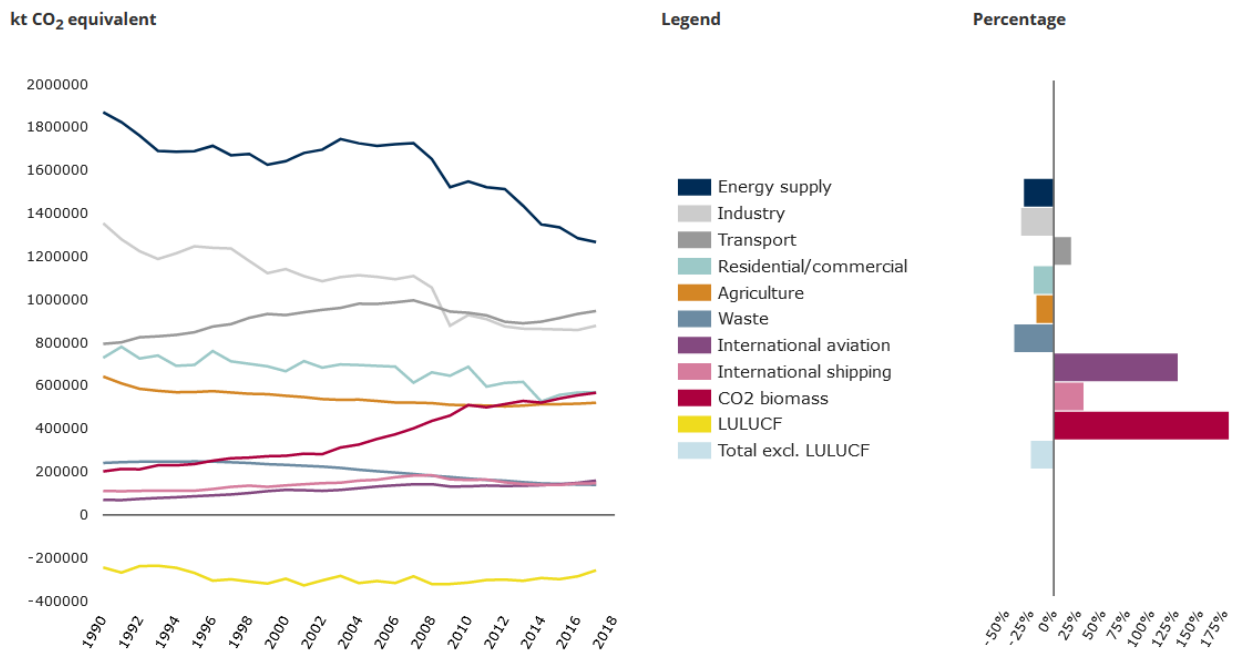
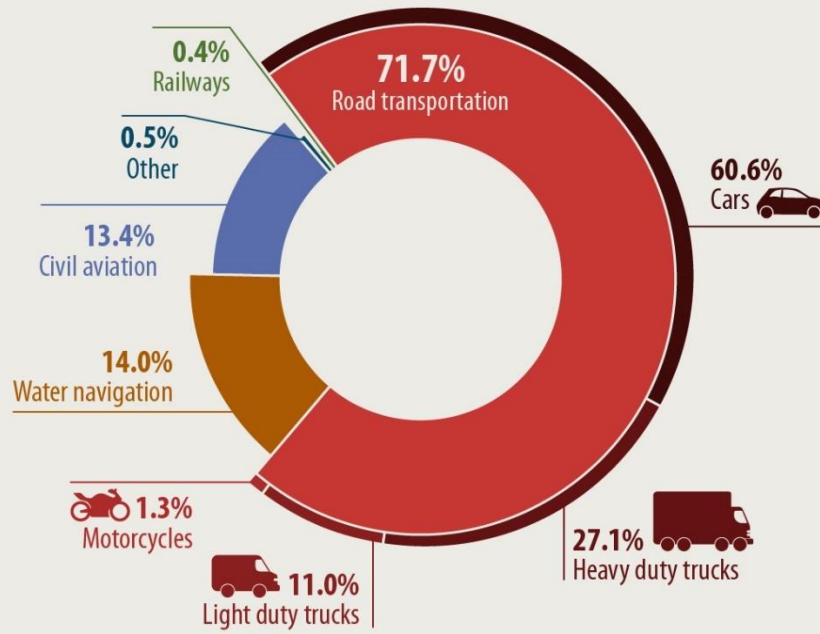


Figure 1.3 - Greenhouse gas emissions by aggregated sector in the EU from 1990 to 2018 (figure from EEA [4])

Road transport accounts for about a fifth of EU emissions [3]. CO₂ emissions from passenger transport vary significantly depending on the transport mode as illustrated in Figure 1.4.

TRANSPORT EMISSIONS IN THE EU

Greenhouse gas emissions breakdown by transport mode
(2019)



Source: European Environment Agency (2022)



Figure 1.4 – Greenhouse gas emissions in the EU by transport mode (figure from [3])

Despite the decreasing trend of the g/km CO₂ emissions of newly certified vehicles with respect to their predecessor, global CO₂ emissions from road transport in Europe are decreasing at a slower rate than the desirable one [5], so it's possible to understand the crucial role of the CO₂ regulations for achieving the goal of limiting GHG emissions.

1.2 CO₂ emission certification in Europe

Since September 2017, as reported in [6], the European Union began a transition from the New European Driving Cycle (NEDC) to the Worldwide Harmonized Light Vehicles Test Procedure (WLTP) for new-vehicle emissions certification. With respect to the 2025 and 2030, the percentage reduction targets in the CO₂ regulation are fixed and are depending on the fleet average WLTP starting point of all manufactures in 2021 (Figure 1.5).

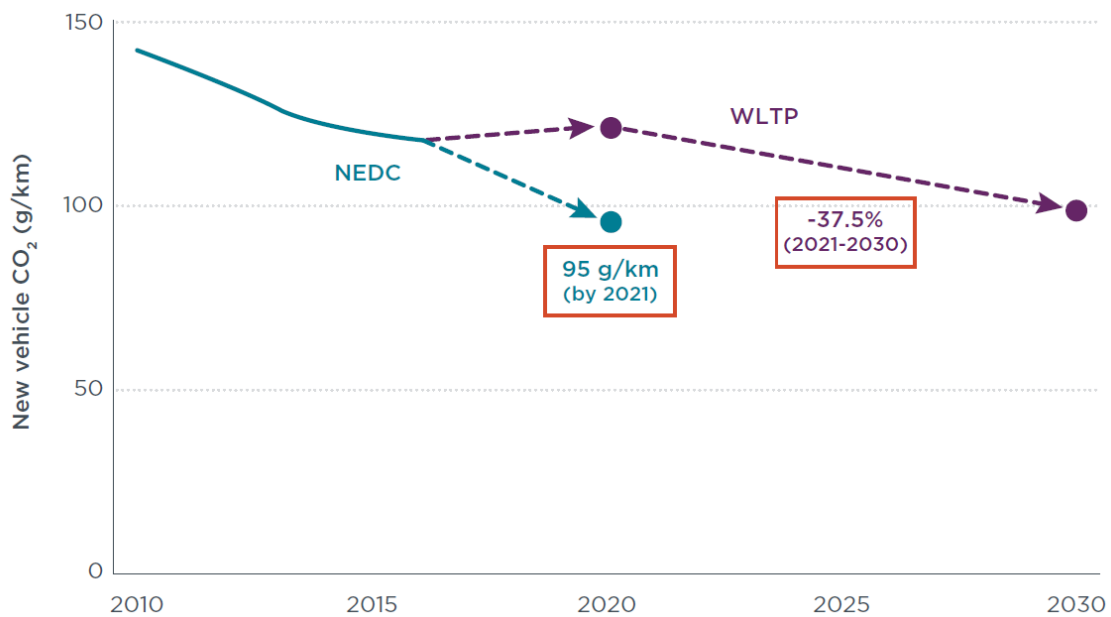


Figure 1.5 - Schematic illustration (the percentage could vary due to possible developments in the regulations) showing how after 2021 the CO₂ emissions target is a reduction percentage relative to the 2021 starting point (figure from [6])

In [7] the main procedural differences and consequences between the WLTP and the NEDC driving cycles and procedures are evaluated.

In particular the main differences between the two test procedures are identified and their impact on CO₂ emissions quantified using a simulation software. The main differences between the two protocols can be grouped in four categories as Table 1.1 summarises: road load determination from the test track, laboratory test, post-processing of the results, declaration of CO₂ results.

	Factor	NEDC	WLTP
Impact of road load determination procedure	Vehicle test mass	Kerb mass + 100 kg	Each individual vehicle of the vehicle family has its own test mass
	Vehicle tires	The widest tire has to be chosen, not necessarily implying the worst RRC, no prescription concerning the tire pressure, minimum tire tread depth 50%	CO ₂ interpolation method based on the RRC class values, tire pressure set at its minimum prescribed value, minimum tire tread depth 80%
	Calculation of resistant forces	Average of the test times in the coast down tests	Average of the test forces in the coast down tests
	Inertia of rotating parts	Increase in the WLTP of 3% in F ₀ , F ₁ and F ₂ road load coefficient relative to NEDC ones	
Impact of laboratory testing	Gearshift strategy	Same fixed gear positions for all vehicles	Gear position calculated for each vehicle and in the function of the engine and vehicle characteristics
	Driving cycle	Lower dynamicity	Higher dynamicity
	Test Temperature	The test temperature in the laboratory shall be set between 20 °C to 30 °C	The test temperature in the laboratory shall be set to 23 ± 3 °C
	Vehicle inertia	The effect of the rotational mass is neglected	The inertia mass shall be set to test mass plus 50% of the rotational mass
	Vehicle preconditioning for chassis dynamometer setup	No prescription on the preconditioning	The preconditioning consists in executing a complete WLTC

Impact of post-processing of test results	SOC correction	Not present	The battery SOC is monitored over the whole test, FC and CO ₂ emissions are corrected, if needed, for the imbalances of the SOC and the battery is not charged during the vehicle soak
	Correction of cycle flexibilities	Integration in the WLTP of the correction procedures compared to NEDC	
Impact of declaration of CO ₂ emissions		The final type approval CO ₂ value becomes the OEM declared value if the test result does not exceed the declared value by more than 4 %	The procedure for the determination of the final CO ₂ type approval value is different and more complex

Table 1.1 - Differences between NEDC and WLTP (source [7])

Results of [7] show how the largest impact on total CO₂ emissions is related to:

- the increase of the test mass;
- the introduction of the new driving cycle and gearshift schedule;
- the correction of speed and distance flexibilities.

So the introduction of new WLTP test procedures would increase the average CO₂ emissions in the worst case scenario by more than 25%. In addition the WLTP can contribute to significantly reduce the gap, occurred when the NEDC was in use, between the type approval fuel consumption and the real-world one. In this way the laboratory test results, despite their intrinsic limitations, can come closer to the real-life conditions. Although in the future, as happened with the NEDC, it's possible that the fuel consumption gap begin to increase again because of the test procedure margins potentially exploitable.

1.3 Real world CO₂ emissions

In this paragraph, some matters that concern the real-world CO₂ emissions are evaluated and the differences from the laboratory tests are examined.

1.3.1 CO₂ emissions GAP between certification and real-world

As it's possible to see in [8], the Worldwide Harmonized Light Vehicles Test Procedure (WLTP), as other tests, cannot fully address all possible operating situation and it includes some margins that might be exploited, therefore there is a gap between tests and real-world contexts as far as the CO₂ emissions, and so fuel consumption (FC), and vehicle energy demands are concerned. In addition, since 2009 when the mandatory CO₂ targets in the European Union regulations were introduced, the gap between laboratory and real-world CO₂ emissions increased to about 40% in 2017.

In [9] it's possible to observe that the problem of the FC gap was already known with the New European Driving Cycle (NEDC); indeed this was one of the reasons that lead to the creation of the WLTP. In [9] from a series of WLTP and NEDC tests carried out at the European Commission's Joint Research Centre (JRC), a simulation model that could accurately reproduce vehicle CO₂ emissions over the two test cycles was obtained and different scenarios were simulated: two cases based on the NEDC, two cases based on the WLTP and a fifth case aiming to simulate the real-world driving conditions. Three different configurations were assumed based on the basis characteristics of an average naturally aspirated (NA) petrol, an average turbo charged (TC) petrol and an average diesel passenger car. The results are presented in Figure 1.6 and a graphical summary is shown in Figure 1.7 that indicates how the shortfall between the NEDC and the WLTP was estimated in the order of 13%, between the NEDC and the estimated real-world scenario to about 32%.

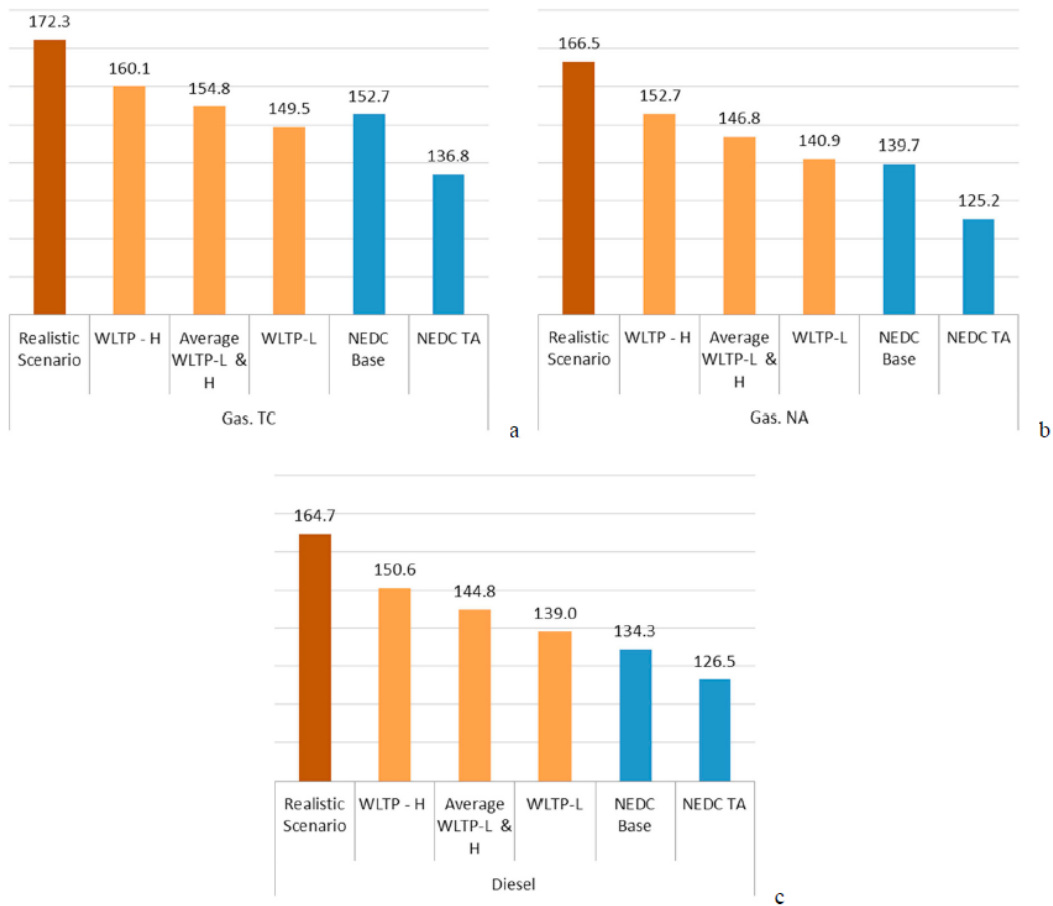


Figure 1.6 - Simulation results for all three vehicle considered over six different scenarios. All values are expressed in g CO₂ / km (figure from [9])

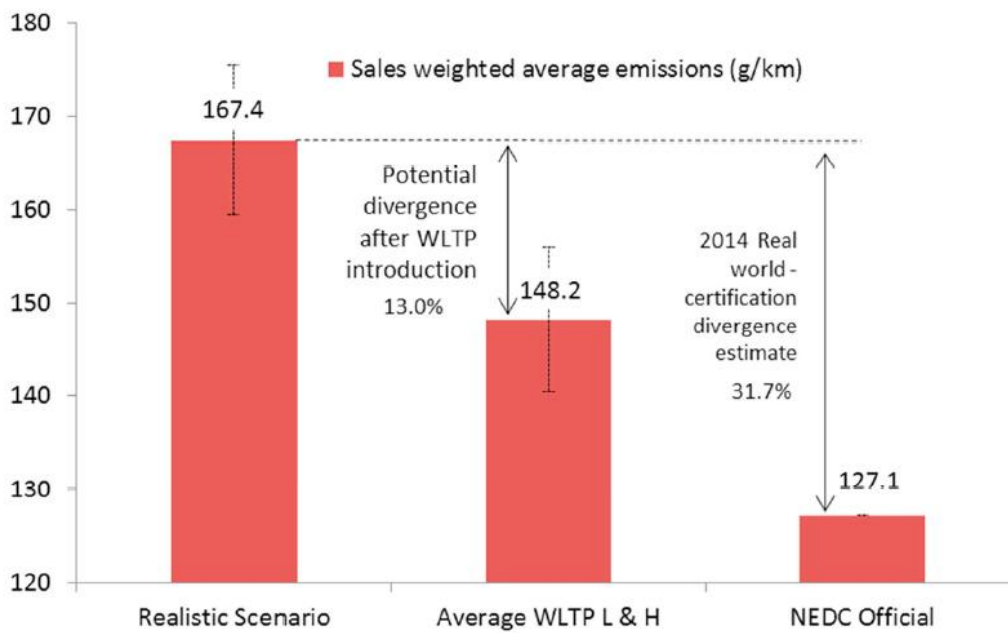


Figure 1.7 - Weighted average emissions for NEDC type approval, WLTP (High and Low) and realistic scenario with errors bars (figure from [9])

In [10] a method to monitor the in-use fuel consumption, and so the FC gap, is presented. In fact, to avoid a gradual recurrence of the gap's increase, in the regulation for light-duty vehicles (LDVs) and heavy-duty vehicles (HDVs) new requirements are present for regular monitoring of real-world CO₂ emissions. Therefore the European Commission shall collect fuel and energy consumption data from vehicles on the road using on-board fuel consumption monitoring (OBFCM) devices, these data have to be accessible via the On-board diagnostics (OBD) port. For the light-duty vehicles, the accuracy of the fuel consumed reported by the OBFCM is set to $\pm 5\%$ compared to the WLTP type-approval test fuel consumption. In [10] an investigation about the accuracy of the recorded fuel consumption from the OBD is carried out referring to the laboratory (WLTP) and on-road, with portable emissions monitoring system (PEMS), experiments. Results are shown in Table 1.2.

ACCURACY OF THE OBD MEASUREMENTS IN LDVs		
	Compared to laboratory test measurements	Compared to PEMS measurements
Fuel consumption (FC)	The majority within $\pm 5\%$ (Lowest accuracy at low vehicle speeds under transient conditions)	The majority within $\pm 5\%$ (Lowest accuracy in the urban phase)
Travelled distance	The majority within $\pm 1,1\%$ (all are lower)	In average from $-0,7\%$ to $-2,2\%$ (all are lower)

Table 1.2 - Summary of the accuracy results of the OBD measurements (values from [10])

So the analysis in [10] demonstrates that the requirements set by the European regulation in terms of real-world FC monitoring can be fulfilled.

1.3.2 Real-world factors which affect fuel consumption

To assess the real-world factors that affect on the fuel consumption, the study carried out in [8] is considered. Its aim is to analyse and quantify the intrinsic variability in the fuel consumption gap considering a single vehicle and different driving measurements: New European Driving Cycle (NEDC), WLTP, Real Driving Emissions (RDE) and real-world driving (RWD) conditions without specific testing boundaries. The type-approval cycles were conducted on the JRC's chassis dynamometer, the RDE one on the road using a Portable emissions measurement system (PEMS) and RWD with a normal vehicle usage and with parameters logged from OBD. The focus is on environmental and traffic conditions, and driving factors, which are independent of vehicle manufactures (Original equipment manufacturers, OEMs).

In Table 1.3 the data of fuel consumption are compared with the declared NEDC values and it's possible to notice how the FC gap increases in the case of RDE conditions.

Test	Fuel consumption [l/100 km] (FC gap [%])				
	Phase 1	Phase 2	Phase 3	Phase 4	Combined
Declared (NEDC)	6,5	4,9			5,5
NEDC-cold	7,5 (37%)	5,0 (-8%)			5,9 (8%)
WLTP-cold	8,0 (45%)	5,7 (4%)	4,7 (-15%)	6,7 (22%)	6,1 (10%)
PEMS	8,1 (47%)	5,3 (-3%)	7,8 (42%)		7,2 (31%)

Table 1.3 - FC declared and measured from the laboratory and on road test (PEMS) (values from [8])

Therefore in [8] the divergence in FC between type-approval tests and real-world driving trips is confirmed, moreover almost 60% of the RWD trips had an average FC higher than the average one measured with PEMS on RDE trips.

In addition, in Figure 1.8 the total FC gap variability of individual factors, divided in environmental and traffic factors and driver factors and considering all of them together, is represented. It's possible to observe that the most influent parameters on the FC gap are the vehicle average speed, the road grade and the journey distance. At the same time, the driver factors are not negligible.

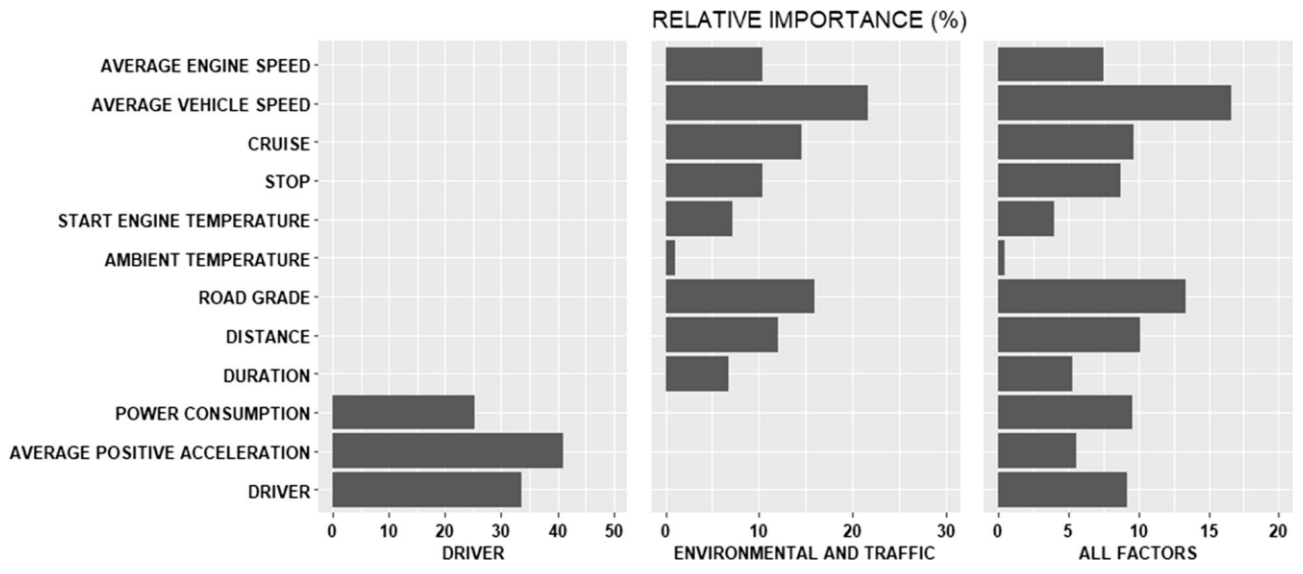


Figure 1.8 - The relative importance (% of contribution) of individual factors to the total FC gap variability (figure from [8])

2 Hybrid Electric Vehicles (HEVs)

As it's possible to see in [11] and [12], a hybrid vehicle combines two or more sources of power that can directly or indirectly provide propulsion. Considering this definition, several kinds of hybrid vehicles can be created, however only hybrid electric vehicles (HEVs) have reached the mass market, essentially they feature integration of an internal combustion engine (ICE) with one or more electric machines, aiming to optimize the operation of the ICE and maximize the efficiency of the energy conversion [11].

2.1 Architectures

Hybrid electric vehicles can be classified in series, parallel and complex depending on the power flow's path from the energy sources to the wheels.

In a series HEV only the electric motor (EM) is mechanically coupled to the wheels while the ICE is connected to a generator. Therefore the EM can receive electric power either from the battery pack or the generator, or from both. This arrangement presents the advantage that the ICE can work in a narrow power range near the optimum efficiency. Nevertheless, the high-energy conversion losses due to the long efficiency chain are disadvantageous [12].

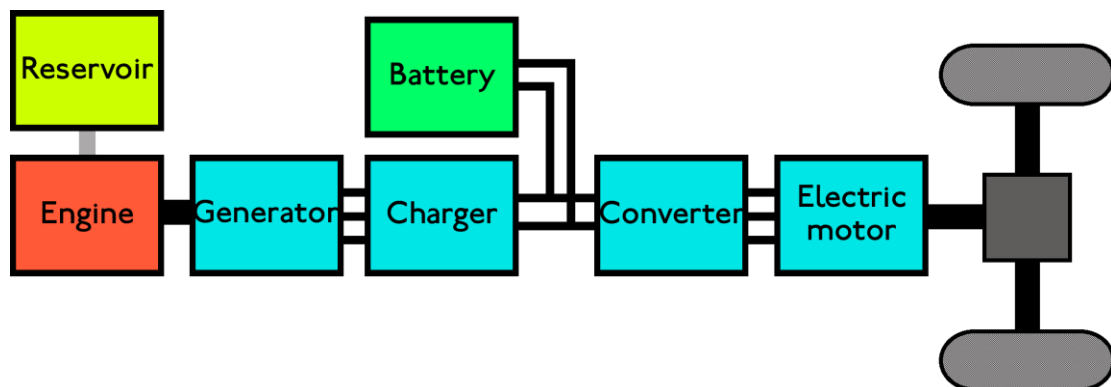


Figure 2.1 - Scheme of a series hybrid architecture

In a parallel HEV both the EM and the ICE can be directly connected to the driveline and can therefore both supply mechanical power to the wheels, the power deriving from the two on-board energy sources, chemical and electrical, is summed mechanically. The main advantages of the parallel architecture over the series one include a lack of multiple electric machines considering that there's not the generator, the elimination of the multiple power conversions from mechanical to electrical and again to mechanical one, a smaller EM with the same performances guaranteed. On the other hand, the control of the parallel hybrid powertrain becomes more complex.

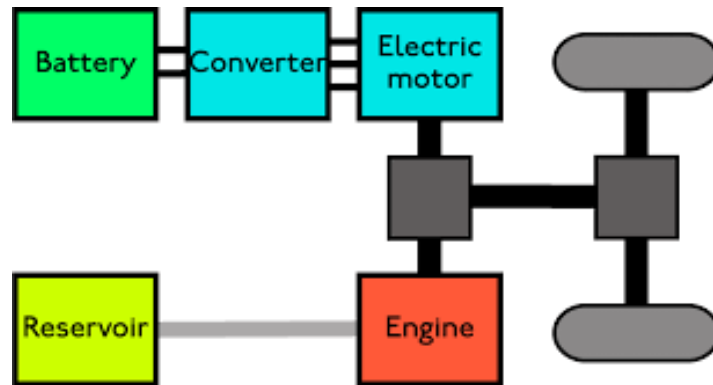


Figure 2.2 - Scheme of a parallel hybrid architecture

Parallel hybrids are further categorized according to the position of the electric machine with a categorization from P0 to P5 as illustrated in Figure 2.3 [13].

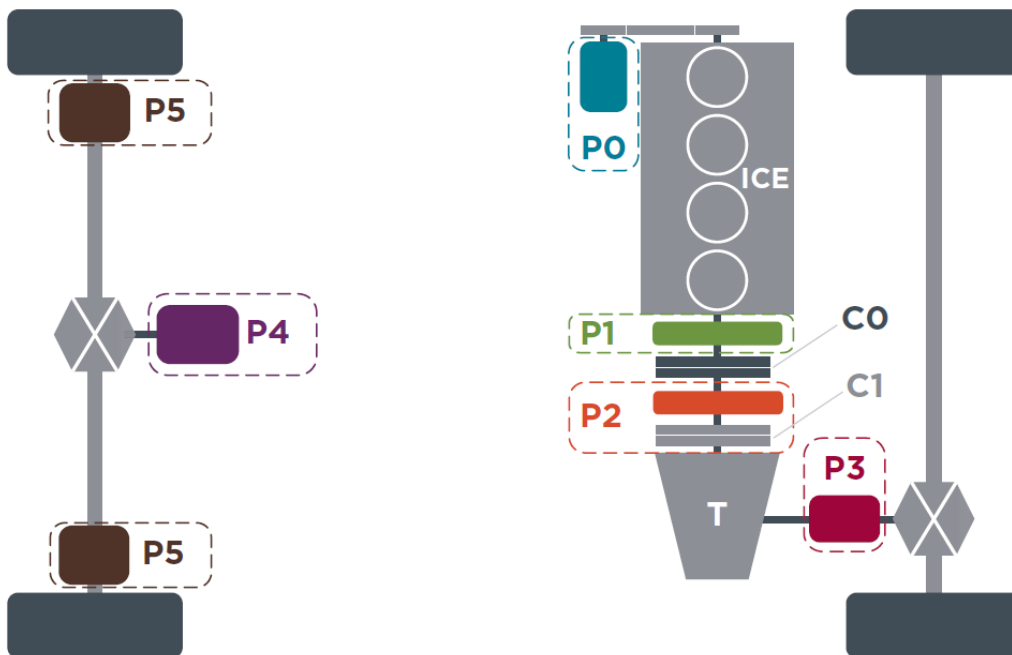


Figure 2.3 - P0 to P5 parallel hybrid architectures, Cx: Clutch x, T: Transmission, Px: Position of the electric machine(s) in each configuration x (figure from [13])

As described in [13]:

- in the P0 the EM is permanently connected to the ICE in the front-end accessory drive and cannot be decoupled, usually called belt starter generator (BSG) or belt alternator starter (BAS);
- in the P1 the EM is attached directly to the crankshaft of the ICE in front of the clutch;
- in the P2 the layout is similar to the P1 except an additional clutch is added between the ICE and the EM, this allows the EM to be decoupled from the ICE;
- in the P3 the EM is attached to the output shaft of the transmission and is thereby permanently connected to the wheels;
- in the P4 the EM is connected to the axle which is not driven by the ICE, also called “e-axle”;
- in the P5 the layout is similar to the P4, but in this configuration two EMs are integrated in the wheel hubs, directly acting on the wheels, also called “e-wheel”.

A complex HEV is obtained adding powertrain’s degrees of freedom with different technology approaches:

- increase of the number of traction systems and therefore of the mechanical or electrical links;
- increase of the number of on-board energy and power sources;
- coexistence in the same architecture of a parallel path with a series one.

Among complex hybrid architectures, there are two quite relevant cases: the series/parallel architecture and the powersplit architecture.

The first one (Figure 2.4) combines the series and parallel architectures often using one or more clutches: there’s a single ICE which is mechanically connected directly to the wheels and to a generator so it’s possible to use a parallel power flow or a series one in which only the EM powers the wheels. Thus it’s possible to use each traction system when the corresponding optimal operation conditions occur, for example the parallel configuration at high speed and in the highway, while the series one at lower speeds disconnecting the ICE from the wheels.

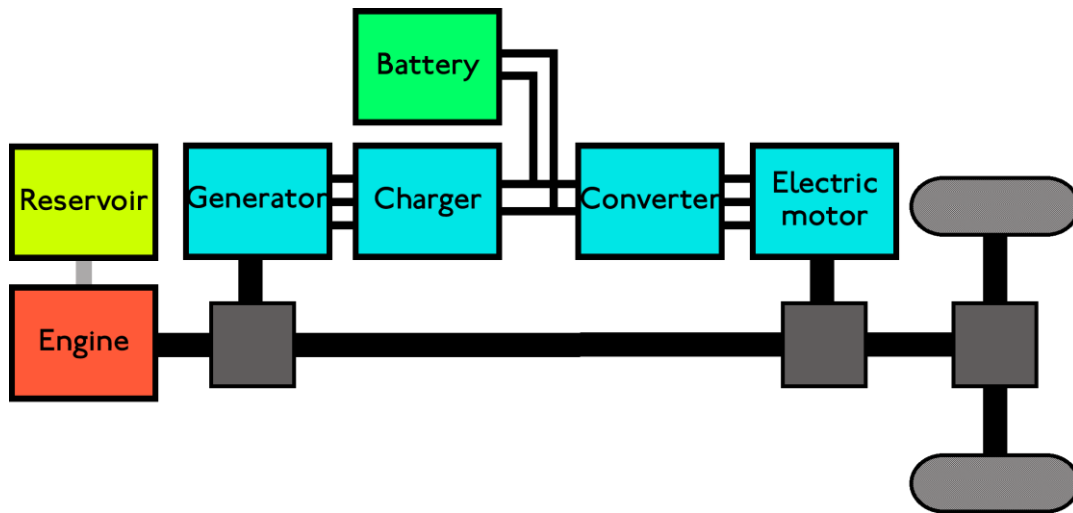


Figure 2.4 - Scheme of a complex series-parallel hybrid architecture

The Powersplit architecture (Figure 2.5) consists in a complex hybrid system where the power is still split between a series and parallel architecture, but the combination of the operating modes is obtained with an epicyclic gear train: the generator is connected to the sun gear, the internal combustion engine to the planetary carrier and the electric motor to the ring gear. With this system it's possible to vary the power split changing the components speeds with the aim of achieve the best overall efficiency.

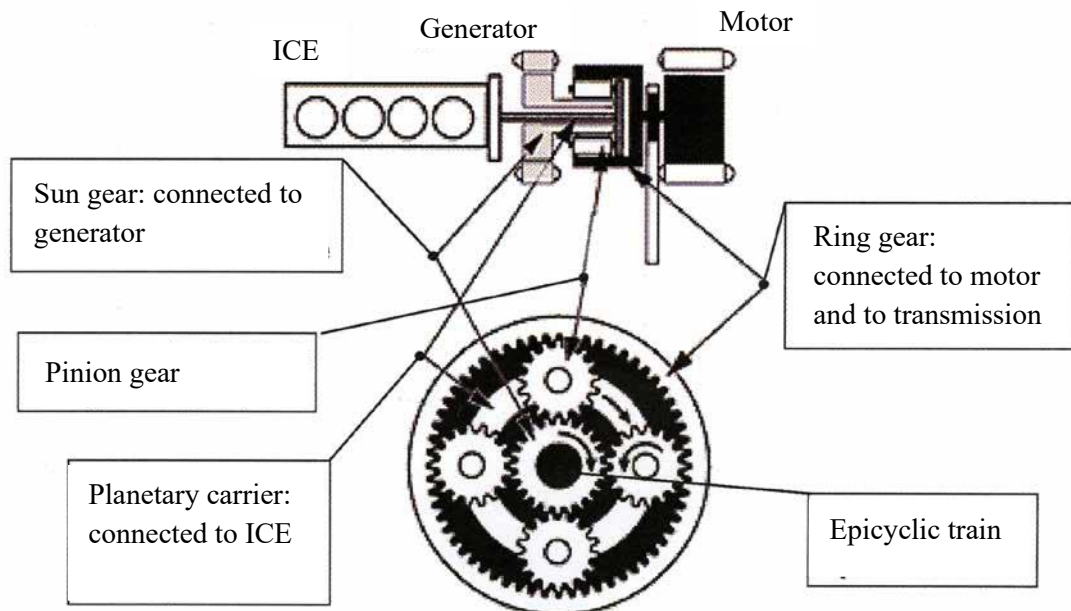


Figure 2.5 - Scheme of a complex powersplit hybrid architecture

2.2 HEVs and PHEVs

One of the most important classifications is between Hybrid Electric Vehicle (HEVs) and Plug-in Hybrid Electric Vehicle (PHEVs). In the European Union's regulation [14], the HEVs are formally defined as Not Off-Vehicle Charging Hybrid Electric Vehicles (NOVC-HEVs) while the PHEVs are formally defined as Off-Vehicle Charging Hybrid Electric Vehicles (OVC-HEVs).

The HEVs can't be recharged from external sources and they can operate essentially only in charge sustaining (CS) mode therefore the battery state of charge (SOC) is maintained close to a reference value and the battery works as an "energy buffer" powering the electric motor (EM) when it's more appropriate and recharging when the proper conditions occur, for example in the regenerative braking. Thus the HEVs' batteries are smaller than PHEVs and naturally than battery electric vehicles (BEVs).

The PHEVs can be recharged from external sources and so they have bigger batteries and electric motors than HEVs.

2.3 PHEVs operating strategies

As it's possible to see in [11], in a conventional vehicle the power request is given by the driver through accelerator and brake pedals and a low-level controller translate these requests into actions. In a HEV the presence of multiple energy sources significantly increases the powertrain complexity and requires the development of a suitable Energy Management System (EMS) [15] which determines the power split between the different power actuators (for example between the ICE and the EM) [11]. In particular it is composed by two parts: the one which is, strictly speaking, the energy management system and the supervisory controller. The first one decides how to split the power demand indicating the best operating mode and the second one is used to split the power between the power actuators.

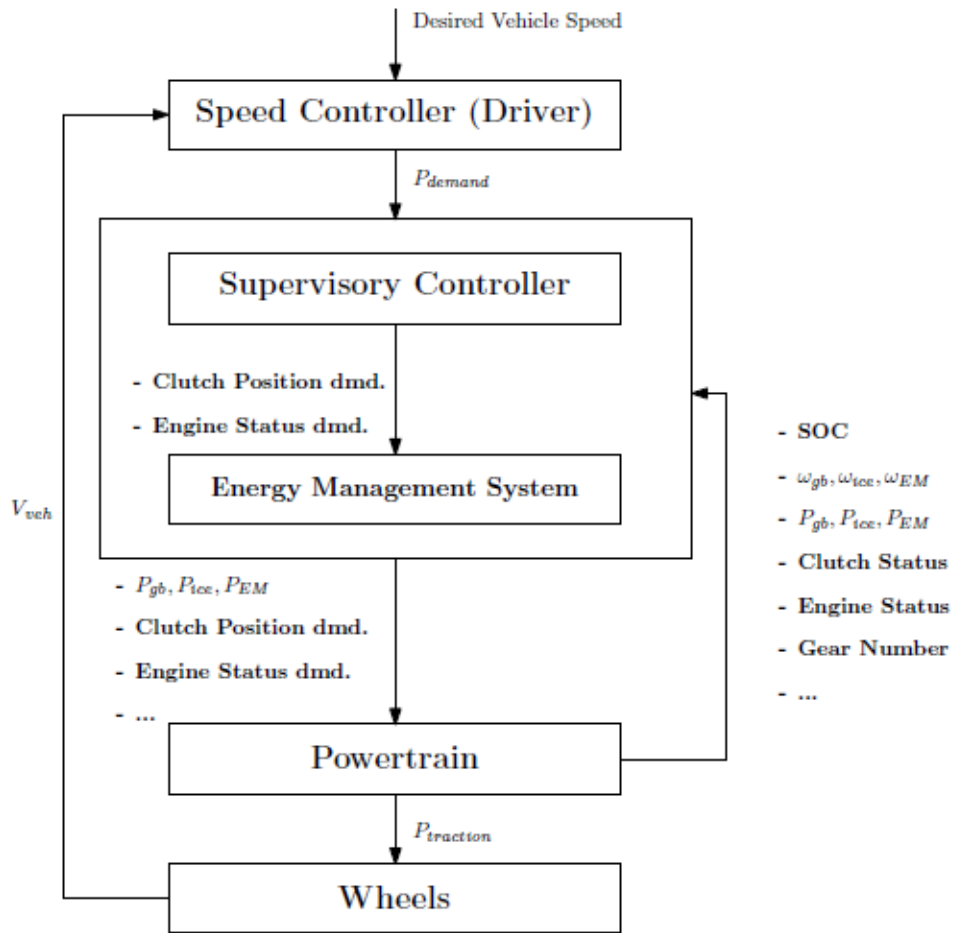


Figure 2.6 - The role of the EMS in a hybrid electric vehicle (figure from [11])

In a HEV it's possible to use a charge sustaining control strategy whereas PHEVs can employ different and more complex operating strategies due to the size of their batteries and electric motors. The most common one is the so-called charge depleting and charge sustaining (CD-CS) strategy, in this thesis another one is analysed: the blended mode.

2.4 Charge Depleting and Charge Sustaining mode

The most common operating strategy in a PHEV is the charge depleting and charge sustaining (CD-CS) strategy. Using this strategy, the vehicle initially follows the charge depleting (CD) phase where the power demand is fulfilled only by the electric motor until the battery state of charge (SOC) reaches a determined lower value.

The state of charge is a dimensionless parameter which describes the amount of usable charge in a battery as a function of time conveyed as a ratio, typically expressed as a percentage, between the actual capacity $C(t)$ and the rated one C_{nom} (2.1).

$$SOC(t) = \frac{C(t)}{C_{nom}} \quad (2.1)$$

When in the CD phase the power demand exceeds the maximum power the electric motor can supply, the ICE can be anyway started to fulfil the overall requested power.

When the SOC reaches the reference value, the vehicle turns in the charge sustaining (CS) phase where, likewise a HEV strategy, the SOC is maintained around the reference value using a rule based (RB) optimization method. The battery works as an energy buffer and the continuous pure electric driving can't be achieved. In Figure 2.7 it's possible to see an example of a typical SOC trajectory as a function of the time in a trip where the CD-CS strategy was used.

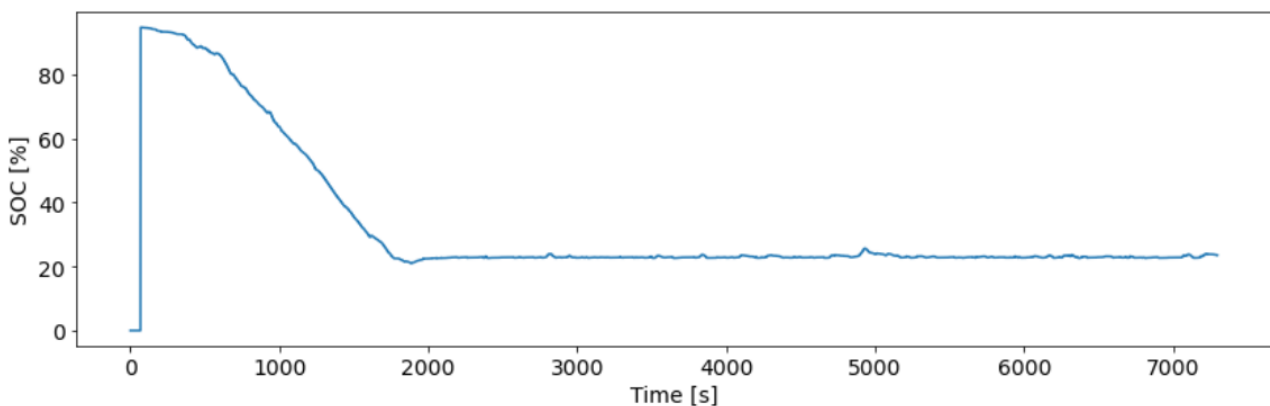


Figure 2.7 - Example of a SOC profile in a CD-CS trip

The CD-CS strategy aims to maximize the only electric driving: this control uses the EM only, except possible high-power demands, since the beginning regardless the type of journey, without considering other parameters like the journey length planned and the road energy demand. Therefore this control strategy is easy to execute in the vehicle because the unique variables involved are the instantaneous SOC and power demand. At the same time the optimisation of the power split, in terms of FC, along the trip, in particular in the long ones, is not guaranteed.

2.5 Blended mode

The blended control strategy has the purpose of overcoming the CD-CS disadvantages improving fuel economy and thus reducing CO₂ emissions. In this mode the EM and the ICE are used along the entire trip depending on the different conditions with the aim of exploiting the most efficient operating points of the propulsion systems in order to improve the overall fuel economy of the trip. Thus the SOC is managed along the trip and it usually presents a more gradual discharging trajectory which the aim to reach the lower limit at the end of the trip. With the latter condition, the entire available battery charge is used in the trip and a possible final part in a necessarily CS operating mode is avoided. Generally the blended mode uses an Equivalent Consumption Minimization Strategy (ECMS) optimization method. The ECMS consider a weighting factor μ between fuel and battery power.

In Figure 2.8 it's possible to see an example of a typical SOC tendency as a function of the time in a trip where the blended strategy was used.

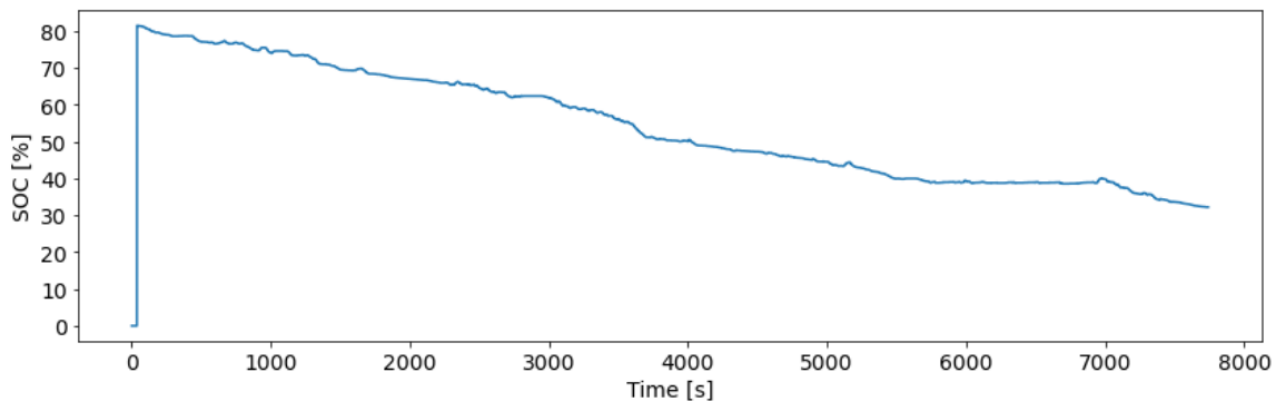


Figure 2.8 - Example of the SOC profile in a blended trip

The blended mode is more difficult to execute on board because it requires the a priori knowledge of diverse variables regarding the journey, for example the total distance and the energy demand and other characteristics such as the slopes along the trip.

2.6 Advantages and disadvantages of the blended mode

In this chapter a literature review about the blended mode is presented in order to evaluate which advantages and disadvantages emerge as far as this control strategy is concerned.

First of all, in [16] a comparison between the CD-CS mode and the blended mode is presented using type approval test driving cycles: the New European Driving Cycle (NEDC) and the Worldwide Harmonized Light Vehicles Test Cycle (WLTC). The tests are carried out in the vehicle emissions laboratories (VELA) of the Joint Research Centre (JRC) on a Euro 6 PHEV and three vehicle modes are considered: Zero Emission Vehicle (ZEV), Blended and Sport. The latter mode is tested in charge sustaining while the other two in charge depleting condition due to their broad use of the electric traction in relation to the sport mode. In Figure 2.9 and Figure 2.10 the time dependency of the ICE switching ON/OFF strategy and of the SOC trajectory are illustrated for the ZEV and blended mode respectively. Figure 2.11 shows the percentage of the share among the different operating modes.

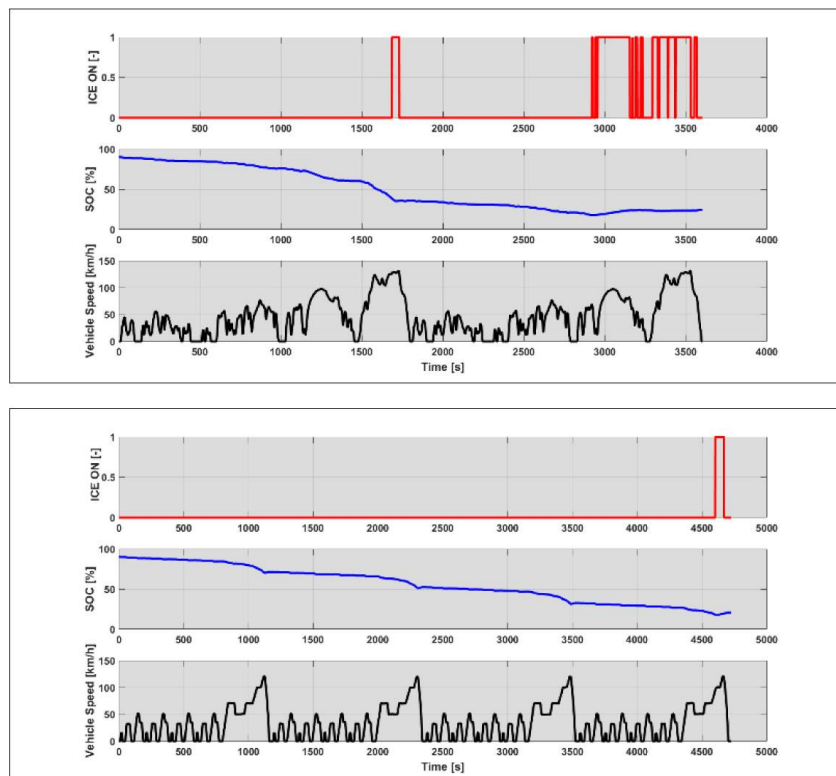


Figure 2.9 - ICE ON/OFF status and battery SOC for the ZEV mode along the WLTP (top) and NEDC (bottom) (figure from [16])

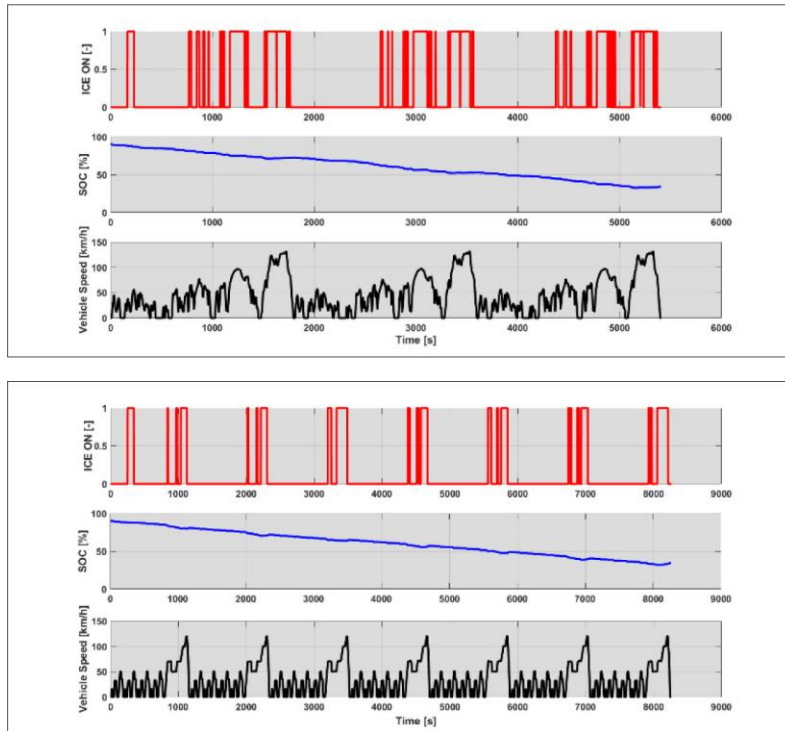


Figure 2.10 - ICE ON/OFF status and battery SOC for the blended mode along the WLTP (top) and NEDC (bottom) (figure from [16])

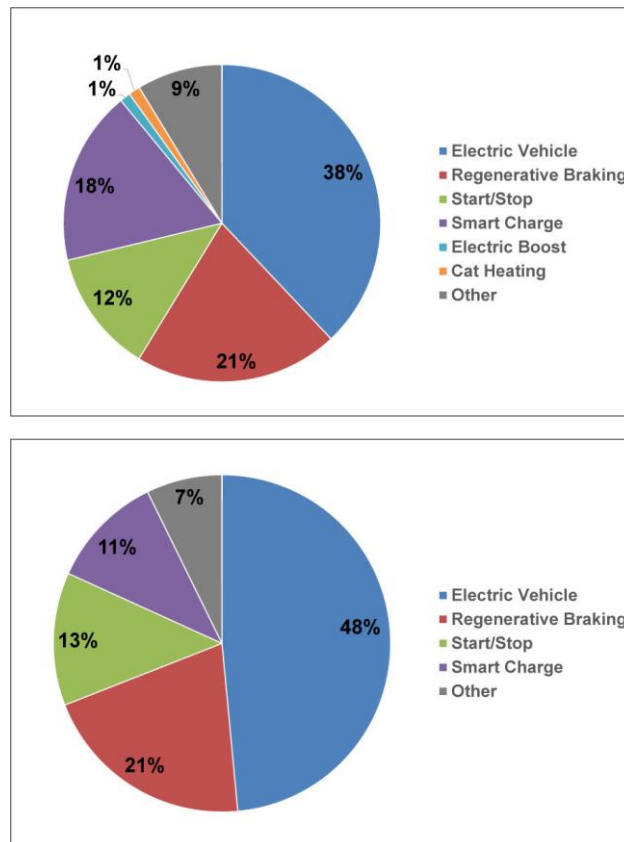


Figure 2.11 - Vehicle operating modes along WLTC for blended (top) and ZEV (bottom) (figure from [16])

In Table 2.1 the operation limits difference between the two modes are summarized.

CONDITION	ZEV MODE	BLENDED MODE
ICE switching ON	Power demand above 60 kW Reaching SOC = 25%	Power demand above 30 kW Reaching SOC = 35%
Only electric driving	Speed up to 120 km/h <ul style="list-style-type: none"> ┌ Acceleration below 0,5 m/s² └ Speed between 50 and 80 km/h ┌ Acceleration below 1,5 m/s² └ Speed below 50 km/h Speed·acceleration between -15 and 25 m²/s³ 	Speed up to 80 km/h Speed·acceleration between -5 and 15 m ² /s ³

Table 2.1 – Operation limits of the ZEV mode and blended mode (data from [16])

It's possible to notice that the blended mode limits the only electric drive for mid and low speeds, typical of the urban driving, while in the ZEV mode the EMS permits the only electric driving in a wider range of speeds, accelerations and power demands.

The difference in type approval (TA) CO₂ calculation are observed in Table 2.2.

NEDC	WLTC
$CO_{2,TA} = \frac{D_{OCV} \cdot M_1 + D_{av} \cdot M_2}{D_{OCV} + D_{av}}$	$CO_{2,TA} = \sum_{j=1}^k (UF_j \cdot CO_{2,CD,j}) + \left(1 - \sum_{j=1}^k UF_j\right) \cdot CO_{2,CS}$
<p>D_{OCV}: electric range $D_{av} = 25 \text{ km}$: average distance between two rechargings</p>	<p>UF_j: utility factor of each WLTC phase during CD $CO_{2,CD,j}$: CO₂ emissions in each WLTC phase during CD $CO_{2,CS}$: CO₂ emission during CS test</p>

Table 2.2 - Summary of the CO₂ calculation in TA test using NEDC and WLTC

In Figure 2.12 and Figure 2.13 it's possible to perceive the results in terms of CO₂ type approval (in green) coming from the combination of the assessed mode, blended or ZEV, use in the CD and the sport mode (in red) used in the CS.

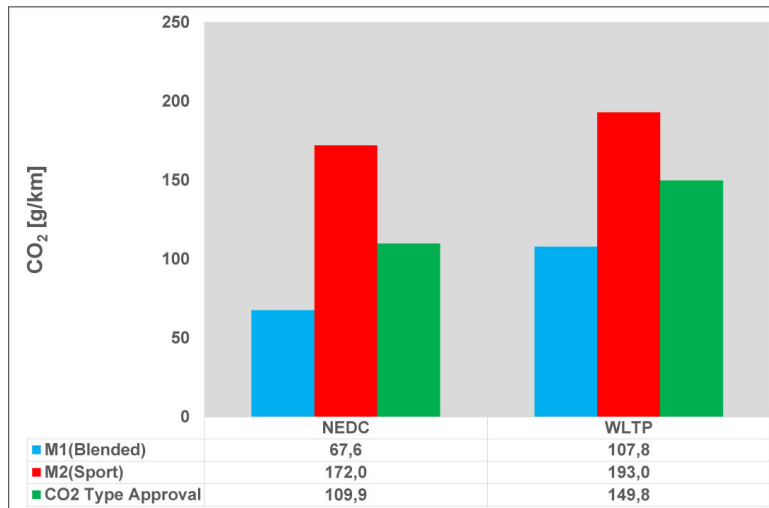


Figure 2.12 – CO₂ emissions along the NEDC and the WLTC combining the blended mode with the sport mode (figure from [16])

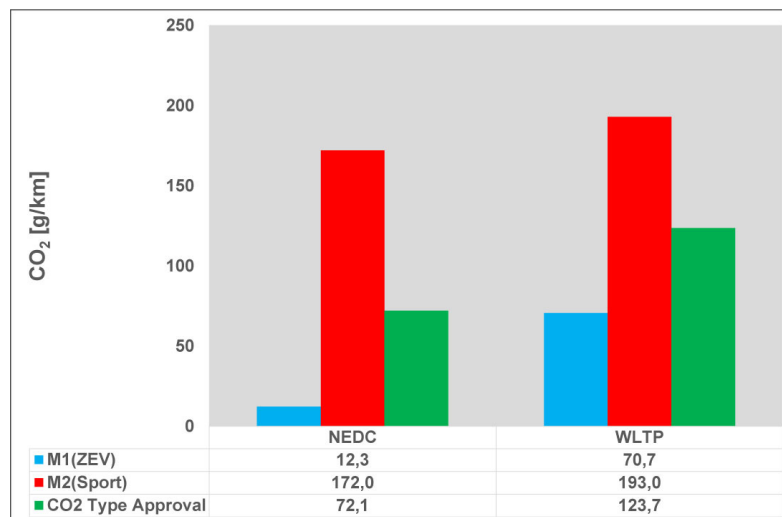


Figure 2.13 – CO₂ emissions along the NEDC and the WLTC combining the ZEV mode with the sport mode (figure from [16])

With M₂ equal in each mode considering the same driving cycle because it derives from the CS part, it's possible to compare the M₁ values which is higher in the blended mode than in the ZEV one. In particular in the WLTC case, if the blended mode would be used in the CD phase, the CO₂ emissions would be greater than in the ZEV mode due to the CO₂ emissions occurred in the first phases of the sequence of cycles because they would have a superior weight in the calculation that uses the utility factor (UF) approach, described in paragraph 3.2.2.

So using the blended mode in the NEDC and WLTC driving cycles is not worthwhile because it leads to higher CO₂ emissions than the ones obtained with a CD-CS strategy.

In [17] a blended rule based EMS is presented, it is formulated over driving information and vehicle trip energy without considering specific vehicle speed or acceleration profiles. As it's summarized in Figure 2.14, the vehicle energy required is estimated considering the driver style, the route distance and the road types (urban or extra urban). In particular it's necessary to know the destination, then trip information is personalised over distance according to road types, the latter information can be obtained using a navigation system, the traffic one from an Intelligent transportation system (ITS) or other highway agencies. For the different road types and driver styles there is a specific energy per km, the estimated energy for each road type is obtained multiplying the specific energy by the corresponding distance. The total estimated trip energy is compared with the total available battery energy calculated considering the current SOC and the target one.

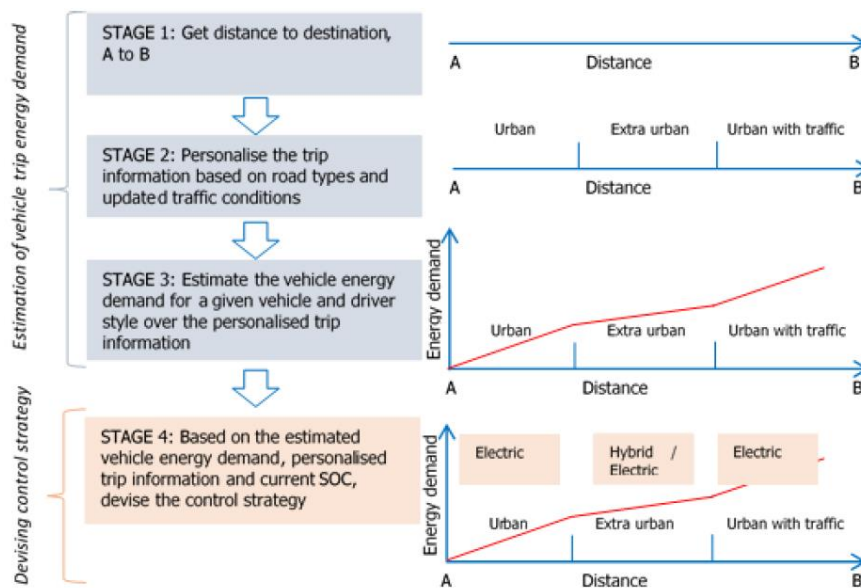


Figure 2.14 - Working principle of the EMS proposed in [17] (figure from [17])

The purpose of the control strategy is to obtain the minimum engine fuel consumption and the EMS operates depending on the surplus or deficit of actual battery energy as compared to the remaining trip one. In case of surplus, the only electric drive is used; conversely in case of deficit it's necessary to provide the remaining necessary energy with the ICE, its timing and operating duration depend on the amount of energy deficit, when it's in smart charging it's operate on the optimal operating line (OOL).

This EMS is compared by simulation whit a conventional rule base one (CD-CS strategy) considering four different real-word driving trips with different urban (U) and extra-urban (E) distances alternation: U/E/U, U/E, E/U, U. The one using the blended strategy gives a grater fuel economy than the conventional one as it's possible to see in Table 2.3, in fact the knowledge of the driving information and the estimated trip energy helps to manage battery energy and to use the ICE more efficiently.

	Proposed EMS				Conventional EMS			
Trip (Road type sequence)	A (U/E/U)	B (U/E)	C (E/U)	D (U)	A (U/E/U)	B (U/E)	C (E/U)	D (U)
Final SOC	0,440	0,442	0,439	0,418	0,443	0,453	0,443	0,451
Actual FE [mpg]	110,8	114,6	133,0	245	101,1	100,6	114,8	171

Table 2.3 - Results for the different four real-world trips in [17] (table from [17])

In [18] a comparison between a parallel PHEV's model based energy management systems and a CD-CS one is illustrated. The purpose is to minimise the fuel consumption while fulfilling the driver power demand and the constraint on the final SOC.

Overall, four different strategies, summarised in Table 2.4, are proposed: charge depleting and charge sustaining (CD-CS), Average cycle prediction + ECMS (ACP + ECMS), Markov based cycle prediction + ECMS (MCP + ECMS) and ECMS. The latter is the off-line optimal solution, calculated knowing in advance the driving cycle and the optimal weighting factor during the complete cycle. The other three control strategies can be implemented online. In the ACP + ECMS the road information are known because the considered rout has been previously covered 50 times, while in the MCP + ECMS the driving cycle is not known in advance and it's predicted.

Strategy	Control type	Control level	Cycle prediction
CD-CS	Online	Heuristic	No
ACP + ECMS	Online	Model-based	Fixed prediction
MCP + ECMS	Online	Model-based	Dynamic prediction
Optimal (ECMS)	Off-line	Model-based Optimal	Known cycle

Table 2.4 - Comparison of the different control strategies in [18] (table from [18])

The performances of the different control strategies are assessed with a simulation campaign, the results are shown in Figure 2.15.

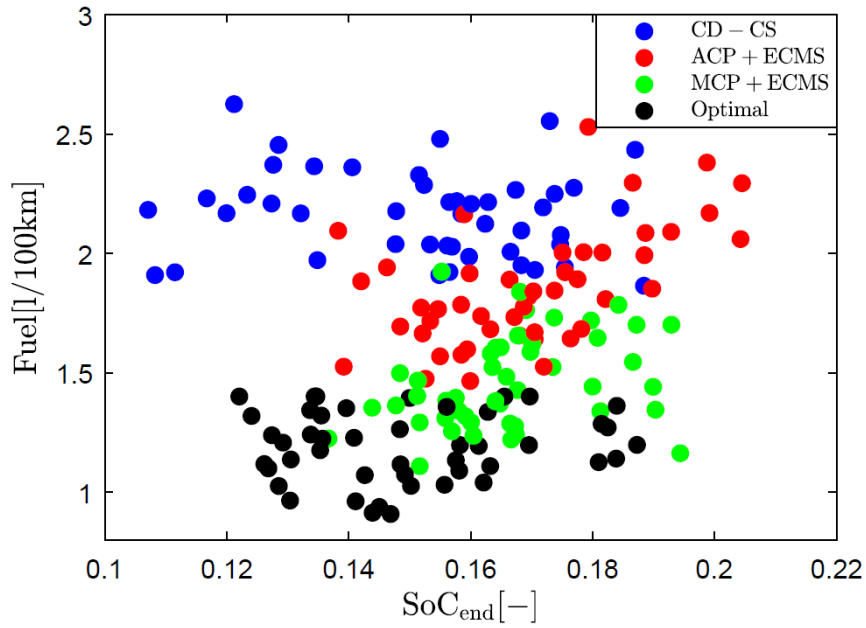


Figure 2.15 - Results of the four control strategies in [18] simulation (figure from [18])

It's possible to notice that the CD-CS strategy presents the farthest results from the optimal ECMS, then the ACP + ECMS and the MCP + ECMS have the nearest results. These results are also shown in Figure 2.16, in the optimal ECMS the weighting factor μ is constant allowing the achievement of the minimum fuel consumption.

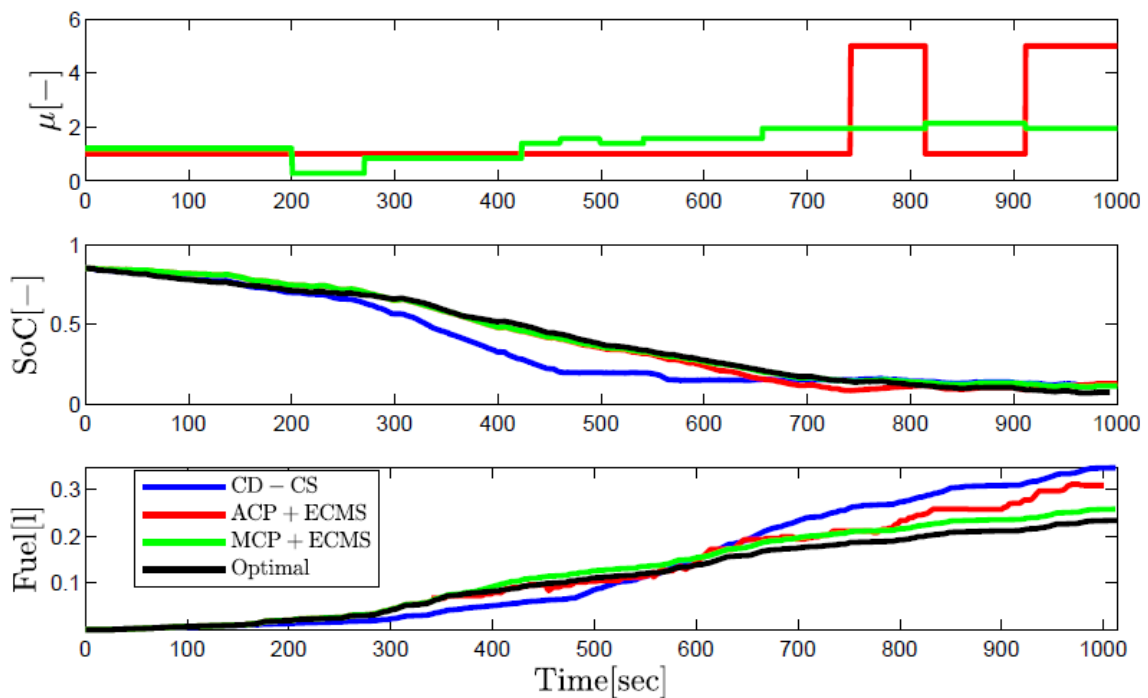


Figure 2.16 - Evolution of the results in the four EMSs of [18] (figure from [18])

In addition in Figure 2.17 the frequency of the ICE operating point are represented over the engine efficiency map. In the case of optimal ECMS the engine works mostly in the high efficiency zone and the dispersion of frequency grows through the different control strategies in the order: MCP + ECMS, ACP + ECMS and at the end CD-CS.

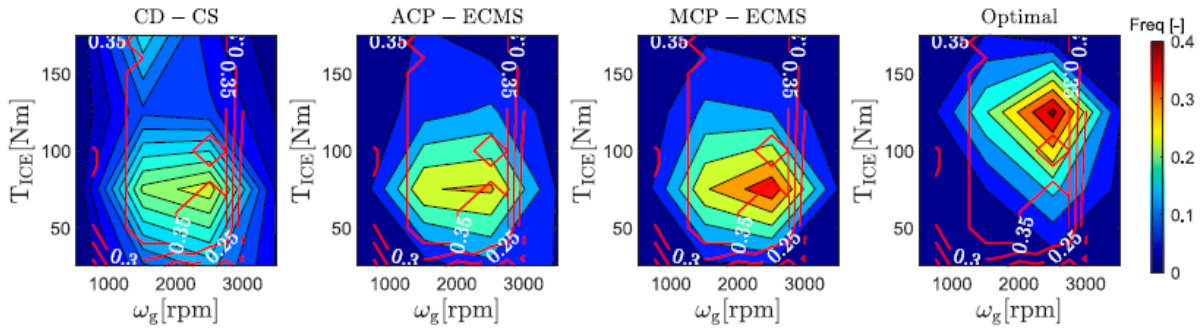


Figure 2.17 - Frequency of the ICE operation points overlapping engine's iso-efficiency lines, in red, in the four control strategies of [18] (figure from [18])

The final results show that the MCP +ECMS is the most efficient online approach while the CD-CS the worst. Providing analogous final SOC and compared to the optimal ECMS result, the MCP + ECMS presents a 11% higher fuel consumption, the ACP + ECMS 35% higher and the CD-CS 52% higher.

In [19] the blended control strategy SOC trajectory is assessed when the low-emission zones (LEZ) that require electric-only driving, and varying road grade are considered. Two driving cycles are considered: a realistic city-bus cycle recorded in the city of Dubrovnik (label as "DUB" cycle) and the Heavy Duty Urban Dynamometer Driving Schedule (HDUDDS). These two driving cycles are replicated several times and designated as $ixDUB$ and $ixHDUDDS$ with i the number of cycle considered. The SOC trajectories are depicted with respect to travel distance, a dynamic programming (DP) optimization is conducted to obtain a globally optimal SOC trajectory for the given driving cycle.

First of all, the SOC trajectory obtained with the DP it's compared with the shortest-length one, that is the linear one, connecting the initial SOC point $SOC_i = 90\%$ and the final one $SOC_f = 30\%$ in the two driving cycle with no LEZ presence and zero road grade. The results are illustrated in Figure 2.18 and it's possible to notice that the optimal DP trajectory is close to the ideal one.

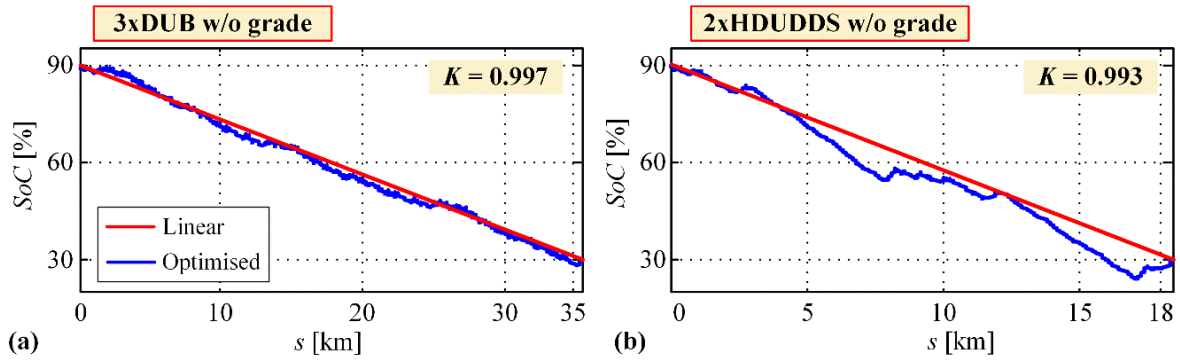


Figure 2.18 - Optimal SOC trajectory (in blue) and linear SOC trajectory (in red) without LEZ and road grade for 3xDUB driving cycle (a) and 2xHDUDDS driving cycle (b) with respect to distance s (figure from [19])

Then an analogue procedure has been conducted in the case of LEZ presence and zero road grade (Figure 2.19) and the obtained optimal SOC trajectories are well aligned with the shorter-length ones also in this case.

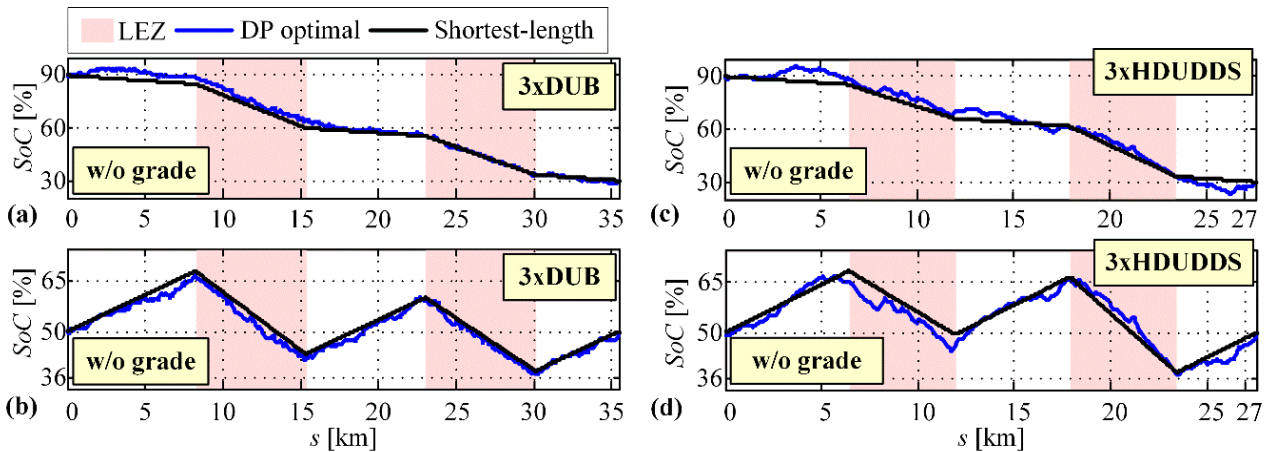


Figure 2.19 - Optimal SOC trajectory (in blue) and shortest-length (piecewise linear, in black) trajectory in case of LEZ presence and without road grade for 3xDUB and 3xHDUDDS with $SOC_i = 90\%$, $SOC_f = 30\%$ (a, c) and $SOC_i = 50\%$, $SOC_f = 50\%$ (b, d) (figure from [19])

Introducing the recorded road grade, an offset and a distortion take place from the shortest-length trajectories as it's possible to see in Figure 2.20.

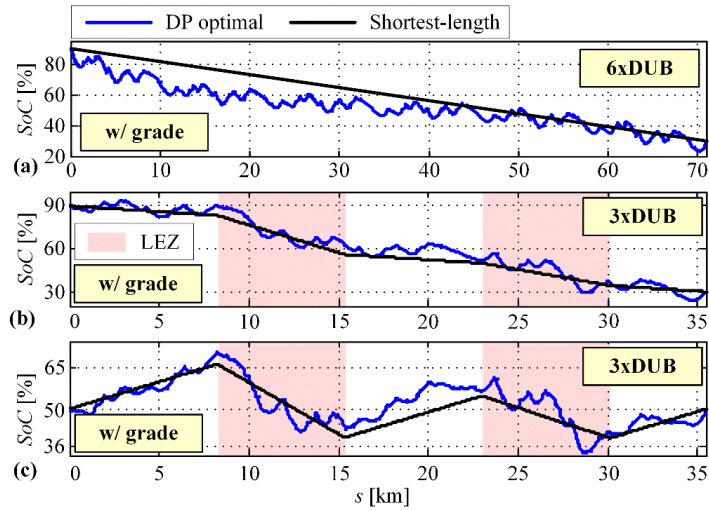


Figure 2.20 - Optimal SOC trajectory (in blue) and shortest-length (piecewise linear, in black) trajectory in case of registered road grade, for 3xDUB also with LEZ (b, c), with different SOC_i and SOC_f (figure from [19])

In the case of sinusoidal road grade profiles, Figure 2.21, it's possible to discern that the divergence from the linear trajectory is more accentuate in case of low-frequency road grade profile because the SOC rapidly decreases in case of uphill driving and increase during downhill driving due to the regenerative braking.

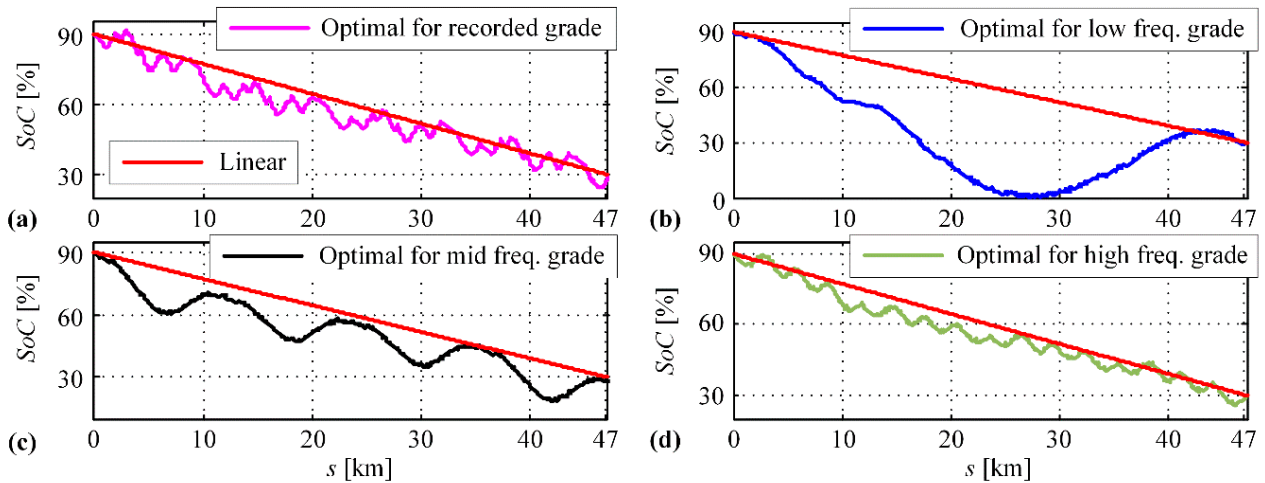


Figure 2.21 - Optimal SOC trajectories and linear ones for 4xDUB driving cycle and recorded road grade (a), low frequency (b), mid frequency (c) and high frequency sinusoidal road grades (figure from [19])

Decomposing and rearranging the SOC linear trajectory in a discharging and charging section, it's possible to obtain two linear sections close to the optimal SOC trajectory. Plotting the SOC time derivative with respect to the power demand P_d , Figure 2.22, a 2nd order polynomial functional dependence can be detected from negative to mid positive power demands (regenerative braking and electric-only driving).

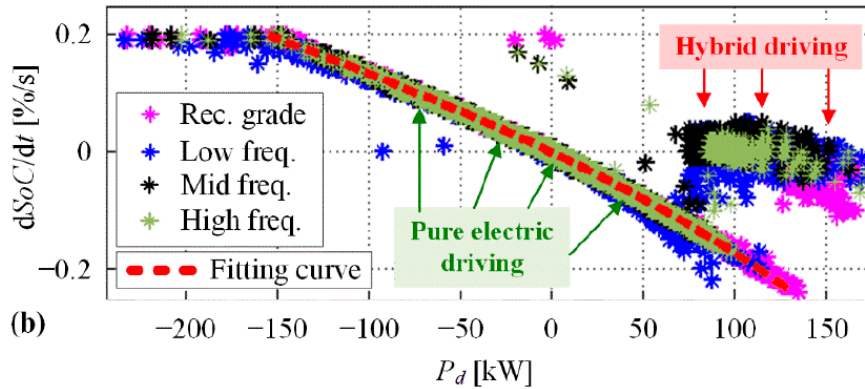


Figure 2.22 - SOC time derivative with respect to power demand P_d (figure from [19])

Using this correlation (Figure 2.22) and assuming that the power demand and the vehicle speed are known in advance or properly estimated, a SOC trajectory is calculated with a synthesis procedure. This synthesized trajectories, as it's possible to note in Figure 2.23, closely follow the optimal ones obtained with DP.

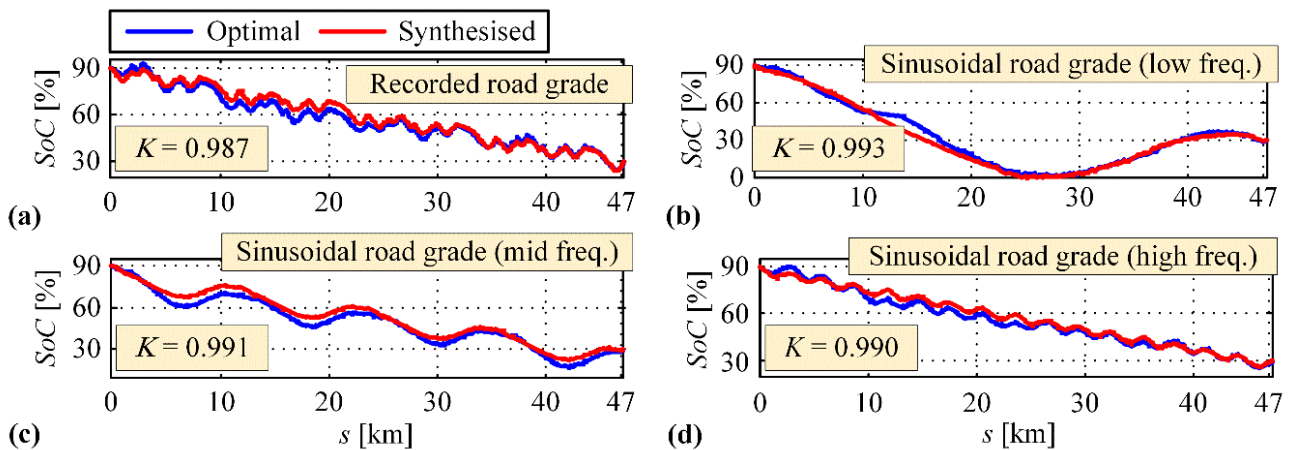


Figure 2.23 - Optimal and synthesized SOC trajectories for recorded road grade (a) and for sinusoidal profiles (b, c, d) (figure from [19])

Results in Figure 2.24 show that the blended mode (BLND) approaches the DP reference within a margin of 2% and the CD-CS mode within a margin of 5% in terms of total fuel consumption V_f .

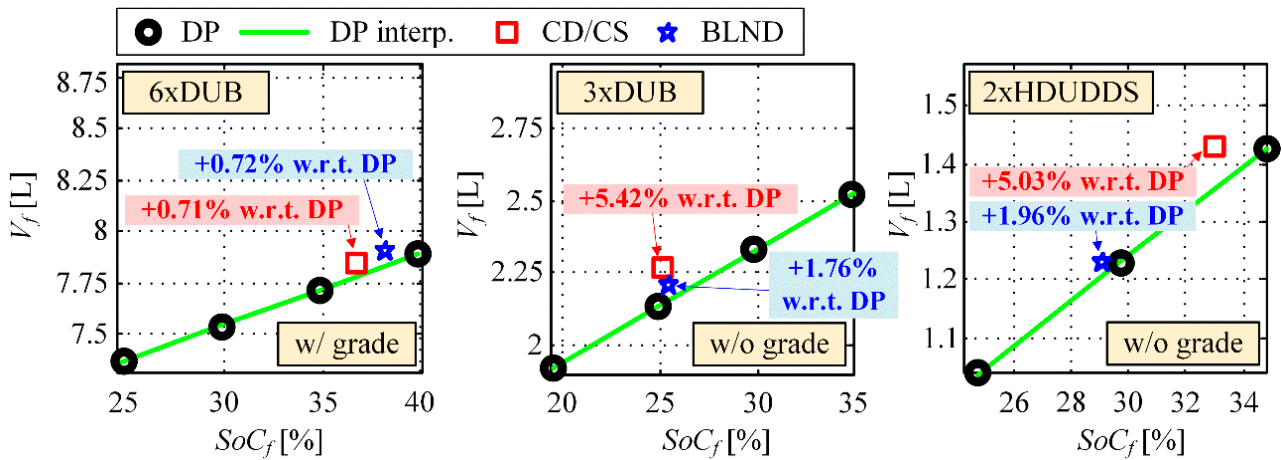


Figure 2.24 - Total fuel consumption for CD-CS and blended mode for different driving cycle without LEZ (figure from [19])

Eventually a fuel consumption comparison is conducted on the 4xDUB driving cycle considering two reference trajectory synthesis, the linear trajectory based and the 2nd order polynomial based. The results, displayed in Figure 2.25, reveal that the difference between the two references became higher in case of lower sinusoidal road grades.

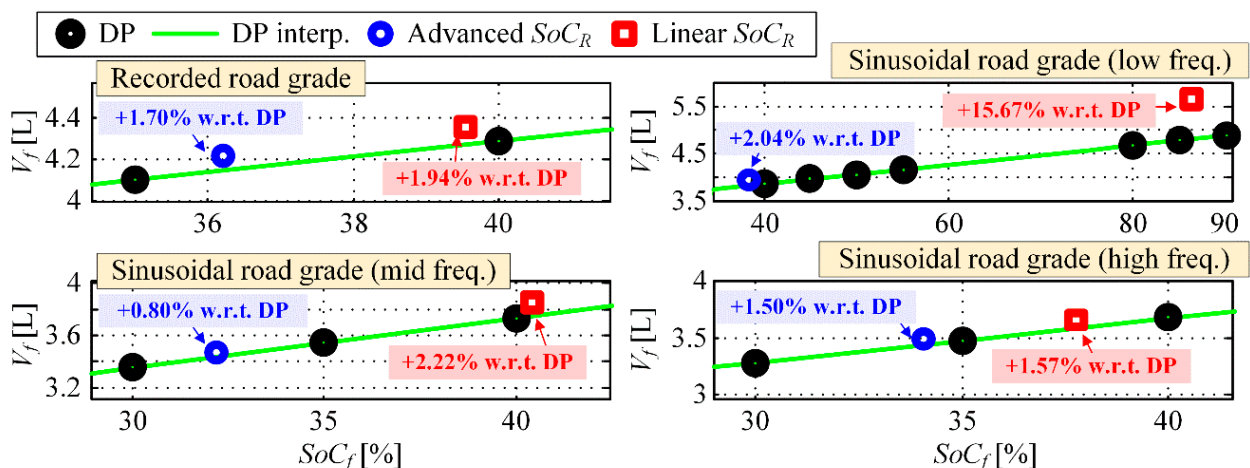


Figure 2.25 – Total fuel consumption for the 4xDUB driving cycle and for different reference trajectory synthesis, linear and non-linear (advanced) one, for 4xDUB driving cycle and for recorded road grade (a), low frequency (b), mid frequency (c) and high frequency sinusoidal road grades (figure from [19])

It's possible to summarize that in the driving cycles without road grade, when a blended mode based on a linear shortest-length SOC trajectory is used, the fuel consumption is rather close to the optimal one obtained with a dynamic programming strategy. Introducing road grade, the same blended strategy, for the mid and high frequencies of the sinusoidal road grade profile, gives FC results not so distant from the DP benchmark. In the case of low frequencies of the sinusoidal road grade, it's necessary to use a more complex non-linear strategy to obtain good FC results.

In [20] it's possible to analyse how in a parallel PHEV the uncertainties regarding the predicted trip length affect the discharging strategy compared to the optimal one. A blended mode is calculated with dynamic programming to minimise fuel cost while the predicted length of the trip is modelled as a normally distributed stochastic variable as it's possible to see in Figure 2.26.

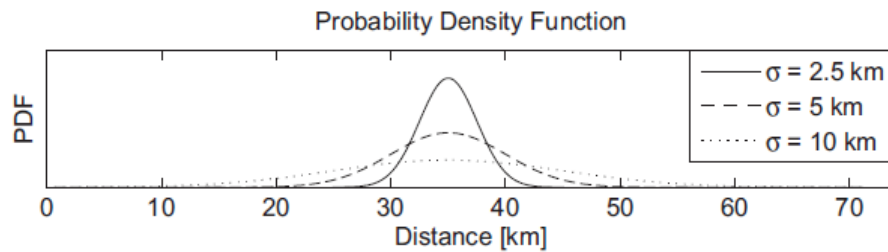


Figure 2.26 - Normal distribution of the probability density function when the predicted trip length is 35 km (figure from [20])

When the predicted trip length is shorter than the all-electric range (AER), the charge depleting and charge sustaining (CD-CS) is already the optimal strategy because the CD phase is sufficient to cover the entire predicted journey.

To assess the other cases, two predicted trip length $\mu = 35 \text{ km}$ $\mu = 55 \text{ km}$ and three different standard deviation $\sigma = 2,5 \text{ km}$, $\sigma = 5 \text{ km}$ and $\sigma = 10 \text{ km}$ are considered on three diverse speed profiles: A (Figure 2.27), B (Figure 2.28) and C (Figure 2.29).

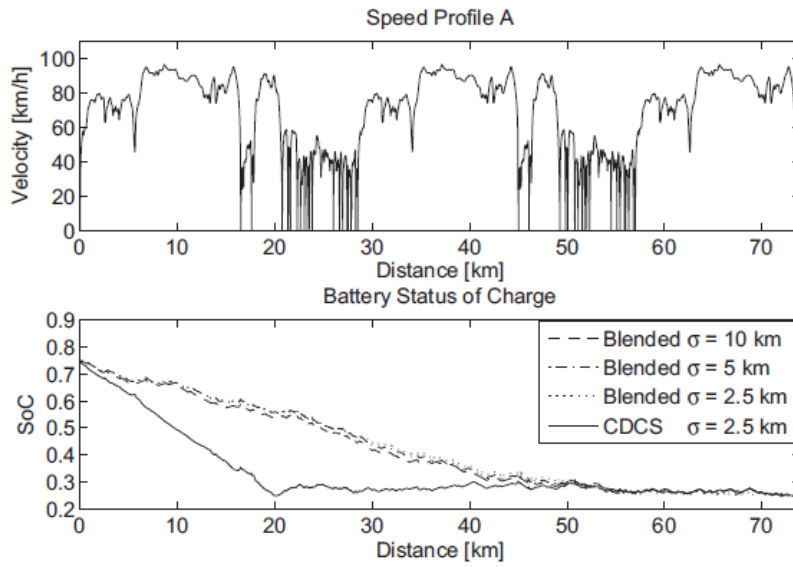


Figure 2.27 - Speed and SOC trajectories for profile A with predicted trip length $\mu = 55 \text{ km}$ (figure from [20])

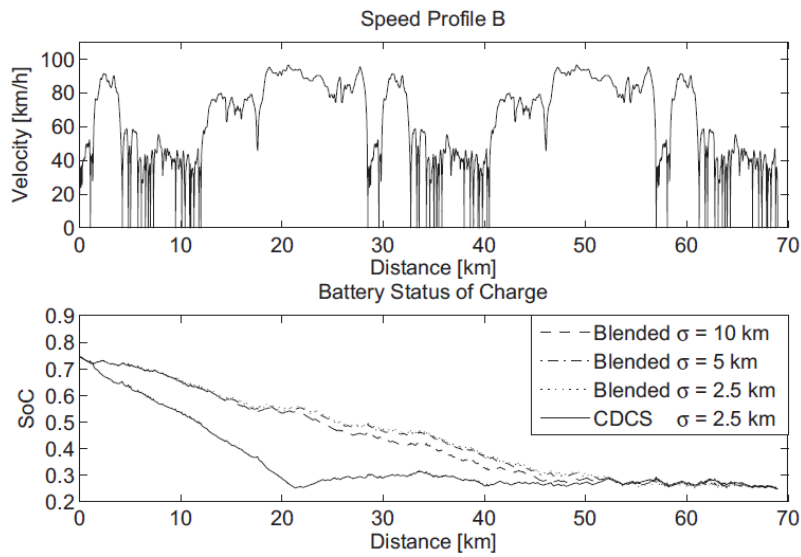


Figure 2.28 - Speed and SOC trajectories for profile B with predicted trip length $\mu = 55 \text{ km}$ (figure from [20])

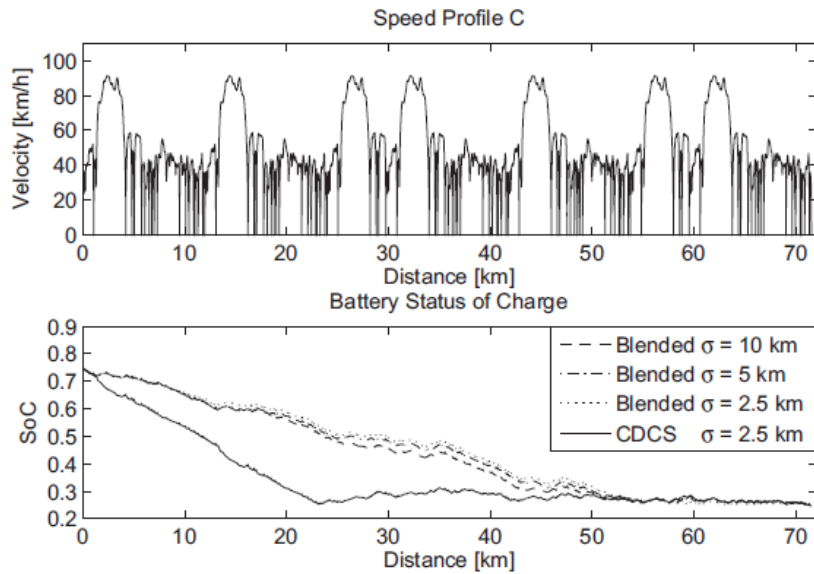


Figure 2.29 - Speed and SOC trajectories for profile C with predicted trip length $\mu = 55 \text{ km}$ (figure from [20])

It's possible to observe that as the standard deviation decreases, the lower SOC limit is reached by the blended trajectory in a position increasingly closer to the predicted trip length. In Table 2.5 and in Table 2.6 the blended mode fuel cost improvements are shown compared to the CD-CS strategy respectively for predicted trip length $\mu = 35 \text{ km}$ and $\mu = 55 \text{ km}$.

Speed Profile	σ [km]	Cost [%] $x = \mu - \sigma$	Cost [%] $x = \mu$	Cost [%] $x = \mu + \sigma$
A	2,5	0,34	1,94	3,15
	5	-3,92	3,46	1,43
	10	-14,9	2,20	1,40
B	2,5	2,05	1,88	2,93
	5	-4,30	-0,09	1,39
	10	-15,9	1,41	1,93
C	2,5	-1	2,25	2,04
	5	-8,17	2,38	2,32
	10	-19,6	-0,34	1,64

Table 2.5 - Blended mode fuel cost improvements compared to the CD-CS strategy for $\mu = 35 \text{ km}$ referred to the distance x (table from [20])

Speed Profile	σ [km]	Cost [%] $x = \mu - \sigma$	Cost [%] $x = \mu$	Cost [%] $x = \mu + \sigma$
A	2,5	1,72	1,24	1,71
	5	0,64	1,77	1,10
	10	-0,17	1,33	1,36
B	2,5	1,41	1,35	1,28
	5	-0,75	1,30	0,94
	10	-0,86	1,79	1,43
C	2,5	1,48	2,63	1,58
	5	-0,44	1,90	1,70
	10	-0,92	2,17	1,67

Table 2.6 - Blended mode fuel cost improvements compared to the CD-CS strategy for $\mu = 55$ km referred to the distance x (table from [20])

In the profile A with predicted trip length $\mu = 35$ km, the cost savings are higher because in profile A the first part is highway with high power demand and disadvantages for the CD-CS strategy. Moreover the savings for $x = \mu$ and $x = \mu + \sigma$ are higher for $\mu = 35$ km than $\mu = 55$ km because significant cost savings of the blended mode are obtained during the corresponding CD phase, so the greatest cost savings occur for distance near to AER or a bit longer. Therefore, a blended mode is advantageous in case of predicted trip length almost exact or underestimated compared to the real trip length.

In conclusion, considering the results of the studies in this paragraph, the blended mode, except in the cases of the type approval driving cycles, proves to be better than the CD-CS strategy in terms of fuel economy.

3 CO₂ emission certification for HEVs

The actual European Union regulation for the hybrid electric vehicles is included in the document Commission Regulation (EU) 2017/1151 of 1 June 2017 (latest consolidated version 25/01/2020) available in [14]. The ANNEX XXI contains the procedure for determining the levels of emissions of gaseous compounds, particulate matter, particle number, CO₂ emissions, fuel consumption, electric energy consumption and electric range from light-duty vehicles. In particular Sub-Annex 8 (Pure electric, hybrid electric and compressed hydrogen fuel cell hybrid vehicles) defines the specific provisions for the hybrid electric vehicles. The reference test for the emission measurements is the Type 1.

The regulation establishes two different procedures for the HEVs and PHEVs which in the EU legislation framework are denominated respectively “not off-vehicle charging hybrid electric vehicle” (NOVC-HEVs) and “off-vehicle charging hybrid electric vehicle” (OVC-HEVs). The battery has also a specific denomination which is “rechargeable electric energy storage system” (REESS).

In addition the CD and CS conditions are defined in [14] as follows:

- Charge-depleting operating condition means an operating condition in which the energy stored in the REESS may fluctuate but decreases on average while the vehicle is driven until transition to charge-sustaining operation;
- Charge-sustaining operating condition means an operating condition in which the energy stored in the REESS may fluctuate but, on average, is maintained at a neutral charging balance level while the vehicle is driven.

To determine in the charge-depleting test when the transition from CD to CS has occurred, the break-off criterion is used. The break-off criterion is reached when the relative electric energy change $REEC_i$ as calculated using equation (3.1), is less than 0,04.

$$REEC_i = \frac{|\Delta E_{REESS,i}|}{E_{cycle} \times \frac{1}{3600}} \quad (3.1)$$

where:

- $REEC_i$ is the relative electric energy change of the applicable test cycle considered i of the charge-depleting test;
- E_{cycle} is the cycle energy demand of the considered applicable WLTP test cycle calculated, Wh;
- i is the index number for the considered applicable WLTP test cycle;
- $\frac{1}{3600}$ is a conversion factor to Wh for the cycle energy demand;
- $\Delta E_{REESS,i}$ is the change of electric energy of all REESSs for the considered charge-depleting Type 1 test cycle i , Wh.

The change of electric energy of all REESSs for the considered charge depleting Type 1 test cycle i is computed with equations (3.2) and (3.3).

$$\Delta E_{REESS,j} = \sum_{j=1}^n \Delta E_{REESS,j,i} \quad (3.2)$$

where:

$\Delta E_{REESS,j,i}$ is the electric energy change of REESS i during the considered period j , Wh;

and

$$\Delta E_{REESS,j,i} = \frac{1}{3600} \times \int_{t_0}^{t_{end}} U(t)_{REESS,j,i} \times I(t)_{j,i} dt \quad (3.3)$$

where:

$U(t)_{REESS,j,i}$ is the voltage of REESS i during the considered period j ;

t_0 is the time at the beginning of the considered period j , s;

t_{end} is the time at the end of the considered period j , s;

$I(t)_{j,i}$ is the electric current of REESS i during the considered period j ;

i is the index number of the considered REESS;

n is the total number of REESS;

j is the index for the considered period, where a period can be any combination of phases or cycles;

$\frac{1}{3600}$ is the conversion factor from Ws to Wh.

The Type 1 test shall consist of vehicle operation on a chassis dynamometer on the Class 3 WLTC, shown in Figure 3.1.

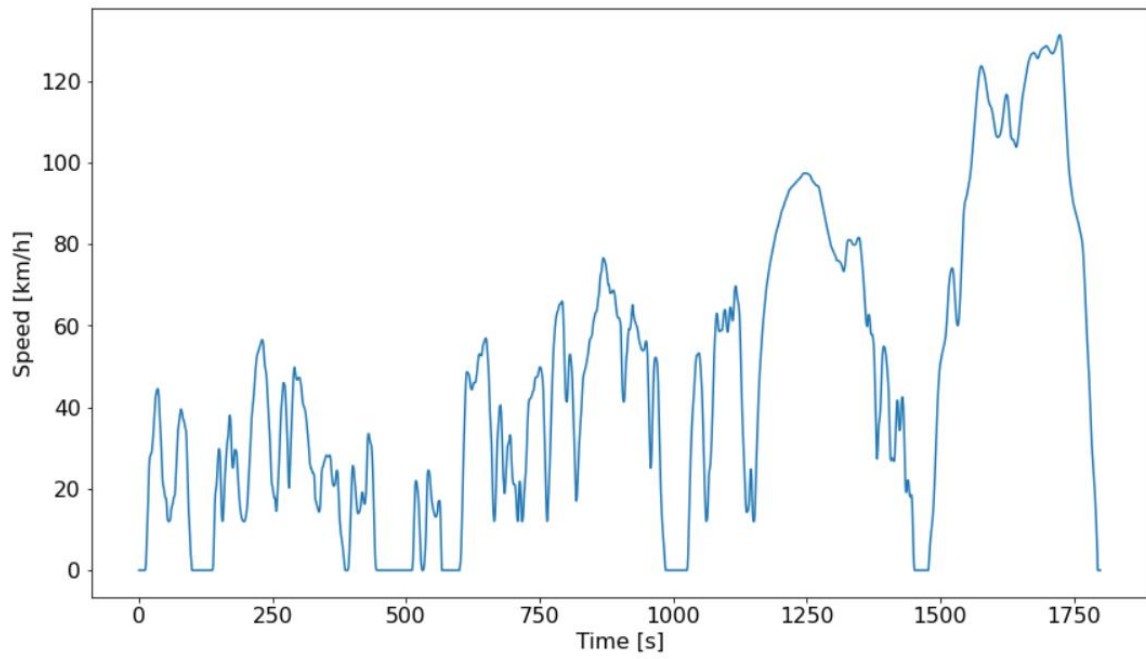


Figure 3.1 - Class 3 WLTC

In paragraph 3.1, the procedures for the NOVC-HEVs are reported and in paragraph 3.2 the OVC-HEVs ones.

3.1 NOVC-HEVs

As described in [14], a not off-vehicle charging hybrid electric vehicle (NOVC-HEVs) means a hybrid electric vehicle that cannot be charged from an external source.

Namely the NOVC-HEV are the vehicles usually simply called hybrid electric vehicles (HEVs).

3.1.1 Test procedure for NOVC-HEVs

For the NOVC-HEVs the test procedure is represented in Figure 3.2.

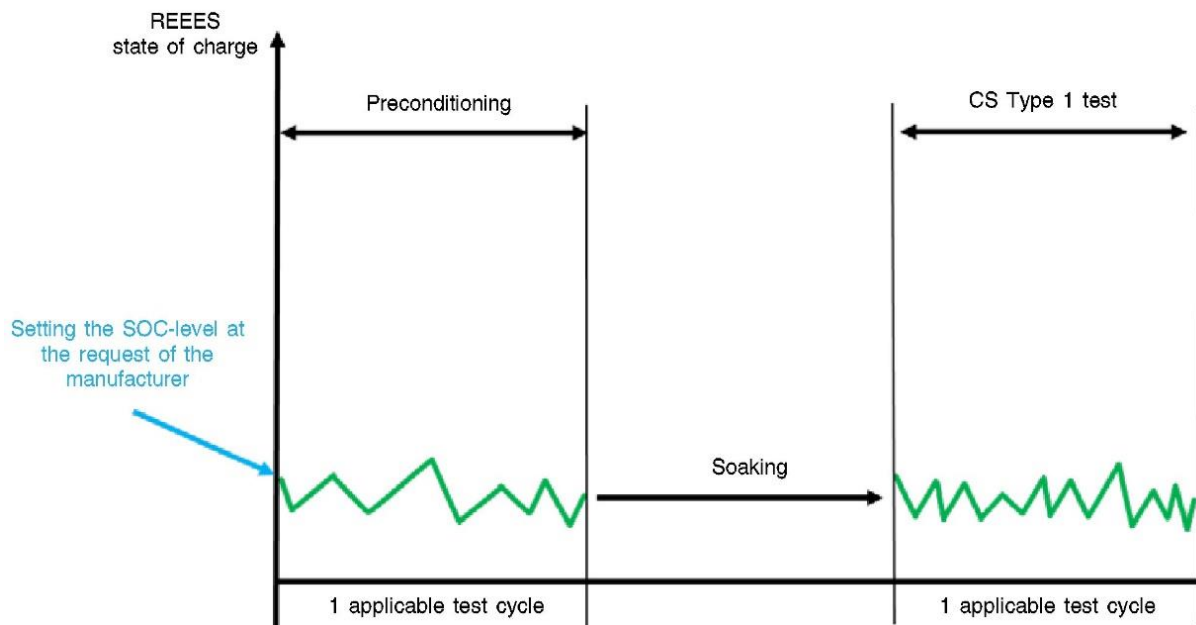


Figure 3.2 - NOVC-HEVs charge-sustaining Type 1 test (figure from [14])

The tests shall consist of vehicle operation on a chassis dynamometer which can present different configurations as Figure 3.3 shows. The test vehicle shall be placed on the dynamometer and operated through the applicable WLTCs.

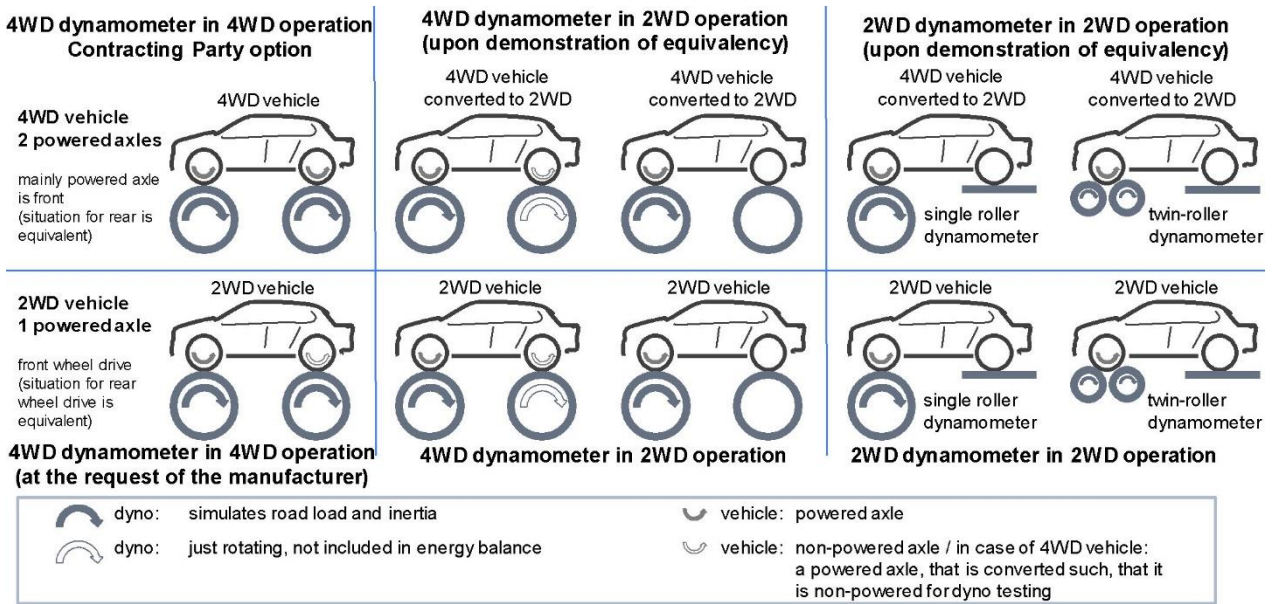


Figure 3.3 - Selection of a driver-selectable mode for OVC-HEVs, NOVC-HEVs and NOVC- FCHVs under charge-sustaining operating condition (figure from [14])

The preconditioning consists in driving the applicable WLTC. After preconditioning and before testing, the test vehicle shall be kept in an area with ambient conditions defined as temperature set point of 23 °C with the tolerance of the actual value within ± 3 °C. The vehicle shall be soaked for a minimum of 6 hours and a maximum of 36 hours.

The Type 1 test shall be conducted under charge-sustaining operating condition and, for vehicles equipped with a driver-selectable mode, the mode for the charge-sustaining test shall be selected according to Figure 3.4.

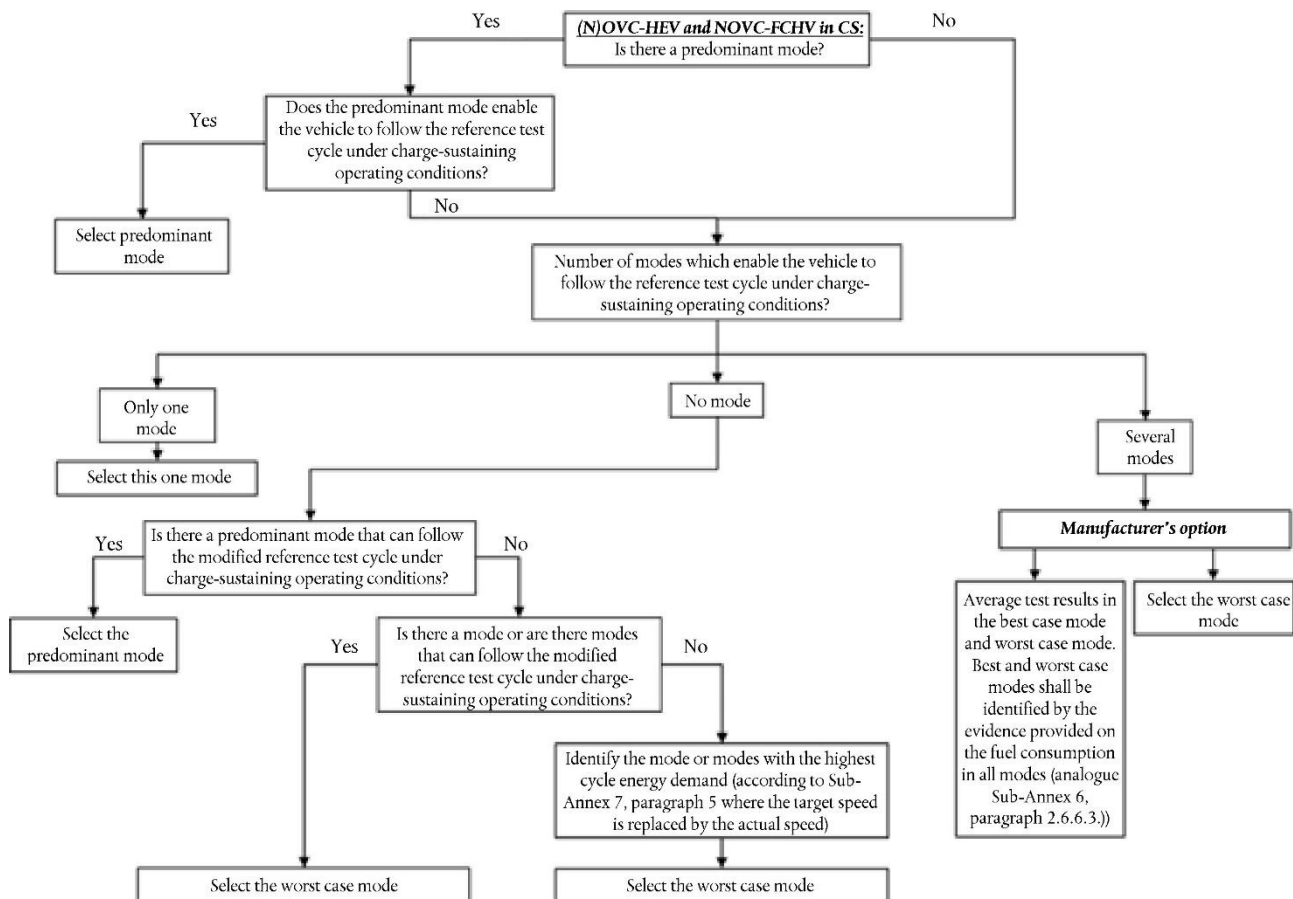


Figure 3.4 - Selection of a driver-selectable mode for OVC-HEVs, NOVC-HEVs and NOVC- FCHVs under charge-sustaining operating condition (figure from [14])

For the Type 1 test, the vehicle shall be pushed onto a dynamometer, the drive wheels of the vehicle shall be placed on the dynamometer without starting the engine, the engine compartment cover shall be closed and an exhaust connecting tube shall be attached to the vehicle tailpipe(s) immediately before starting the engine. The powertrain start procedure shall be initiated by means of the devices provided for this purpose in accordance with the manufacturer's instructions.

The vehicle shall be driven over the applicable WLTC and, if required, CO₂ mass emission shall be corrected as described in paragraph 3.1.2.

3.1.2 Charge sustaining CO₂ correction

The correction of the charge-sustaining Type 1 test CO₂ mass emission, implemented using the CO₂ mass emission correction coefficient K_{CO_2} , shall be applied if $\Delta E_{REESS,CS}$ is negative which corresponds to REESS discharging and the correction criterion c is greater than the applicable threshold in accordance with Table 3.1.

Applicable Type 1 test cycle	Low + Medium	Low + Medium + High	Low + Medium + High + Extra High
Thresholds for correction criterion c	0,015	0,01	0,005

Table 3.1 - RCB correction criteria thresholds (table from [14])

The correction criterion c is the ratio between the absolute value of the REESS electric energy change $\Delta E_{REESS,CS}$ and the fuel energy and shall be calculated as represented in equation (3.4).

$$c = \frac{|\Delta E_{REESS,CS}|}{E_{fuel,CS}} \quad (3.4)$$

where:

$\Delta E_{REESS,CS}$ is the charge-sustaining REESS energy change, Wh;

$E_{fuel,CS}$ is the charge-sustaining energy content of the consumed fuel, Wh.

The CS energy content of the consumed fuel shall be calculated using equation (3.5):

$$E_{fuels,CS} = 10 \times HV \times FC_{CS,nb} \times d_{CS} \quad (3.5)$$

where:

$E_{fuels,CS}$ is the charge-sustaining energy content of the consumed fuel of the applicable WLTP test cycle of the charge-sustaining Type 1 test, Wh;

HV is the heating value, kWh/l;

$FC_{CS,nb}$ is the non-balanced charge-sustaining fuel consumption of the charge-sustaining Type 1 test, not corrected for the energy balance, l/100 km;

d_{CS} is the distance driven over the corresponding applicable WLTP test cycle, km;

10 conversion factor to Wh.

In the case that the correction was not applied, the charge-sustaining CO₂ mass emission is directly the one measured during the charge-sustaining Type 1 test as equation (3.6) shows.

$$M_{CO_2,CS} = M_{CO_2,CS,nb} \quad (3.6)$$

where:

- $M_{CO_2,CS}$ is the charge-sustaining CO₂ mass emission of the CS Type 1 test, g/km;
- $M_{CO_2,CS,nb}$ is the non-balanced charge-sustaining CO₂ mass emission of the charge-sustaining Type 1 test, not corrected for the energy balance, determined, g/km.

If the correction of the charge-sustaining CO₂ mass emission is required, the CO₂ mass emission correction coefficient K_{CO_2} shall be determined and the corrected charge-sustaining CO₂ mass emission shall be computed using equation (3.7). In Appendix A it's possible to find the calculus procedure for K_{CO_2} .

$$M_{CO_2,CS} = M_{CO_2,CS,nb} - K_{CO_2} \times EC_{DC,CS} \quad (3.7)$$

where:

- $M_{CO_2,CS}$ is the charge-sustaining CO₂ mass emission of the CS Type 1 test, g/km;
- $M_{CO_2,CS,nb}$ is the non-balanced CO₂ mass emission of the charge-sustaining Type 1 test, not corrected for the energy balance, determined, g/km;
- K_{CO_2} is the CO₂ mass emission correction coefficient, (g/km)/(Wh/km);
- $EC_{DC,CS}$ is the electric energy consumption of the charge-sustaining, Wh/km.

It's possible to notice that the part of electric energy $EC_{DC,CS}$ that at the end of the driving cycle has contributed to the power demand, so that has a negative sign, is considered and converted in an equivalent CO₂ mass with the CO₂ mass emission correction coefficient K_{CO_2} . Thus this contribute is summed to the non-balanced CO₂ mass emission $M_{CO_2,CS,nb}$ to obtain the actual CO₂ mass emission $M_{CO_2,CS}$. In this way the possible fuel economy caused by the usage of some electric energy from the battery is taken into account.

3.2 OVC-HEVs

As described in [14], an off-vehicle charging hybrid electric vehicle (OVC-HEVs) means a hybrid electric vehicle that can be charged from an external source.

Namely the OVC-HEV are the vehicles usually called as plug-in hybrid electric vehicles (PHEVs).

3.2.1 Test procedure for OVC-HEVs and CO₂ correction

For the OVC-HEVs the test procedure is outlined in Figure 3.5 and Figure 3.6. Vehicles shall be tested under charge-depleting (CD) operating condition, and charge-sustaining (CS) operating condition. The tests shall consist of vehicle operation on a chassis dynamometer as happens for the NOVC-HEVs.

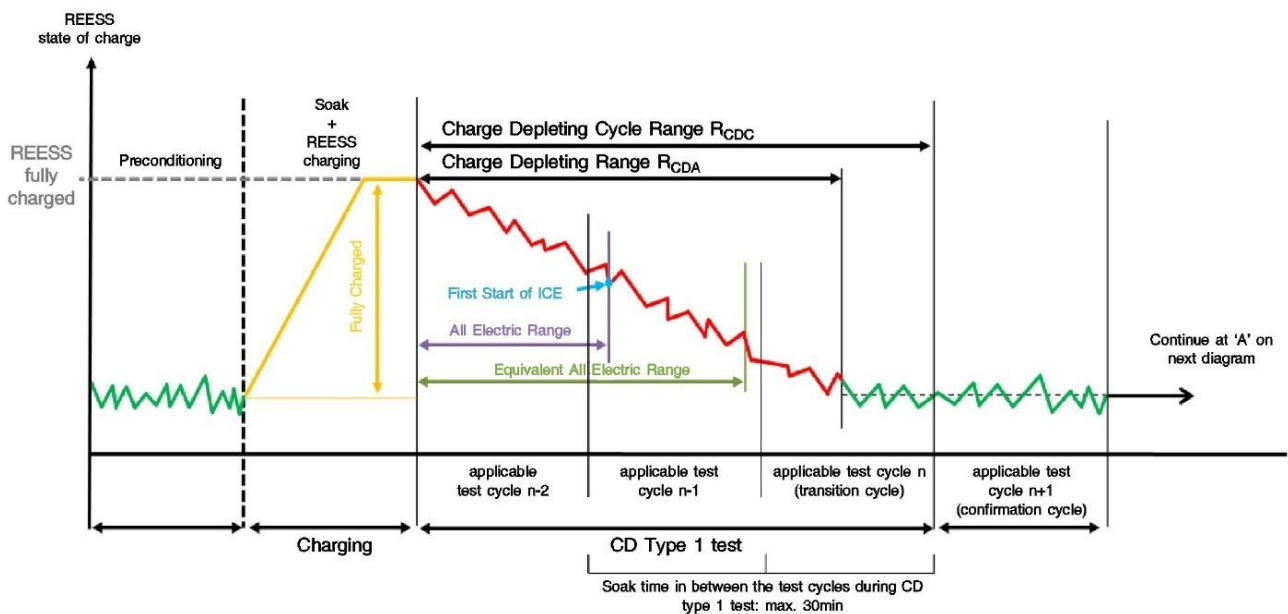


Figure 3.5 - Charge-depleting type 1 test for OVC-HEV (figure from [14])

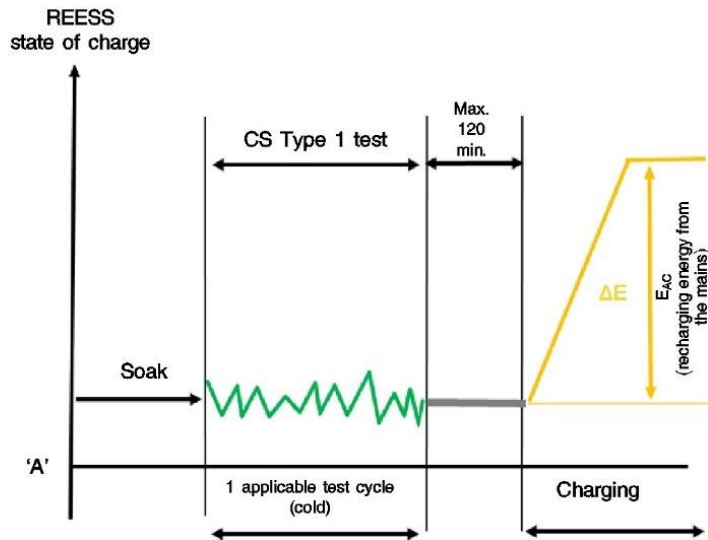


Figure 3.6 - Subsequent charge-sustaining Type 1 test for OVC-HEV (figure from [14])

At the beginning there is the preconditioning phase where the OVC-HEV shall be driven over at least one applicable WLTP test cycle. During each driven preconditioning cycle, the charging balance of the REESS shall be determined. The preconditioning shall be stopped at the end of the applicable WLTP test cycle during which the break-off criterion, described at the beginning of chapter 3, is fulfilled.

After, there is the soaking of the test vehicle: it shall be kept, for a minimum of 6 hours and a maximum of 36 hours, in an area with ambient conditions defined as temperature set point of 23 °C with the tolerance of the actual value within ± 3 °C. During soak, the REESS shall be charged using the normal charging procedure.

Then the Type 1 CD test is conducted with a fully charged REESS and with the vehicle operated in charge-depleting operating condition. For vehicles equipped with a driver-selectable mode, the mode for the charge-depleting test shall be selected as illustrated in Figure 3.7.

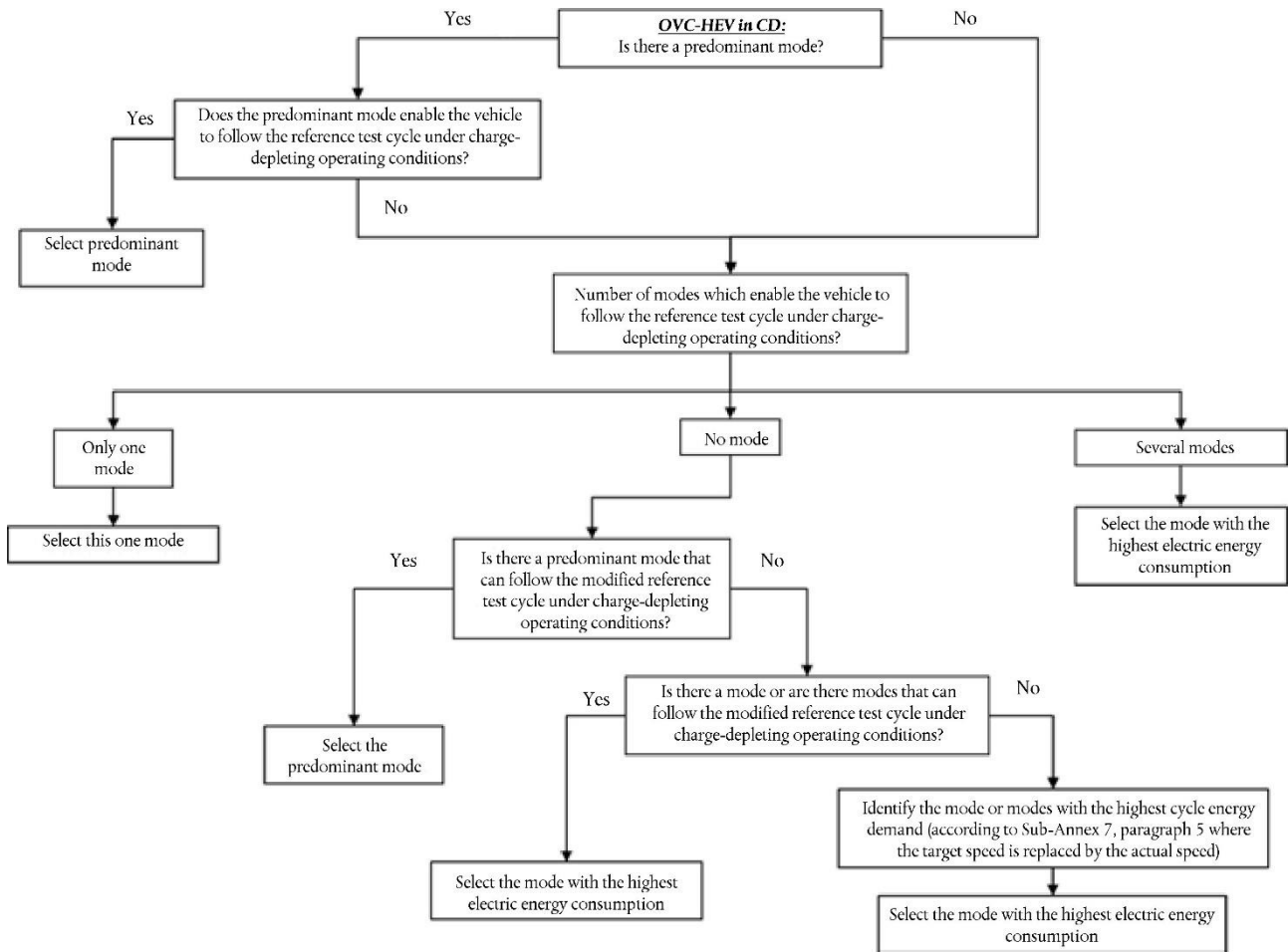


Figure 3.7 - Selection of driver-selectable mode for OVC-HEVs under charge-depleting operating condition (figure from [14])

The charge-depleting Type 1 test procedure shall consist of a number of consecutive cycles, each followed by a soak period of no more than 30 minutes until charge-sustaining operating condition is achieved. During soaking between individual applicable test cycles, the powertrain shall be deactivated and the REESS shall not be recharged from an external electric energy source. The end of the charge-depleting Type 1 test is considered to have been reached when the break-off criterion is reached for the first time. The number of applicable WLTP test cycles up to and including the one where the break-off criterion was reached for the first time is set to $n+1$. The applicable WLTP test cycle n is defined as the transition cycle, the applicable WLTP test cycle $n+1$ is defined to be the confirmation cycle.

Subsequently, there is the charge-sustaining Type 1 test that shall be carried out with the vehicle operated in charge-sustaining operating condition. This test procedure is the same used for the Type 1 test for NOVC-HEVs described in paragraph 3.1.1. If required, CO₂ mass emission shall be corrected. The correction of the CO₂ mass emission is implemented using the CO₂ mass emission correction coefficient K_{CO_2} as it happens in paragraph 3.1.2 for NOVC-HEVs.

After the conclusion of the charge-sustaining test, the vehicle shall be connected to the mains within 120 minutes. The REESS is fully charged when the end-of-charge criterion is reached, namely when the on-board or external instruments indicate that the REESS is fully charged. The energy measurement equipment, placed between the vehicle charger and the mains, shall measure the recharged electric energy E_{AC} delivered from the mains, as well as its duration. Electric energy measurement may be stopped when the end-of-charge criterion is reached.

3.2.2 Utility factor-weighted CO₂ emissions

After the Type 1 tests, there are two values of CO₂ mass emission: the one referred to the CD test and the one referred to the CS test. To obtain a unique value, a weighted sum is implemented, using a utility factor UF_j for each phase j along the WLTP cycles carried out during the CD test.

The utility factors curve is based on driving statistics, described in SAE J2841 [21], and represents essentially the cumulated probability of the average distance normally travelled by the users. In this way, the CO₂ emissions along the WLTP cycles can be weighted based on the phase where they are emitted and so considering the distance travelled in electric driving from the beginning of the test.

For the calculation of a fractional utility factor UF_j for the weighting of period j , the eq. (3.8) shall be applied by using the coefficients from Table 3.2.

$$UF_j(d_j) = 1 - e^{-\left(\sum_{i=1}^k C_i \times \left(\frac{d_j}{d_n}\right)^i\right)} - \sum_{l=1}^{j-1} UF_l \quad (3.8)$$

where:

UF_j	utility factor for period j ;
d_j	measured distance driven at the end of period j , km;
C_i	i^{th} coefficient;
d_n	normalized distance;
k	number of terms and coefficients in the exponent;
j	number of period considered;
i	number of considered term/coefficient;
$\sum_{l=1}^{j-1} UF_l$	sum of calculated utility factors up to period $(j - 1)$.

Parameter	Value
d_n	800 km
C1	26,25
C2	-38,94
C3	-631,05
C4	5964,83
C5	-25095
C6	60380,2
C7	-87517
C8	75513,8
C9	-35749
C10	7154,94

Table 3.2 - Parameters for the determination of fractional utility factors (values from [14])

The utility factor-weighted mass emission of gaseous compounds shall be calculated using the following equation (3.9):

$$M_{CO_2,weighted} = \sum_{j=1}^k (UF_j \times M_{CO_2,CD,j}) + \left(1 - \sum_{j=1}^k UF_j \right) \times M_{CO_2,CS} \quad (3.9)$$

where:

- $M_{CO_2,weighted}$ is the utility factor-weighted CO₂ mass emission, g/km;
- UF_j is the utility factor of phase j ;
- $M_{CO_2,CD,j}$ the CO₂ mass emission of determined of phase j of the charge-depleting Type 1 test, g/km;
- $M_{CO_2,CS}$ the CO₂ charge-sustaining mass emission for the charge-sustaining Type 1 test, g/km;
- j is the index number of the phase considered;
- k is the number of phases driven until the end of the transition cycle.

As it's possible to read in [22], the UF curve for Europe is valid from 0 to 800 km, at the latter distance the UF converges to 1. With increasing electric range, CD phase-CO₂ emissions contribute less to $M_{CO_2,CD}$ and their phase-UFs decrease with increasing the number of WLTP tests in CD mode.

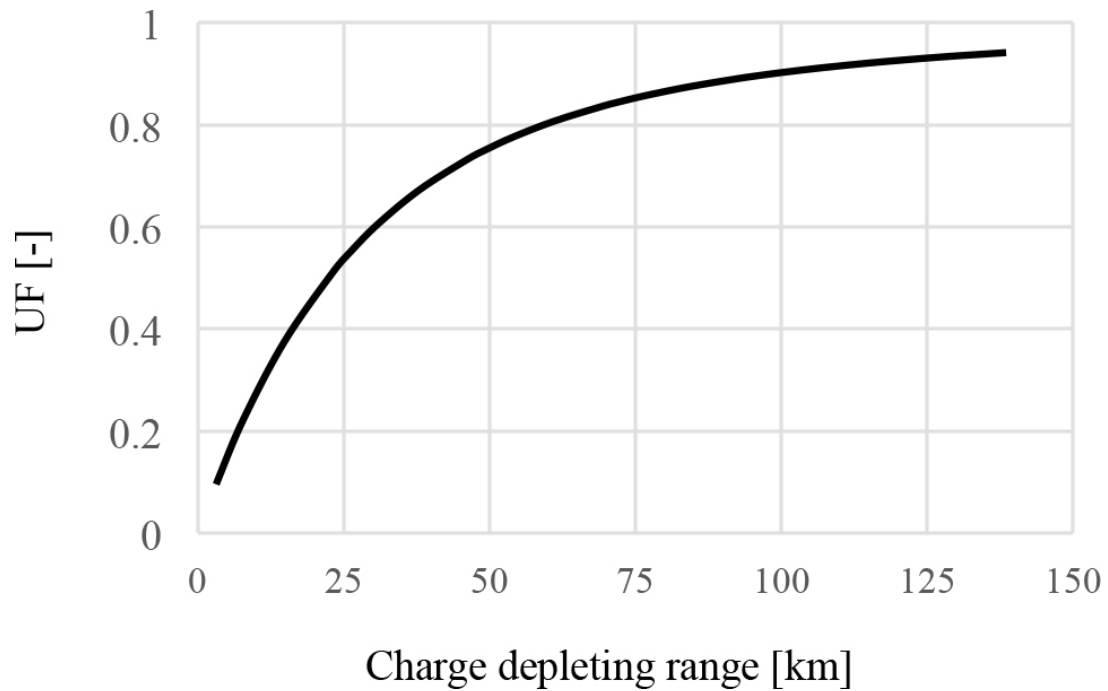


Figure 3.8 - WLTP Utility Factor curve (figure from [22])

Looking to the UF curve in Figure 3.8, it's possible to notice that, in particular for ranges up to around 50 km, the utility factors have a considerable weight on the CO₂ emitted in the initial CD phases of the WLTCs. When the curve tends to flatten in the window between around 50 and 100 km, the utility factor has an increasingly lower contribute.

3.3 Real-world CO₂ emissions in PHEVs

A first comparison between the WLTP and NEDC procedures for what concerns the determination of fuel consumption, CO₂ emissions and electric ranges of two Plug-in Hybrid electric Vehicles is presented in [22] in a context where only a few studies about PHEVs had evaluated the influence of the WLTP introduction. The two PHEVs involved in [22] were tested in the vehicle emissions laboratories (VELA) of the Joint Research Centre (JRC). The results showed that CO₂ emissions and fuel consumption for PHEVs under the WLTP could be higher or lower than the corresponding NEDC values. Besides the regulation procedures, the way the users make use of PHEVs was another factor that could be considered to a better assessment of the CO₂ emissions.

In a subsequent study [23], tests on four Euro 6 PHEVs and related CO₂ emissions and energy consumption were conducted, both in the JRC’s laboratories and on the road. A normalized CO₂ model was extrapolated and was used to calculate some real-world CO₂ values weighted on the milage driven daily and the probability distribution of average trip speed. Two measured dataset were used: one from JRC measurements carried out in the area of northern Italy and one in France from Geco air database. This trends are shown in Figure 3.9 together with the “trip electric-share” concept, abbreviated with “*e – share*” (3.10), a simple CD and CS emission weighting approach presented in [23] that presents two inputs: the Trip Distance (*TD*) and the Expected Electric Range (*EER*).

$$e - share = \min \left(1, \frac{EER}{TD} \right) \quad (3.10)$$

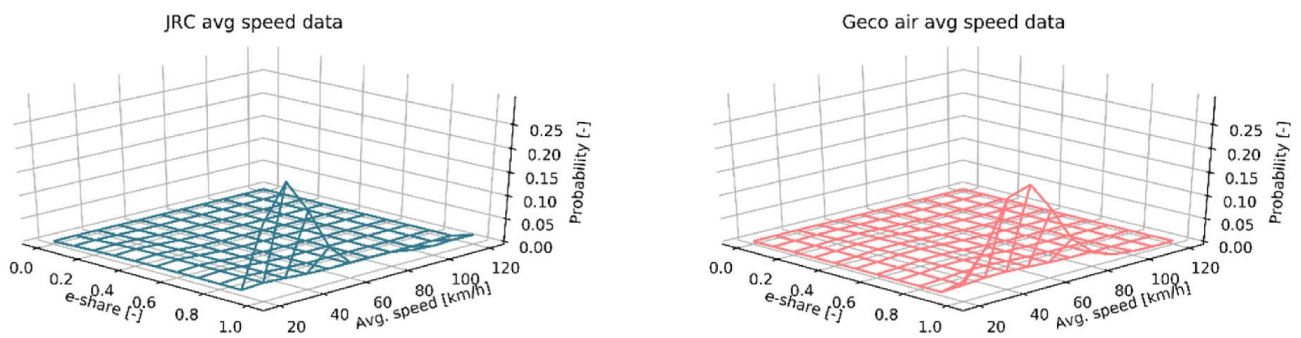


Figure 3.9 - Combined probability distribution used for obtaining the CO₂ emissions under realistic use patterns (on the left the JRC average speed distribution, on the right Geco air average speed distribution (figure from [23])

The resulting distributions in Figure 3.9 appear flat in a wide part of the domain, while exhibit a sharp increase for *e – share* values close to 1 and for average trip speeds between 20 and 60 km/h. Using these probability distributions, the real-world-weighted CO₂ values were calculated. To

consider the charging behaviour of the user, the results are supplied for different levels of initial battery SOC: 100% 90%, 80% and 50%. Results are displayed in Table 3.3, it's possible to notice that, when assuming that the battery is recharged to 100%, the real-world CO₂ emissions gap from the official type approval (TA) values is significant. It worsen for lower values of initial SOC and presents the worst values for the 50% value.

Initial SOC	Average speed distribution	Gap
100%	JRC	+47,3%
	Geco air	+60,7%
90%	JRC	+54,2%
	Geco air	+66,6%
80%	JRC	+61,2%
	Geco air	+72,6%
50%	JRC	+89,4%
	Geco air	+96,8%

Table 3.3 - Results of the CO₂ gap between real-world operation and TA values (values from [23])

Thus it appears realistic that PHEVs real-world CO₂ emissions, compared to the TA ones, are within 150% for initial SOC = 100% and within 200% for initial SOC = 50%. Considering the other analyses in [23], results show that in CS mode the emission stay within a range of 200-600% compared to the TA values. In addition the model demonstrates that the certification values remain representative at low-medium average trip speeds and high initial SOC, whereas the results get worse for high average trip speeds and low battery charge conditions.

4 Case study

The case study of this thesis regards the analysis of data coming from one part of the experimental driving campaign illustrated in [24], where a real-world usage comparison is carried out using two vehicles which present similar characteristics to minimise vehicle-type influence, but with two different traction systems: an ICE conventional vehicle and a PHEV. In particular this thesis deals with the analysis of the data coming from the PHEV.

4.1 Tested vehicle

As it's possible to observe in [24] and [25], the tested vehicle is a 5 doors, C-Segment, parallel P2 PHEV, considered representative of the European market. The technical specifications are summarised in Table 4.1.

Vehicle type	C-Segment, 5 seats
Powertrain	Gasoline PHEV
WLTP test mass [kg]	1698
Engine displacement [cm ³]	1395
Engine power [kW]	110
Electric motor power [kW]	80
Combined power [kW]	150
Equivalent all electric range [km]	70
WLTP fuel consumption [l/100 km]	0,9
F0 [N]	115,5
F1 [N/km/h]	0,106
F2 [N/(km/h) ²]	0,03217
Wheel diameter [mm]	619,262

Table 4.1 - PHEV main specifications

The PHEV have different traction modes which the user can select from the dashboard: Hybrid, Charging level reserve and E-mode. In the Hybrid mode the internal combustion engine and the electric motor interact optimally, thanks also to the information about the journey to cover, coming from the navigation data. In the Charging level reserve mode the selected battery level of charge is reserved up to the end of the trip, namely in this mode the level of battery charge up to which the vehicle can use battery energy is established. In the E-mode the vehicle is propelled by electric energy only, this mode is automatically deactivated when the electric motor cannot supply the power requested or when the battery is low. Thus it's possible to note that the Hybrid and the E-mode selections correspond respectively to the blended and the CD-CS strategies.

4.2 Experimental campaign

In [24] and [25] it's possible to observe that a tailored data-logging system was prepared and mounted on the PHEV relying on availability of signals from the vehicle On-board Diagnostic (OBD) for standardised parameters and Unified Diagnostic Services (UDS) for vehicle-specific parameters. These systems were permanently installed on the vehicle for the whole duration of the activity and all the signals were collected and stored with a sampling frequency of approximately 1 Hz.

The experimental driving campaign has involved a representative sample of 6 users on a voluntary basis and with a rental time of 22 days. The users were selected such they would drive on a mix of urban (vehicle speed below 60 km/h), rural (vehicle speed between 60 and 90 km/h) and motorway (vehicle speed above 90 km/h) driving conditions, however lots of the trips took place in the surroundings of the European Commission's Joint Research Centre (JRC) site in Ispra (Italy), where rural conditions are prevalent, because the users were all affiliated to the JRC. The users were requested to maintain the same driving behaviour as in their normal life in order to guarantee a real-world representativeness of the measurements; in particular the refuelling and the recharging costs were at their expense.

The campaign took up a long period of time in order to capture the variability regarding weather conditions. Further tests in the laboratory were included to ascertain vehicle performance in standard conditions.

During the trips, around 50 parameters were logged, this data enables to capture the operating conditions in real-world operation, for example vehicle speed, battery state of charge, ICE rotational speed, instantaneous fuel consumption. These data were then transfer in the computer as a spreadsheet.

5 Data Analysis

The data analysis was conducted using Python. The trips data were saved in Excel files, one file for each trip, as time series with a resolution of half a second. Some of the main data logged are summarised in Table 5.1.

LOGGED PARAMETER	UNIT OF MEASUREMENT
Battery current	A
Fuel consumption	l/h g/s
EM rotational speed	rpm
EM torque	Nm
SOC	%
Gear selected	-
ICE rotational speed	rpm
ICE torque	Nm
Vehicle speed	km/h
GPS altitude	m
Internal and external temperatures	°C

Table 5.1 - Some of the main data logged along the real-world trips

First of all, the Excel file with raw data had to be processed due to some events that sometimes occurred in the data logging. This processing procedure was conducted by the Joint Research Centre (JRC) staff.

In particular the initial part of the trip could sometimes present a data logging when the vehicle was stationary before the journey, so with vehicle speed and EM voltage (that includes also the inverter) equal to zero. This part was cut off in order to succeed in a better comparison among the trips.

A similar problem sometimes occurred when, at the end of the trip, the PHEV was connected to the grid for the battery recharging. In this case the data logging system continued to register data, with vehicle speed equal to zero and EM voltage different from zero, for a notable period of time where the SOC signal firstly increased because of the recharging process and then remained at a constant value. Also this part had to be cut off for the same reasons of the previous case.

Another issue came up when the PHEV was parked for a quite short period of time, in fact in these cases the system didn't stop to log and therefore, when the vehicle was moved again, the data continued to be recorded. So a unique file with actually two different trips was obtained. To solve this situation, the Excel files with this feature were divided in two different files obtaining two separate trips.

In addition, a first classification of the trips was implemented in order to identify the days when the blended mode was used at least one time. To do this, the last CD time instant and the first CS instant were compared. The condition to identify the CD phase were $SOC > 25\%$ and $FC = 0$ while the condition to identify the CS phase was $SOC < 25\%$. If the two transitions moment were much distant in terms of time, the trip analysed was classified as blended, considering the presence of a long central phase with $SOC > 25\%$ and $FC \neq 0$ and potentially a first short phase in CD and a final one in CS.

With all this processing procedure, data could be correctly elaborated and compared.

5.1 Real-world trips categorization

At the beginning of the Python script used for the data analysis, after importing the libraries needed, the Excel files were loaded in the program. The files were processed as Pandas DataFrames and some other parameters were computed adding new time series in each file: distance, distance travelled in only electric driving, fuel consumption and electric energy consumed. An example of a Python script part is presented in Appendix B.

Then the plots in function of time of the vehicle speed, engine speed and SOC were generated for each trip with an user keyboard input, in this way it was possible to manually categorised them looking at the referred plots.

Later a new dictionary was created to contain some aggregated results that were calculated for each trip: total distance, total distance travelled in only electric driving, initial SOC, final SOC, average speed, total fuel consumed, total electric energy consumed and average temperature. In addition, the category previously assigned, was added in this dictionary for each trip. In particular six types of classification were considered:

A: Blended trips;

B: Blended trips with “not low” final SOC;

C: CD-CS trips;

D: CS only trips or increasing SOC;

E: All electric driving trips (or almost all electric);

F: short trips/others

After, analogously to the previous situation, a dictionary to include the only blended trips was created as well as the aggregated results one.

In the following part, other values related to power, energy and longitudinal dynamic were calculated and added as time series in the only blended trips. In particular these parameters were: acceleration, altitude, alpha (road slope angle), wheels rotational speed, power to the wheels, torque to the wheels, energy to the wheels, battery power, ICE torque, ICE power, ICE energy, EM power, EM torque, powertrain status. The latter parameter was defined using a function with the following possible returns: e-assist, load point moving (LPM), regenerative braking ICE ON (RB ICE ON), regenerative braking ICE OFF (RB ICE OFF), transition, EM only and none of the previous.

The power to the wheels P_w expressed in kW was computed with the formula (5.1):

$$P_w = (F_0 \cos \alpha + F_1 v + F_2 v^2 + 1,03 m a + m g \sin \alpha) \frac{v}{3600} \quad (5.1)$$

with v vehicle speed in km/h, α road slope angle, m vehicle mass in kg, a vehicle acceleration in m/s^2 , g gravitational acceleration, F_0, F_1, F_2 coast down coefficients.

5.2 Comparison between blended trips and CD-CS trips

Among all the real-world trips, the ones which used the charge depleting and charge sustaining (CD-CS) strategy and which were similar to the blended trips, were selected. To do this selection, a JRC's program was used to identify CD-CS trips that presented, compared to blended ones, similar or higher total distance and similar initial SOC and average speed. In total it was possible to choose 10 CD-CS trips. Among the latter, the ones with higher total distance respect to the blended reference trip were cut in the final CS part to obtain a distance similar to the blended one. In this way it was possible to avoid a higher fuel consumption in the comparison due to the exceeding CS part in terms of distance.

These elaborated CD-CS trips were processed with the same procedure carried out for the blended trips in order to go forward with a comparison and analysis.

Different aspect, analysed in the following paragraphs, emerged.

5.2.1 ICE switching ON

First of all, the operating points where the internal combustion engine started, called "switching ON points", were considered.

The switching ON points, were selected and plotted without maintaining the separation among single trips. It was possible to highlight some dependency on the engine control on these conditions. In Figure 5.1 the switching ON points were plotted in the function of vehicle speed and acceleration. In a similar way as in [15] happens, it's possible to glimpse a tendency similar to a hyperbola branch. The more the vehicle acceleration is higher, the more the vehicle speed is lower, namely the ICE is started only when necessary. In addition a sort of lower limit on the vehicle speed is visible around a speed slightly less than 20 km/h and indicates that generally the ICE isn't switched ON below this speed threshold.

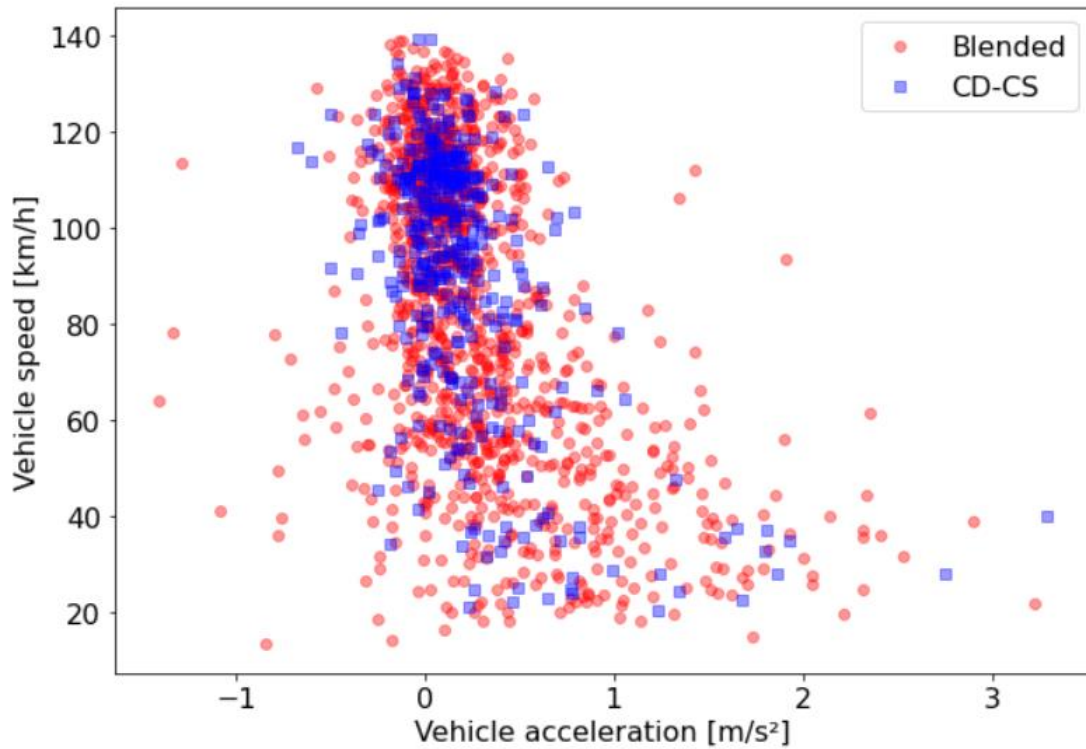


Figure 5.1 - ICE switching ON points in the function of vehicle speed and acceleration

Then it's possible to notice that for the CD-CS strategy, the points are mostly located in the higher speed zone, on the other hand the blended strategy points seem position themselves in a way that covers more the vehicle speeds interval. To avoid wrong considerations caused by the superimposition of the CD-CS points on the blended ones, a more detailed approach, visible in Figure 5.2, was used: two violin plots were added to the sides of the analysed plot.

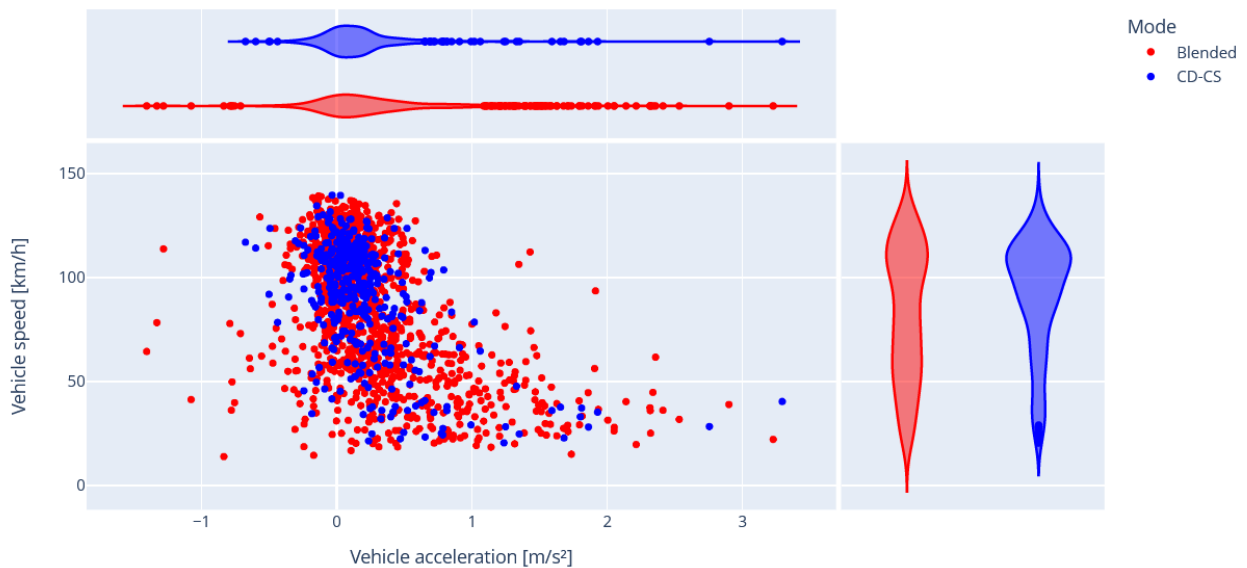


Figure 5.2 - ICE switching ON points in the function of vehicle speed and acceleration with the violin plots addition

As described in [26], the violin plots permit to observe variations in the dataset showing the distribution peaks. On each side of the central axis, there is a kernel density estimation that illustrate the distribution shape of the data. The wider sections of the violin plot represent a higher probability that the point places on the given value, the skinnier sections correspond to a lower probability.

In Figure 5.2 it's possible to note that the blended points actually present a location more distributed along the vehicle speeds range than the CD-CS points which are more aggregate in the higher speeds region. That confirms the last consideration regarding Figure 5.1.

In Figure 5.3 the switching ON tendency is plotted also in the function of vehicle speed and torque to the wheels, called "wheels torque" obtaining a diagram similar to the Figure 5.1 one. It's possible to deduce that in case of lower torques, the ICE starts at greater vehicle speeds, so in these cases, the internal combustion engine switching ON is preferred already at low torques to help the electric motor operation.

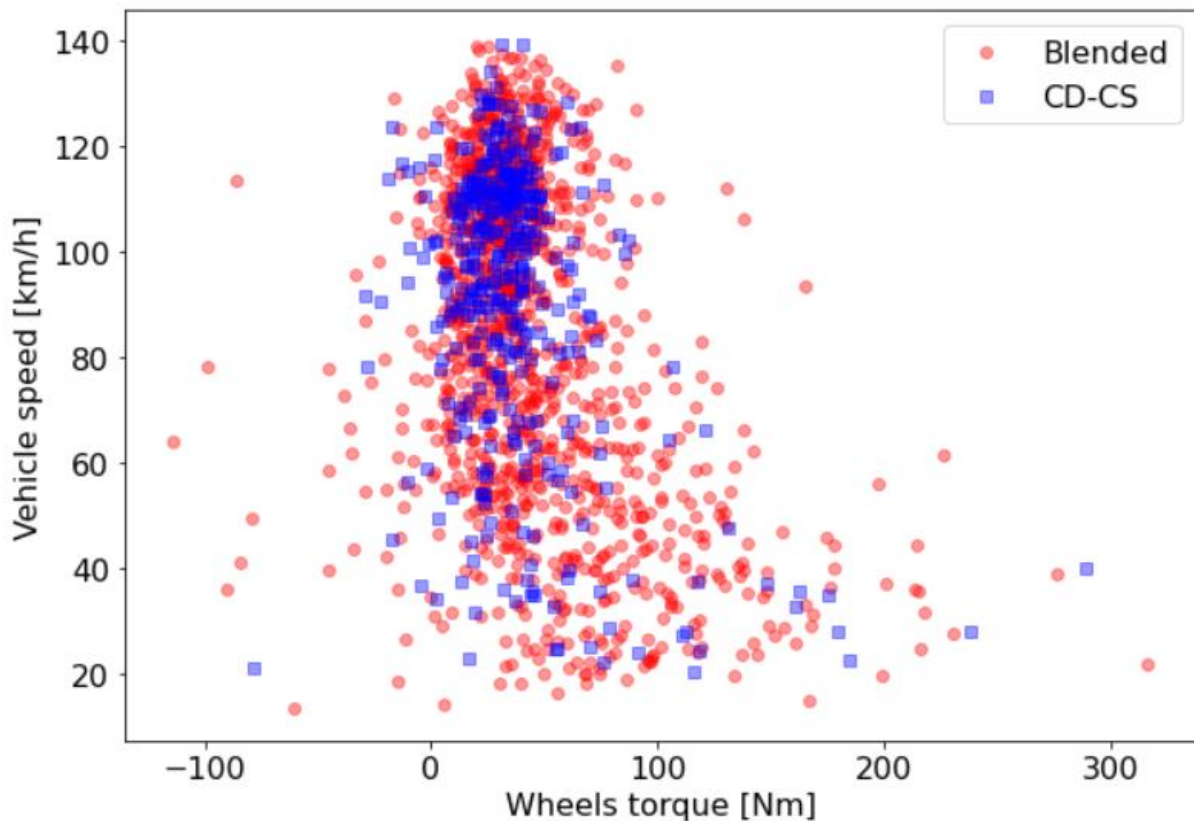


Figure 5.3 - ICE switching ON points in the function of vehicle speed and wheels torque

An analogous difference in distribution between blended and CD-CS plots, as noted in Figure 5.1, is discerned in Figure 5.3. This tendency is confirmed by the violin plots referred to the vehicle speeds visible in Figure 5.4.

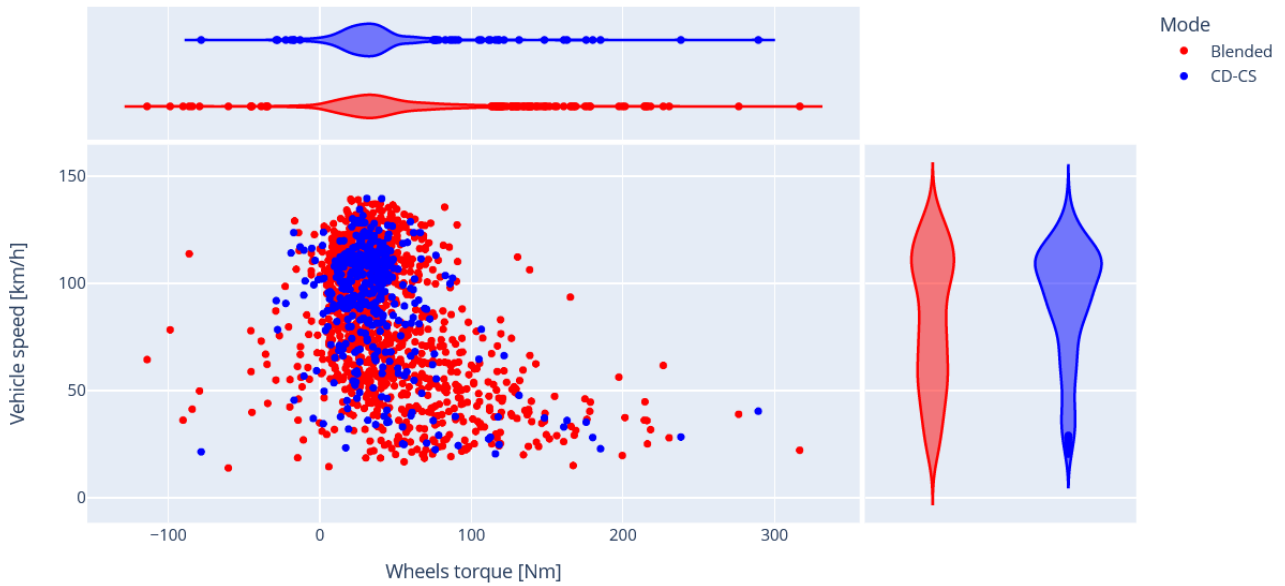


Figure 5.4 - ICE switching ON points in the function of vehicle speed and wheels torque with violin plots

Others significant tendencies can be perceived in the switching ON points diagram in the function of vehicle acceleration and power to the wheels, called “wheels power” and illustrated in Figure 5.5. For the blended points it’s possible to notice a tendency that presents multiple slopes and a wider positioning as far as the vehicle acceleration is concerned, better represented in Figure 5.6 where the violin plots are added.

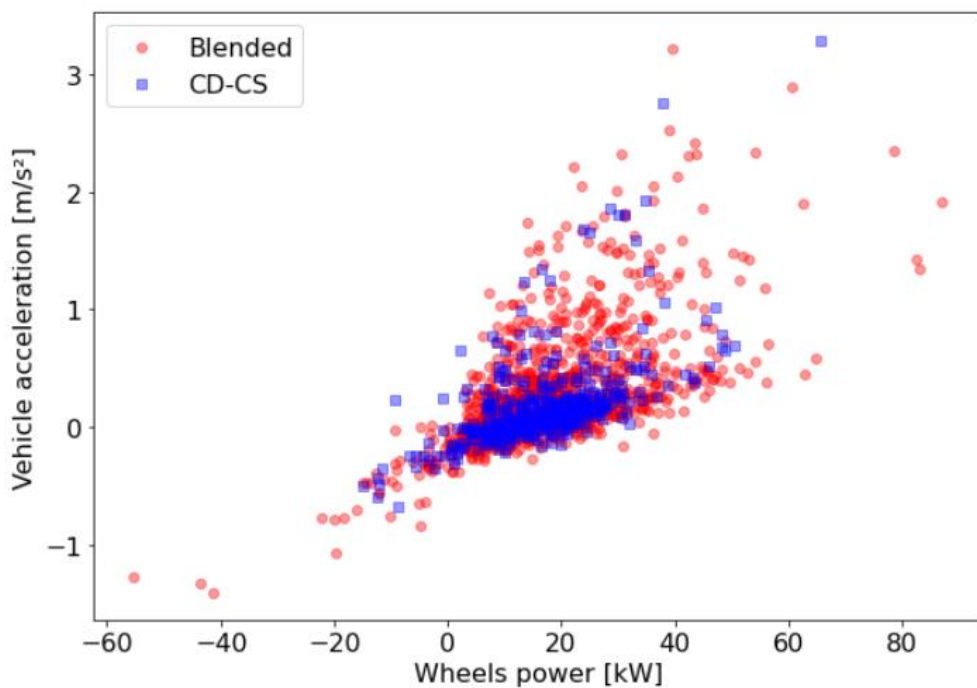


Figure 5.5 - ICE switching ON points of both strategies in the function of vehicle acceleration and wheels power

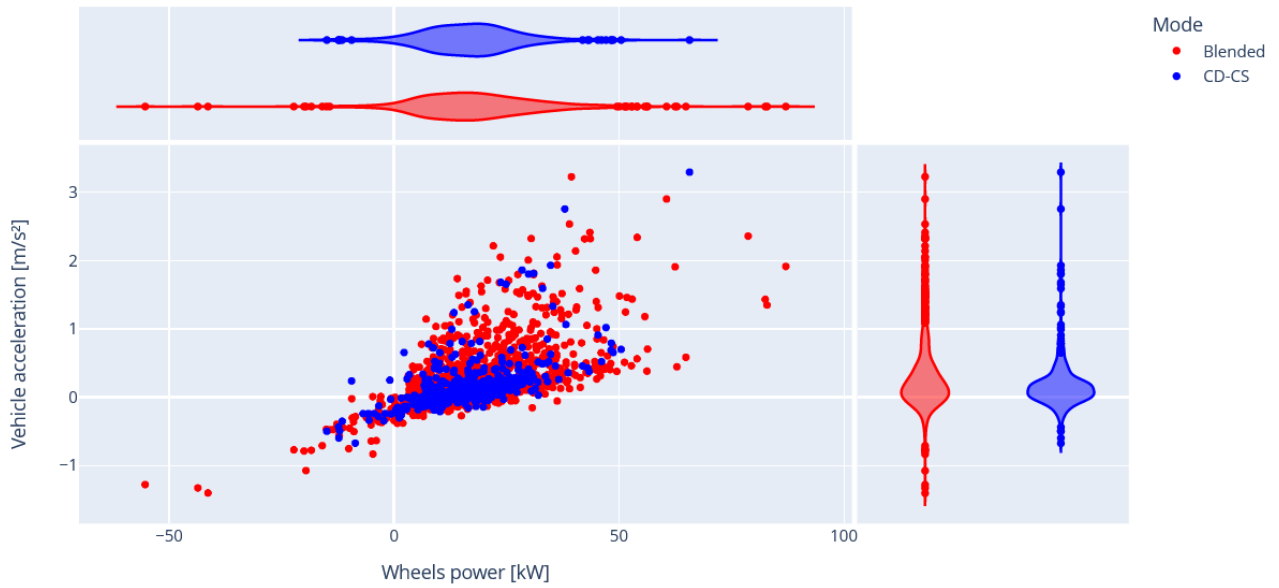


Figure 5.6 - ICE switching ON points of both strategies in the function of vehicle acceleration and wheels power with violins plots

In Figure 5.7 the vehicle speed variability for the blended ICE switching ON points is clarified with a colour bar. It's possible to notice that for lower speeds, the points slopes are higher and vice versa, so it's possible to deduce that for higher vehicle speeds the switching ON occurs already at lower vehicle accelerations. In Figure 5.8 the same approach was used for the CD-CS points, there are a few points for low vehicle speeds while the majority are referred to greater speeds and presents similar slopes and conformity with vehicle speeds compared to the blended diagram in Figure 5.7.

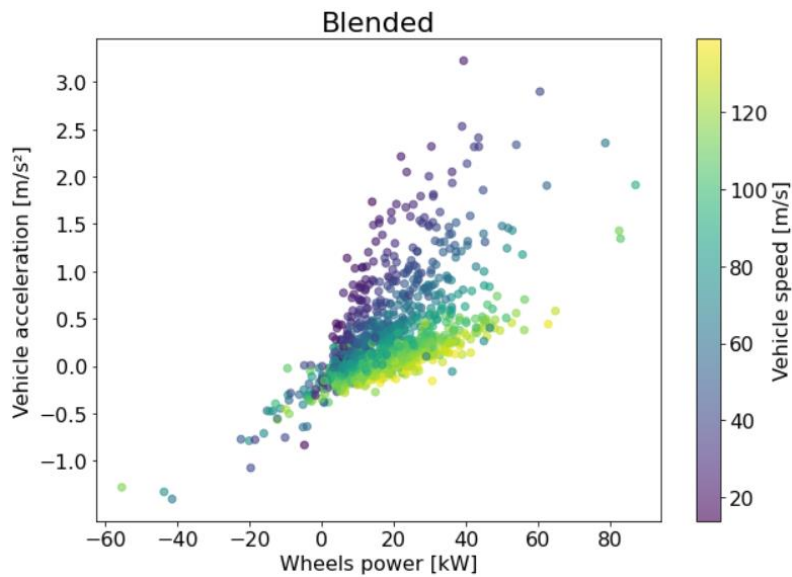


Figure 5.7 - ICE switching ON points of blended strategy in the function of vehicle acceleration, wheels power and vehicle speed with colour bar

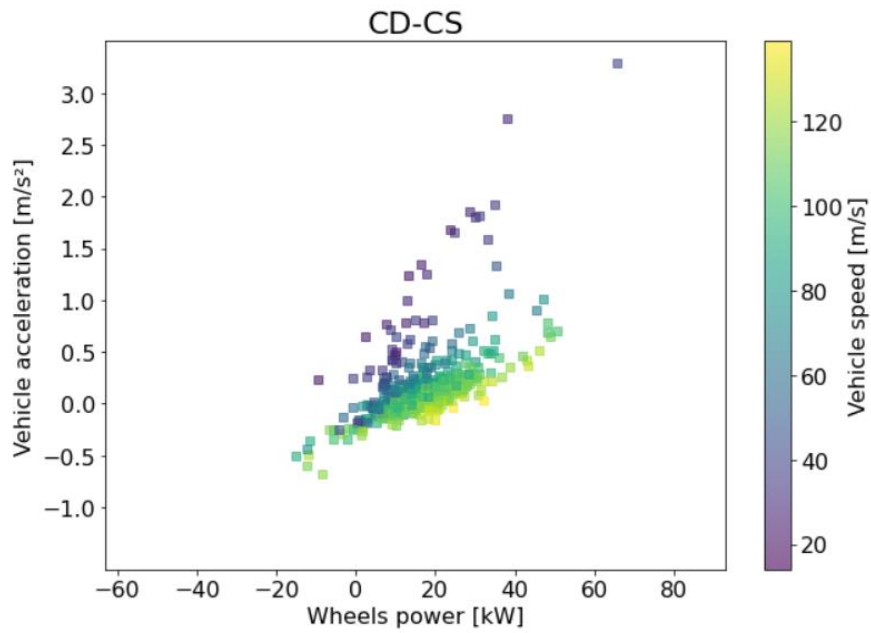


Figure 5.8 - ICE switching ON points of CD-CS strategy in the function of vehicle acceleration, wheels power and vehicle speed with colour bar

Moreover three-dimensional diagrams were created to represent the vehicle speed on a third axis and to extrapolate a fitting surface for the blended and the CD-CS strategy, respectively in Figure 5.9 and in Figure 5.10.

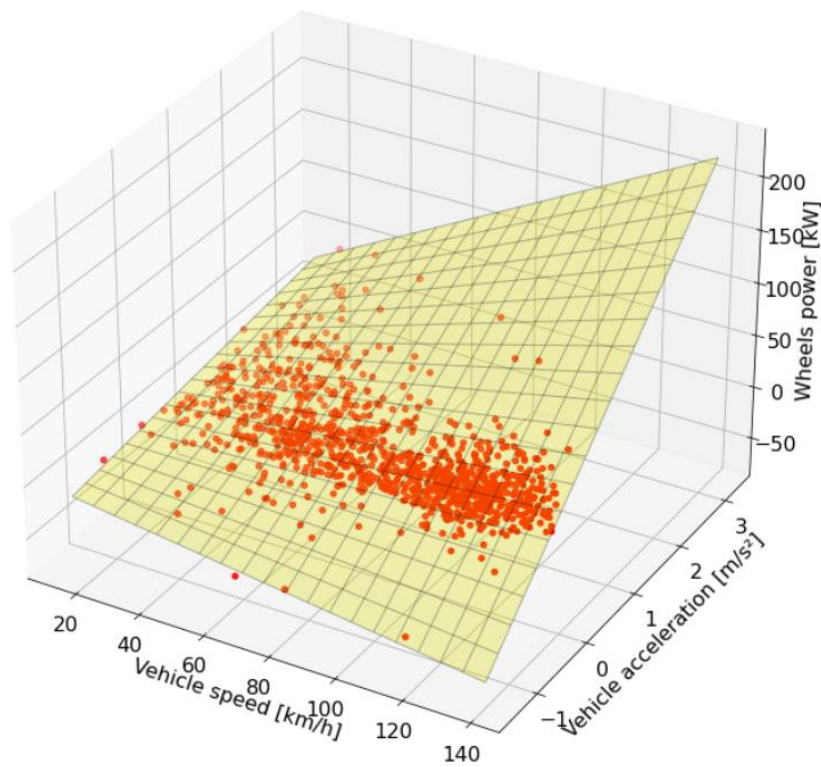


Figure 5.9 - ICE switching ON points of blended strategy in the function of vehicle acceleration, wheels power and vehicle speed

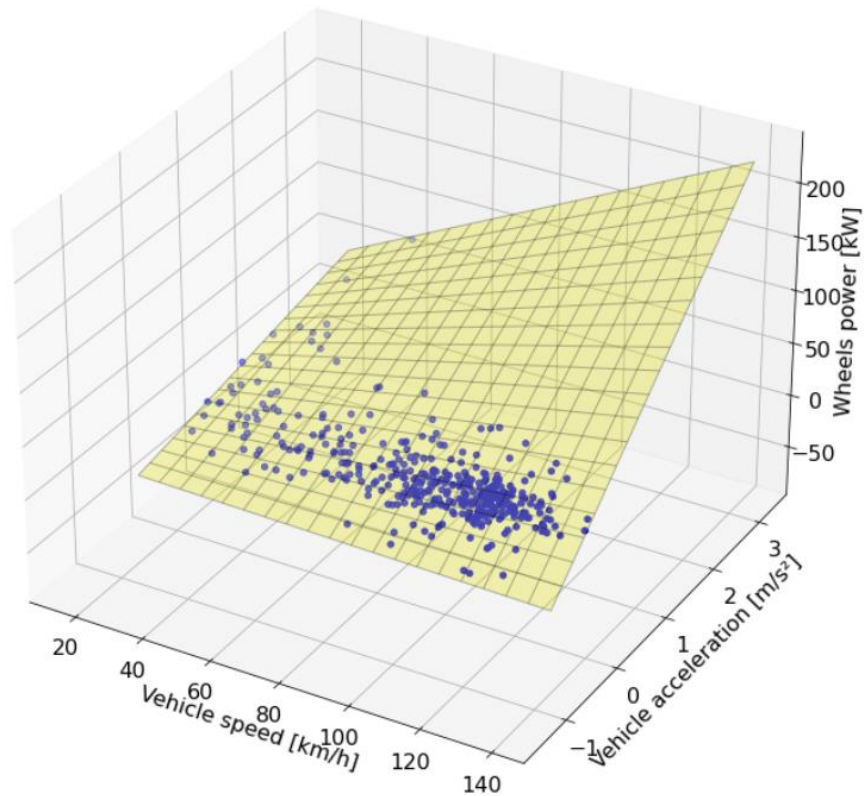


Figure 5.10 - ICE switching ON points of CD-CS strategy in the function of vehicle acceleration, wheels power and vehicle speed

The interpolating surface can provide information on the vehicle control strategy for the ICE switching ON. The two surfaces were compared on a same plot in Figure 5.11 and it's possible to glimpse that they are nearly superimposed. To confirm that, two additional contour plots, one for the blended and one for the CD-CS strategy, were created (Figure 5.12) to can better see the good correspondence.

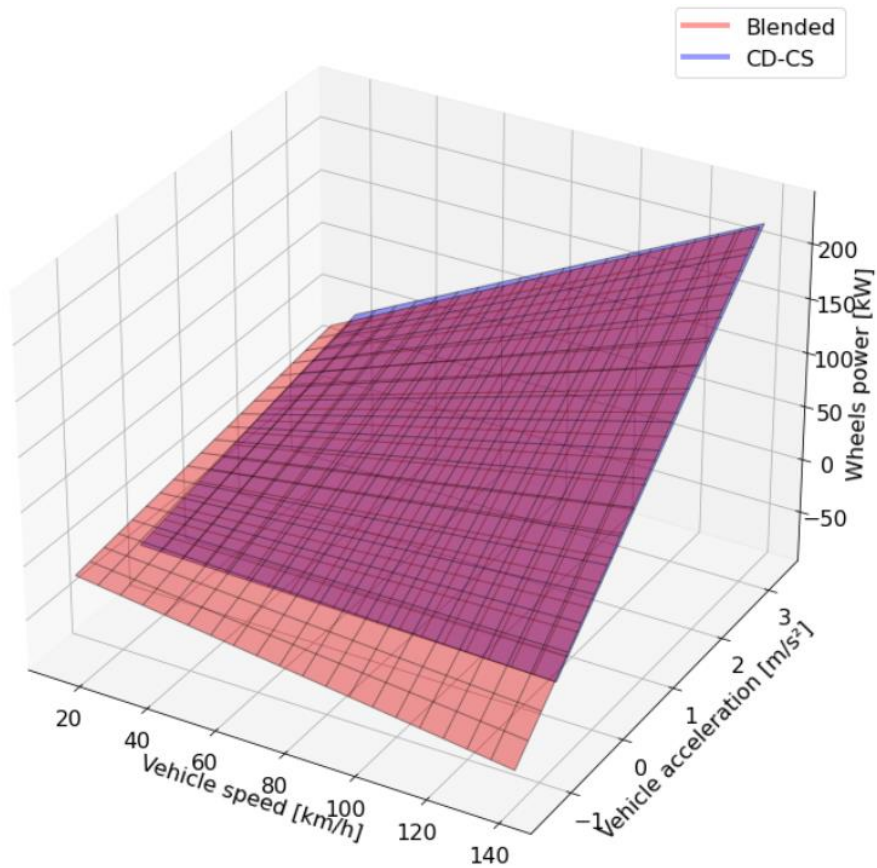


Figure 5.11 - ICE switching ON interpolation surfaces of both strategies in the function of vehicle acceleration, wheels power and vehicle speed

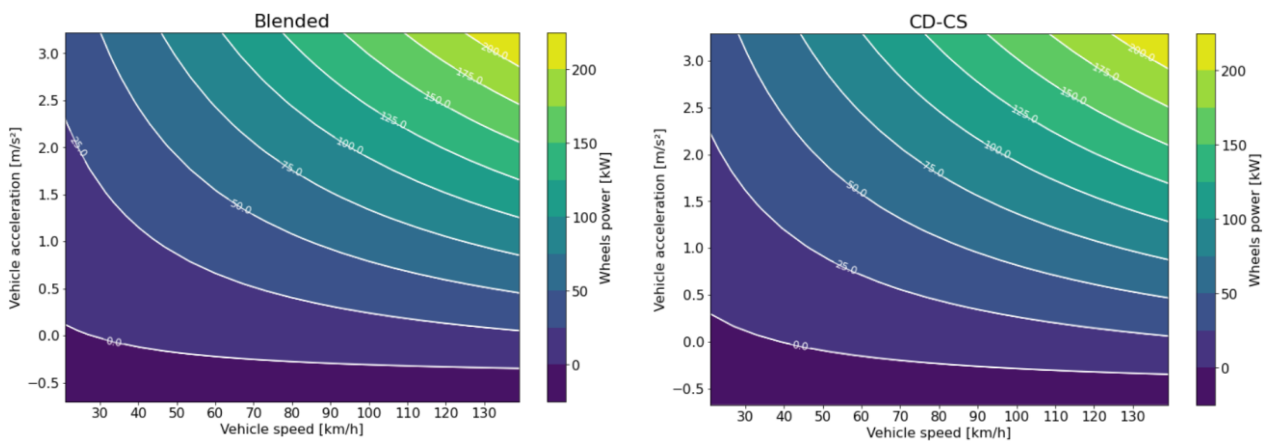


Figure 5.12 - ICE switching ON interpolation surfaces of blended (left) and CD-CS (right) strategy contour plots in the function of vehicle acceleration, wheels power and vehicle speed

5.2.2 ICE switching OFF

An analogous procedure has been conducted to obtain the operating conditions in which the internal combustion engine shut down, called “switching OFF points”. These points were plotted using a single scatter plot for all the trips as done in paragraph 5.2.1.

For the points in the function of the acceleration and power to the wheel (“wheels power”), in Figure 5.13 it’s possible to identify a quite linear trend with the range of vehicle accelerations translated towards negative values, referred to decelerations. It’s possible to notice, as it happens in [15], that the lower the requested torque is, the higher the deceleration threshold for the ICE shutting down. It’s possible that this control strategy can be useful in terms of additional braking power thanks to the internal combustion engine inertia, friction and pumping losses. In Figure 5.14 the violin plots are added and it’s possible to see how the majority of the points are positioned in the low deceleration region.

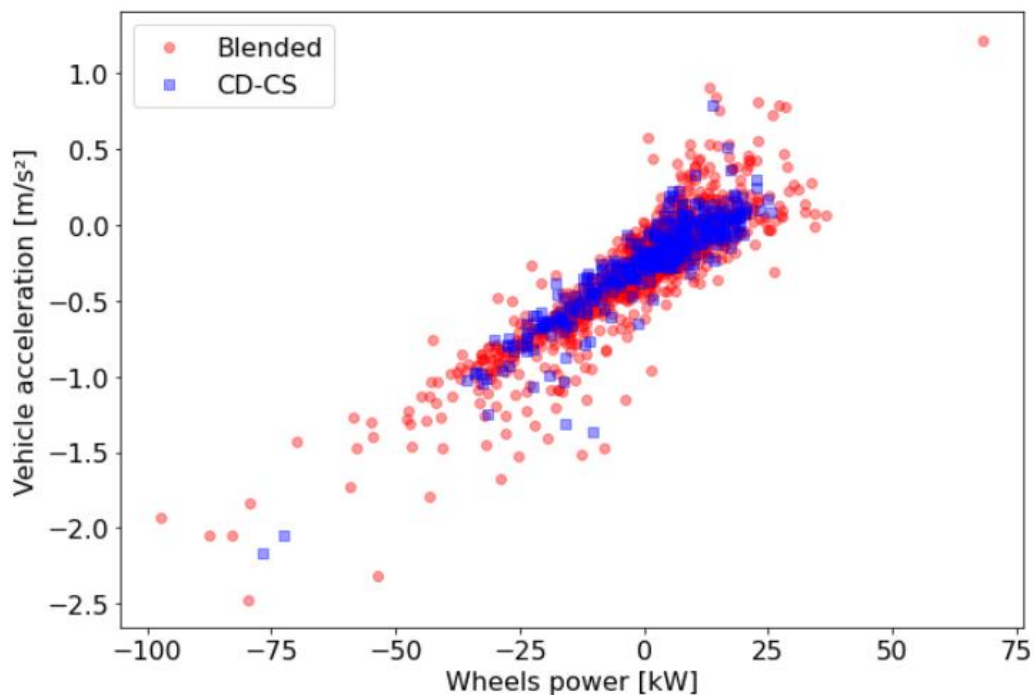


Figure 5.13 - ICE switching OFF points of both strategies in the function of vehicle acceleration and wheels power

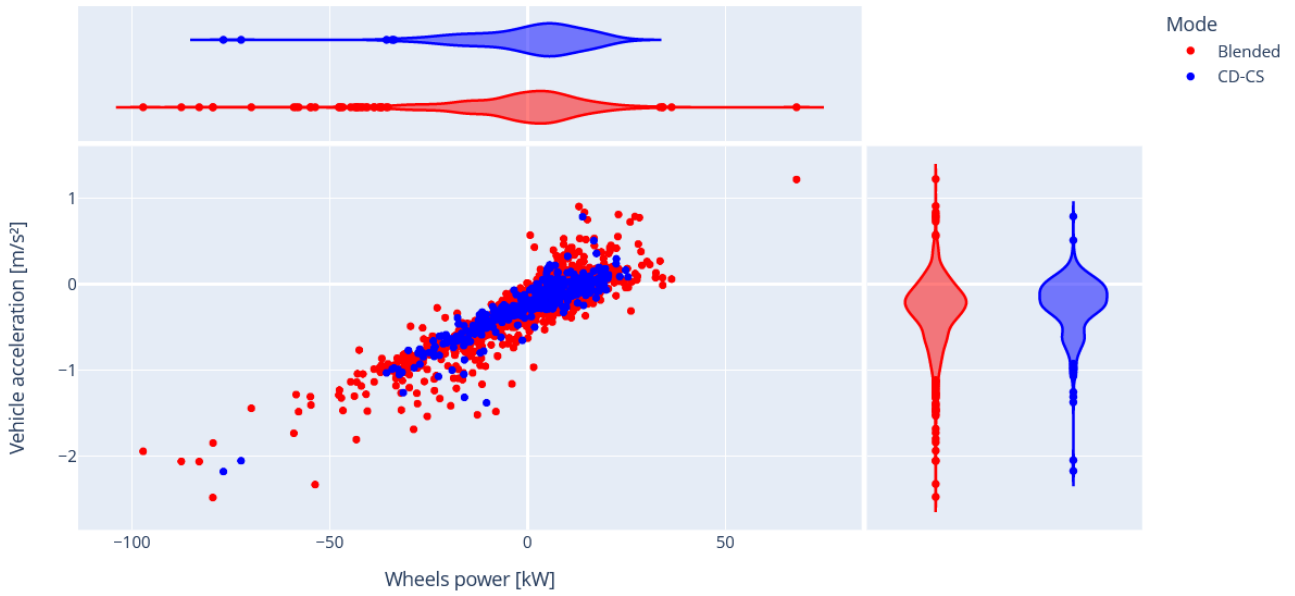


Figure 5.14 - ICE switching OFF points of both strategies in the function of vehicle acceleration and wheels power with violins plots

In Figure 5.15 and in Figure 5.16, the vehicle speed dependency in the two strategies is illustrated using a colour bar. It's possible to discern that in both strategies for lower vehicle speeds there is a higher slope, so the ICE is maintained switched ON longer, while at lower speeds the ICE is switched OFF already for lighter vehicle decelerations.

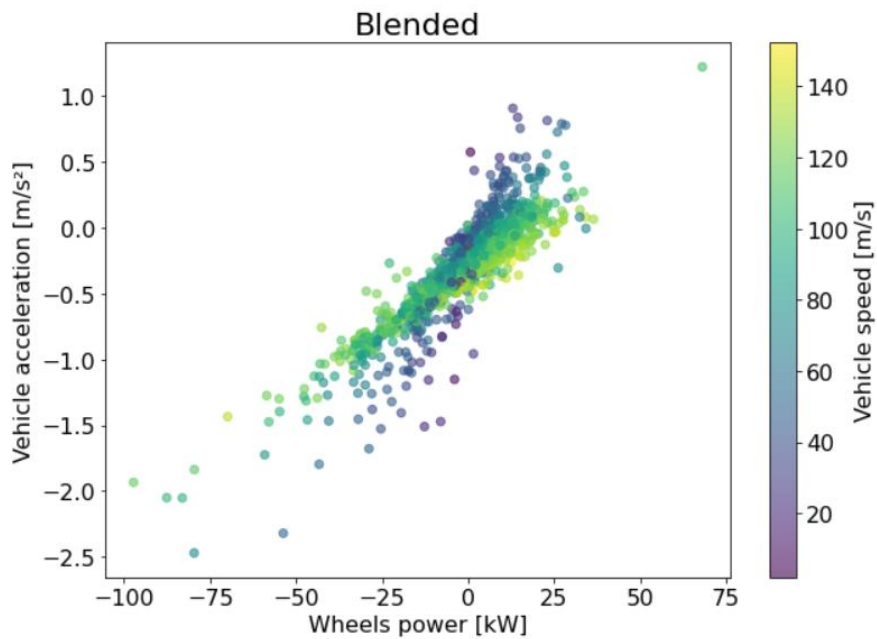


Figure 5.15 - ICE switching OFF points of blended strategy in the function of vehicle acceleration, wheels power and vehicle speed with colour bar

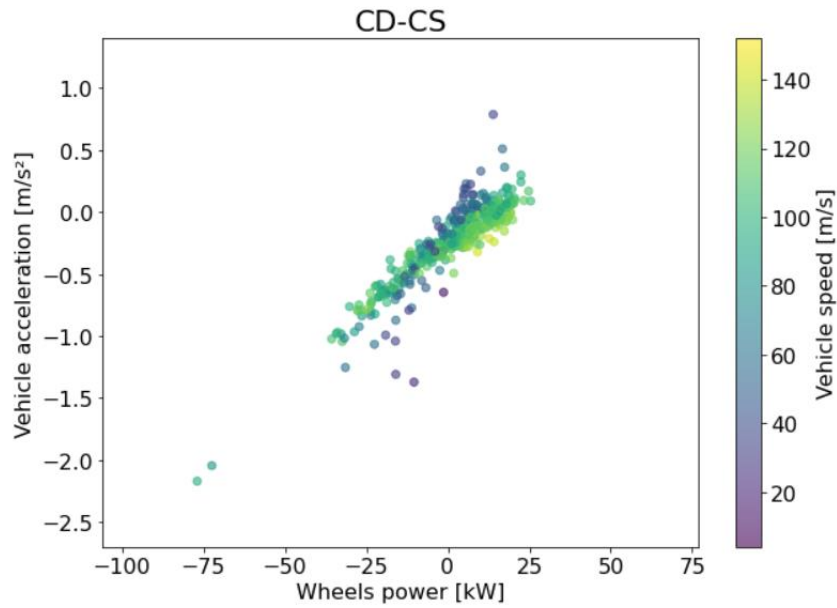


Figure 5.16 - ICE switching OFF points of CD-CS strategy in the function of vehicle acceleration, wheels power and vehicle speed with colour bar

In addition three-dimensional diagrams were created to represent the vehicle speed on a third axis and to extrapolate a fitting surface for the blended strategy in Figure 5.17 and the CD-CS one in Figure 5.18.

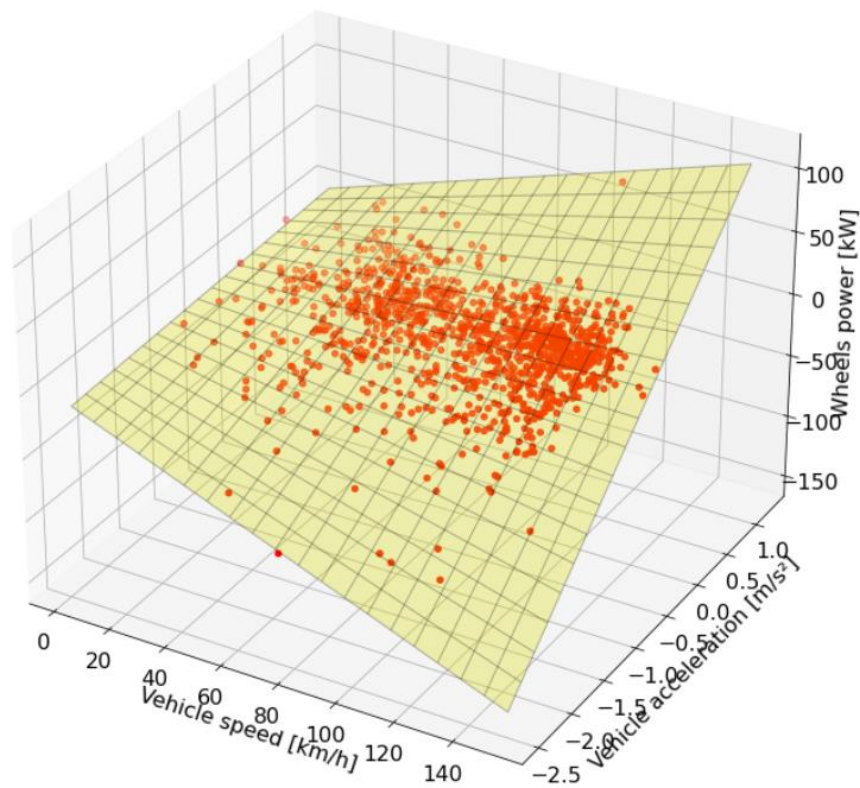


Figure 5.17 - ICE switching OFF points of blended strategy in the function of vehicle acceleration, wheels power and vehicle speed

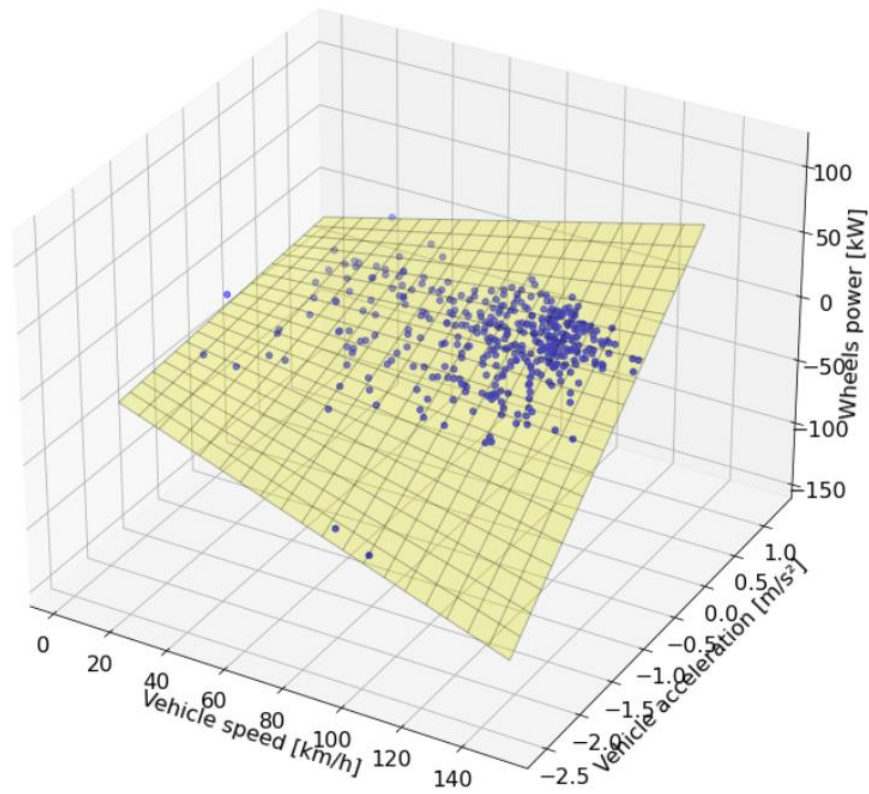


Figure 5.18 - ICE switching OFF points of CD-CS strategy in the function of vehicle acceleration, wheels power and vehicle speed

The two surfaces were compared on a same plot in Figure 5.19 where it's possible to perceive a good superimposition, confirmed in the two additional contour plots for both strategies illustrated in Figure 5.20.

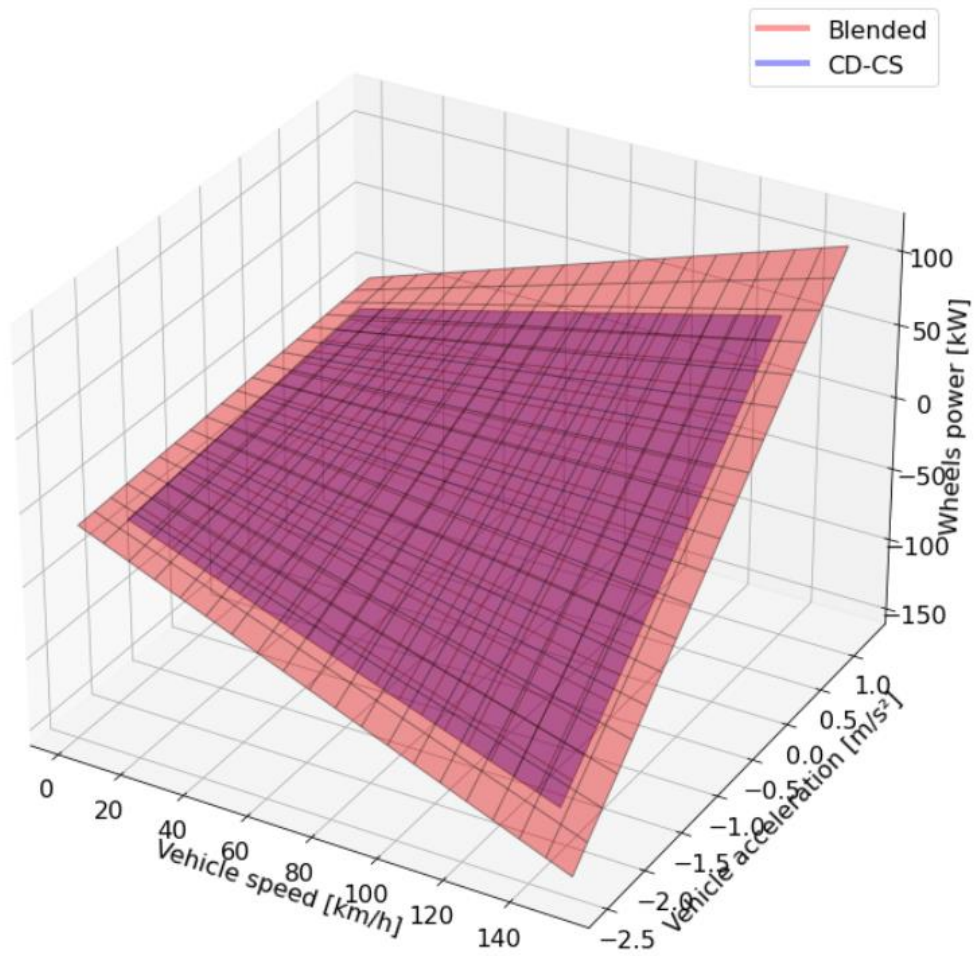


Figure 5.19 - ICE switching OFF interpolation surfaces of both strategies in the function of vehicle acceleration, wheels power and vehicle speed

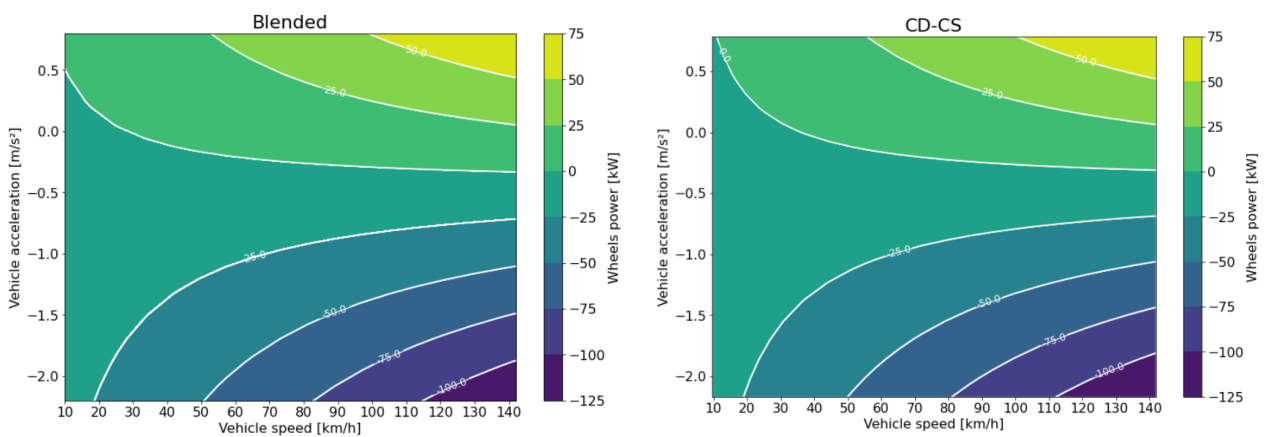


Figure 5.20 - ICE switching OFF interpolation surfaces of blended (left) and CD-CS (right) strategy contour plots in the function of vehicle acceleration, wheels power and vehicle speed

5.2.3 Powersplit

In this chapter, the powersplit between the electric motor and the internal combustion engine, is analysed. In particular the operating points along the trips were divided into different powertrain status using a function implemented in the Python program. Six different statuses, summarised in Table 5.2, were considered (with ω_{ICE} ICE rotational speed, P_w power to the wheels and T_{EM} EM torque).

POWERTRAIN STATUS	CONDITIONS
Operating points	$\omega_{ICE} > 500 \text{ rpm}$ $P_w > 0$
Regenerative braking ICE ON (RB ICE ON)	$\omega_{ICE} > 500 \text{ rpm}$ $P_w \leq 0$ $T_{EM} \leq 0$
Transition phases	$0 < \omega_{ICE} \leq 500 \text{ rpm}$
Electric motor only (EM only)	$\omega_{ICE} = 0$ $T_{EM} > 0$
Regenerative braking ICE OFF (RB ICE OFF)	$\omega_{ICE} = 0$ $T_{EM} < 0$
None of the above	$\omega_{ICE} > 500 \text{ rpm}$ $P_w \leq 0$ $T_{EM} > 0$
	$\omega_{ICE} = 0$ $T_{EM} = 0$

Table 5.2 - Powertrain status conditions

The operating points which are referred to positive powers were represented on a scatter plot of the ICE power in the function of the power to the wheel (“wheels power”), for the blended strategy in Figure 5.21 and for the CD-CS one in Figure 5.22. In a first approximation where the mechanical losses of the transmission are not considered, the points quite above the bisector represent the load point moving statuses because $P_{ICE} > P_w$ while the points quite below the bisector the e-assist ones ($P_{ICE} < P_w$).

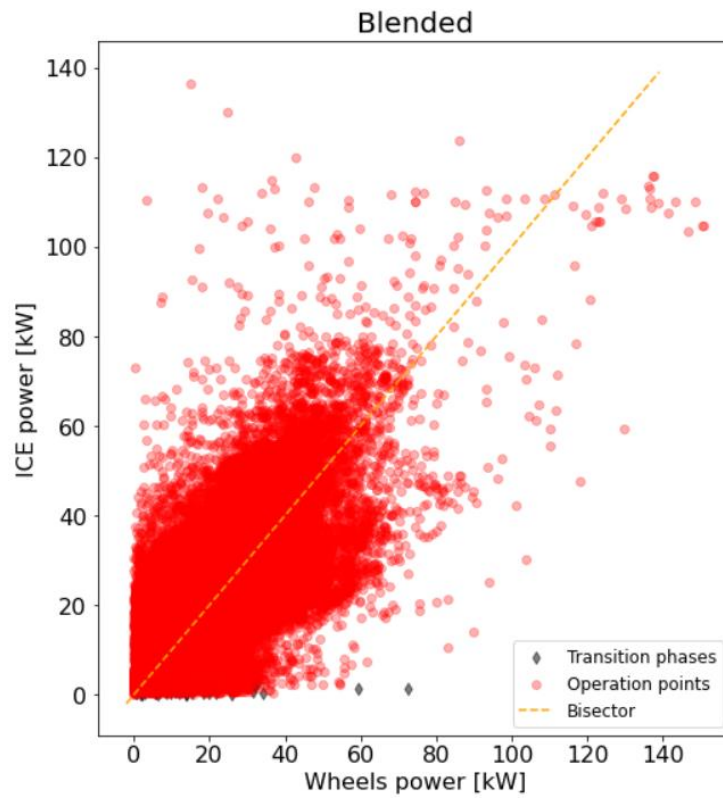


Figure 5.21 - ICE power represented in the function of the total power to the wheels for blended trips

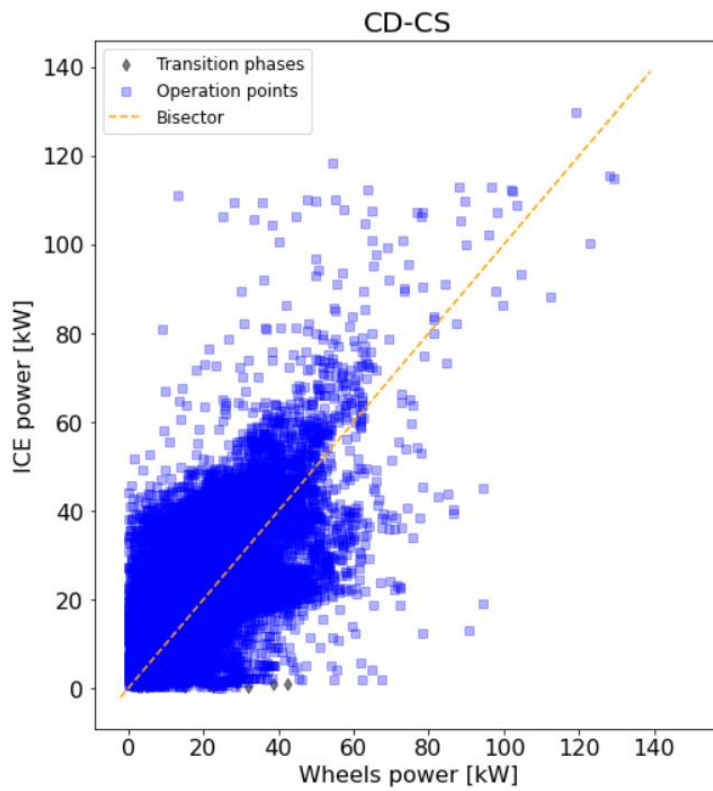


Figure 5.22 - ICE power represented in the function of the total power to the wheels for CD-CS trips

It's possible to observe a quite similar distribution between the two control strategies.

Then the operating point were plotted on the ICE power band as visible in Figure 5.23 for the blended strategy and in Figure 5.24 for the CD-CS strategy. For a better comparison, a common plot with violin plots was created (Figure 5.25), it's possible to notice a small difference in the function of the engine speed: the CD-CS points present two peaks, one corresponding two the blended pattern while the other, more raised, at lower engine speeds.

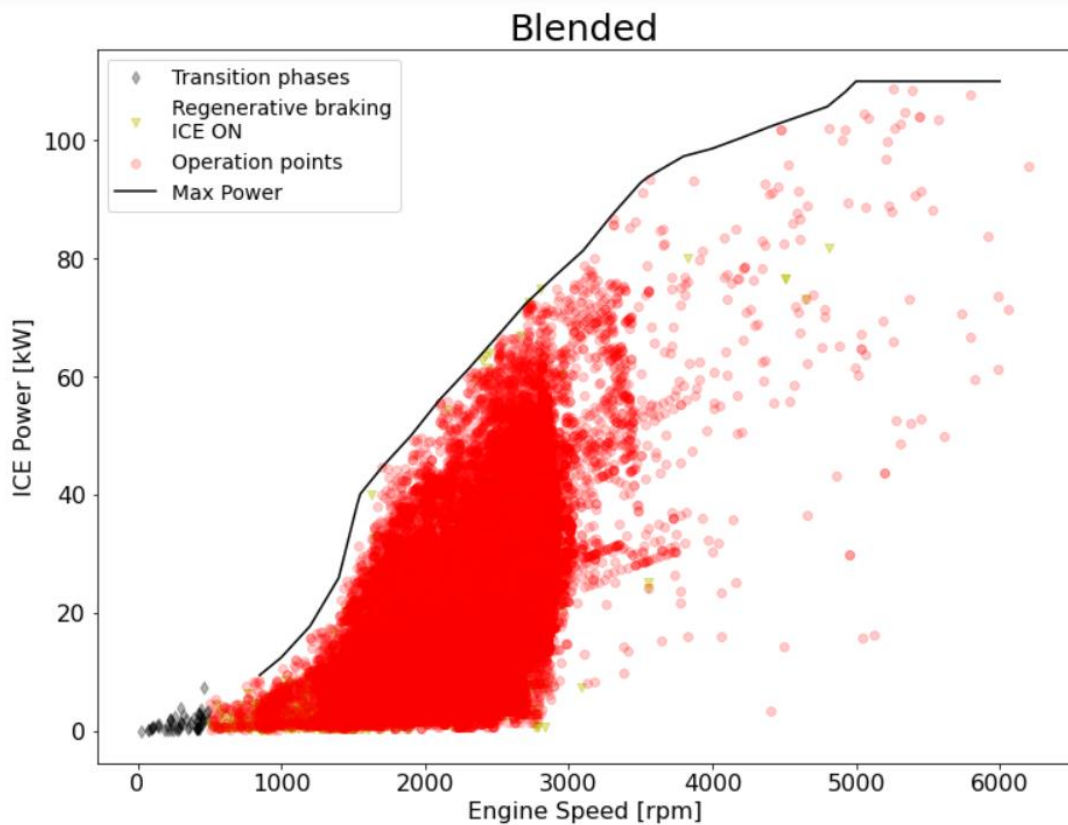


Figure 5.23 - Operating points in the ICE power band for the blended strategy

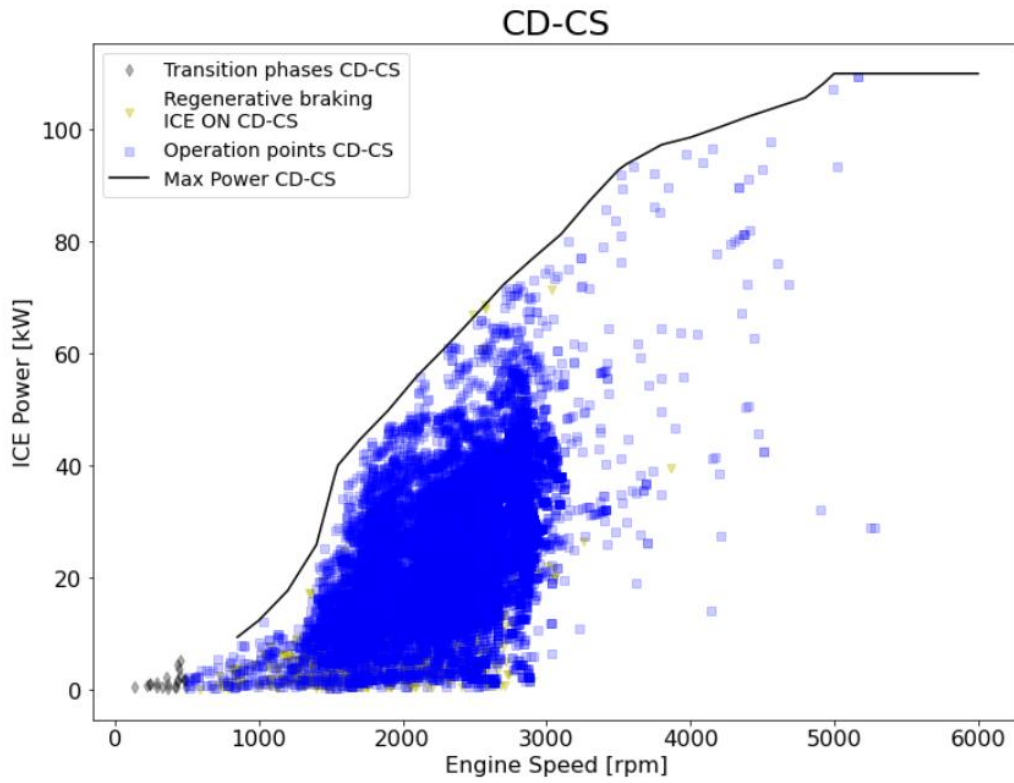


Figure 5.24 - Operating points in the ICE power band for the CD-CS strategy

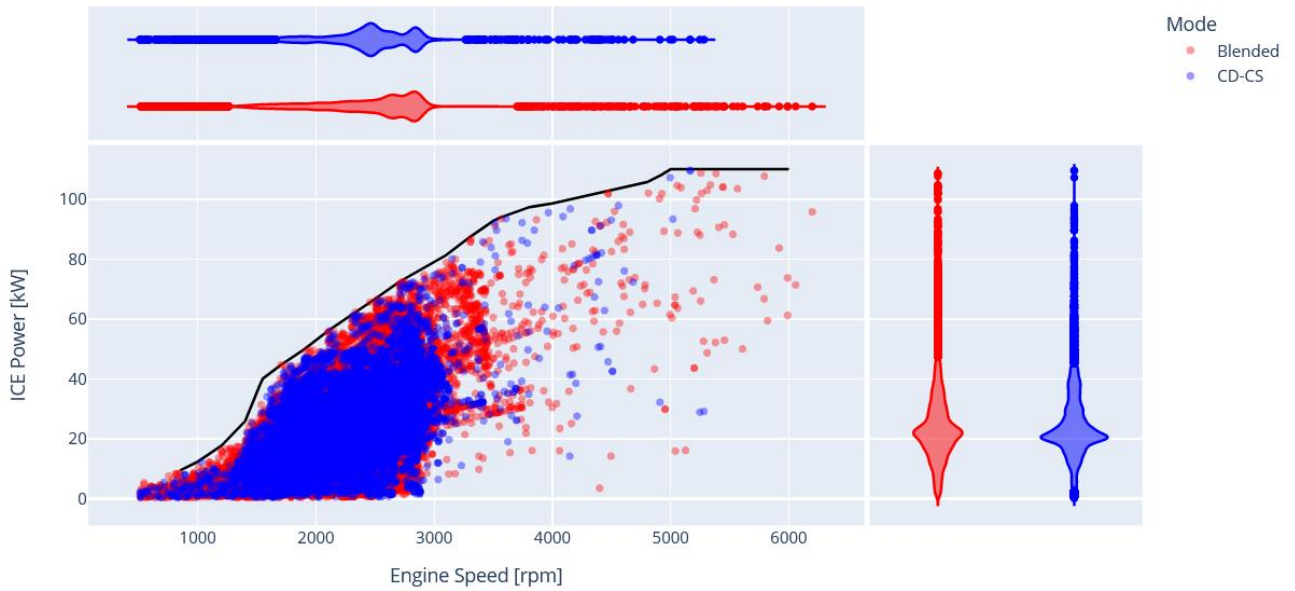


Figure 5.25 - Operating points in the ICE power band for both strategies with violin plots

5.2.4 Gear shifting

In this section a gear shifting analysis is presented with a density of probability approach as Figure 5.26 shows. For the CD-CS strategy, the two different parts are considered separately.

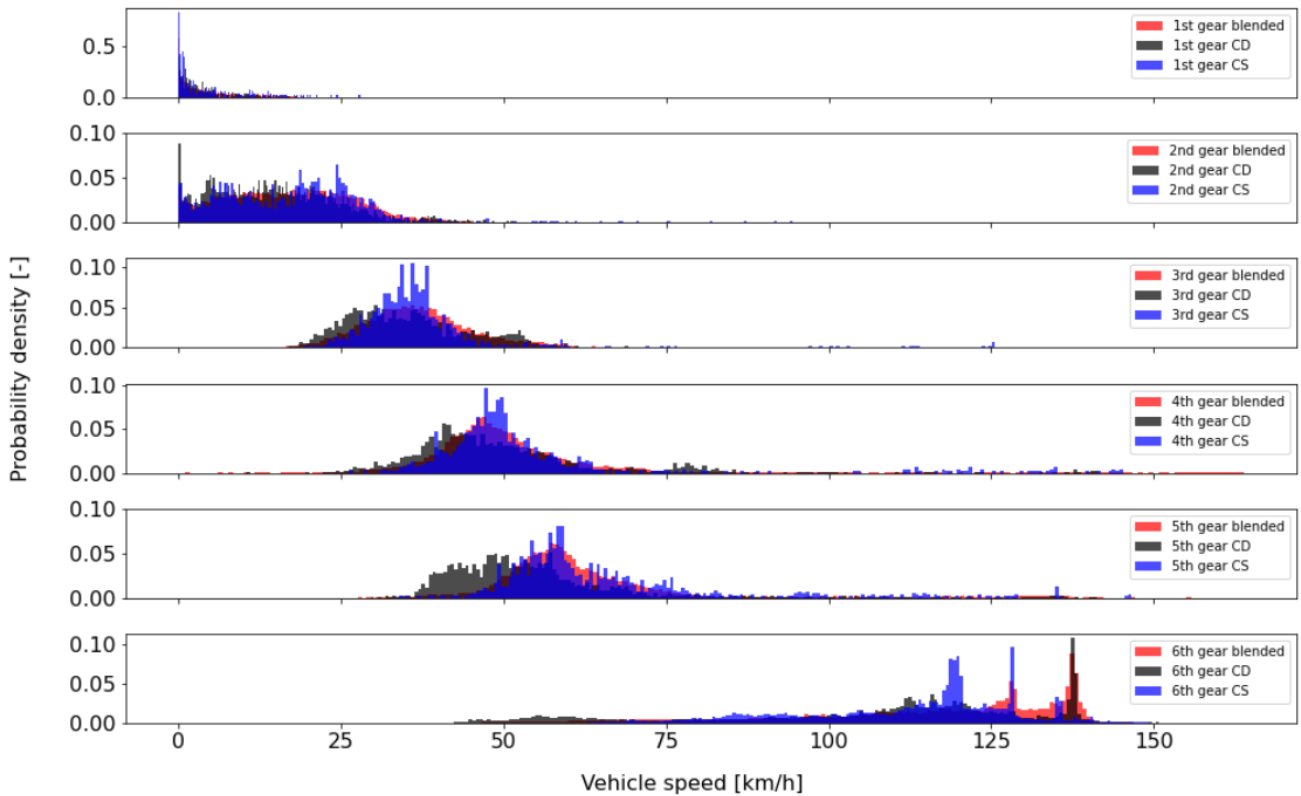


Figure 5.26 - Probability density for the different gears in the function of the vehicle speed

It's possible to see that the 5th gear and in particular the 6th gear are engaged also at lower vehicle speeds for the CD compared to the CS and blended tendencies thanks to the electric motor characteristics. Thus the gears engagement is more limited not only in the CS parts, but also in the blended strategy because of the internal combustion engine less flexible possibilities on the usable gear.

Besides it's possible to detect that, in the 6th gear, usually higher vehicle speeds are maintained with the blended strategy compared to the CS mode. A reason could be that with the blended mode the driver generally maintains the desired cruising speed whereas with the CS the driver tends to keep a lower cruising speed, for example for fuel economy reasons because a considerable usage of the internal combustion engine emerges after the first part of the journey characterised by the electric drive typical of the CD part. This divergence in the cruising speeds in the 6th gear between the CS and blended mode can be found also in the difference in the engine speeds highlighted in the upper violin plot of Figure 5.25 in paragraph 5.2.3: as far as the region of the high vehicle speeds is concerned, the generally lower speeds in CS imply lower internal combustion engine rotational speeds.

5.2.5 Fuel consumption

At the end the total fuel consumption (FC) of the blended and the CD-CS single trips are plotted in the function of the wheels energy rate, a parameter computed to consider the energy demand of the trip in kWh/100km. The results are visible in Figure 5.27.

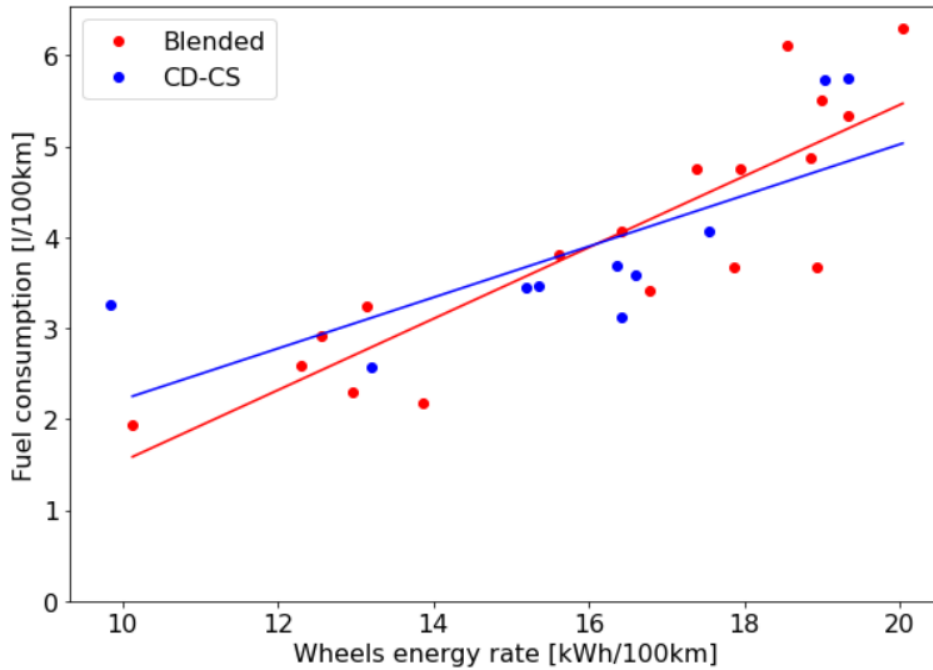


Figure 5.27 - Single trips total fuel consumption plotted referring to the wheels energy rate

It's possible to notice that the fuel consumption values don't present clear differences between the blended and the CD-CS strategies.

Because of the fuel consumption minimisation purpose of the blended mode, one would have expected better results in that strategy in comparison with the CD-CS strategy. Nevertheless it's necessary to consider another factor: the final SOC reached at the end of the trips. In fact the average value of final battery SOC of the blended trips is higher than the CD-CS one, as it's shown in Table 5.3.

Mode	Average final SOC
Blended	30,5%
CD-CS	26,1%

Table 5.3 - Average final battery SOC values in the two strategies

The difference in the average final SOC indicates that in some blended trips the EMS didn't succeed in reaching the lower SOC target value at the end of the journey. Instead in the CD-CS trips the strategy managed to fulfil this condition because the lower reference SOC value is always reached considering that the transition from charge depleting to charge sustaining happens when the SOC has reached this value. Thus it was possible that a blended trips ended with a higher battery SOC, so a part of the energy that should have been used in the trips remained stocked in the battery and was substituted by a greater usage of the ICE entailing a higher fuel consumption. This factor can contribute to obtain underestimated blended fuel economy values.

In Figure 5.28 the trip final battery SOC is plotted with the corresponding trip average vehicle speed. No particular pattern in the function of the average speed can be detected, while it's possible to notice that the CD-CS analysed trips can always reach a final SOC near to the reference value differently from the blended trips. It's possible to observe that also in Figure 5.29 and in Figure 5.30 where the trip final battery SOC is plotted with the trip total distance and trip difference in altitude respectively.

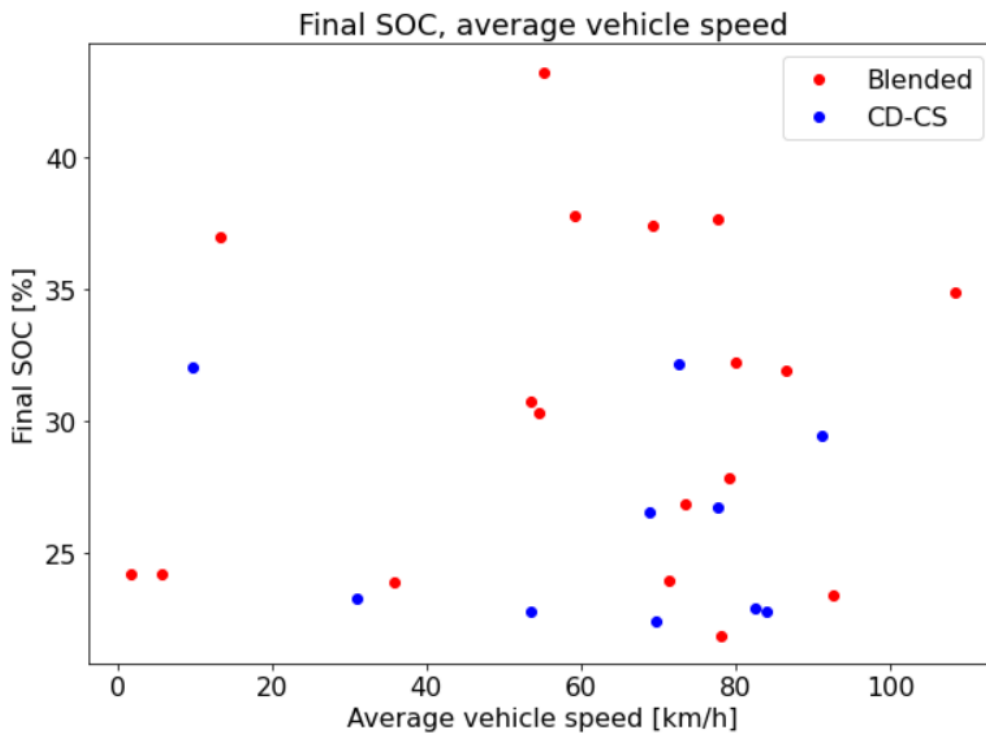


Figure 5.28 - Single trips final SOC plotted with the trip average vehicle speed

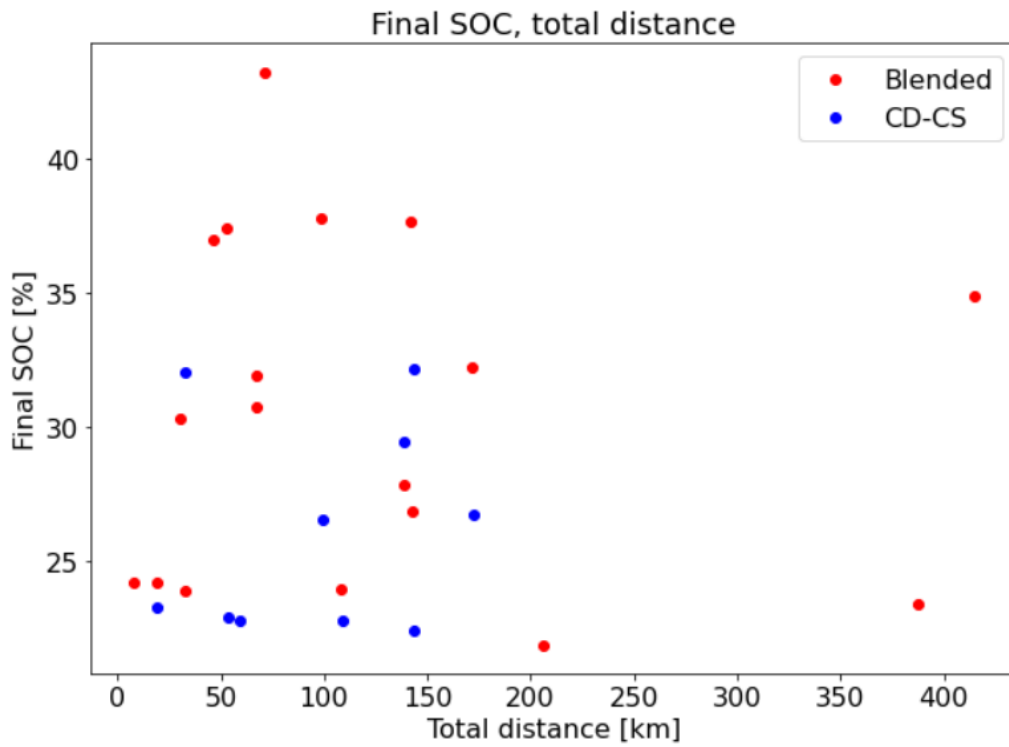


Figure 5.29 - Single trips final SOC plotted with the trip total distance

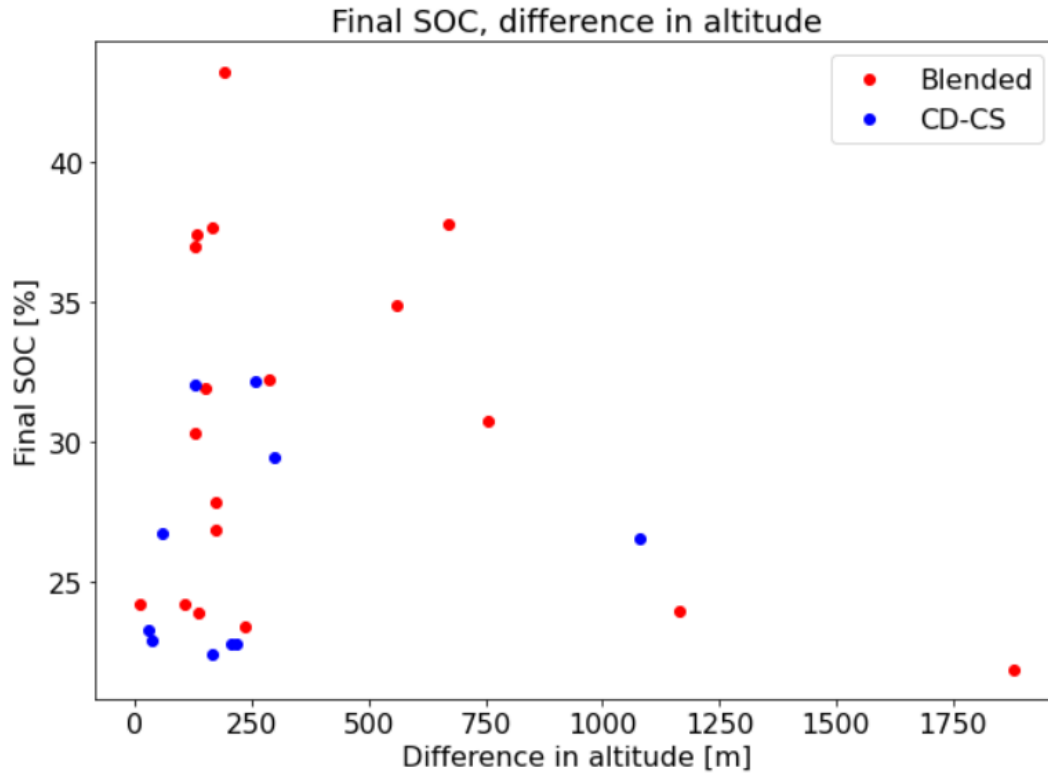


Figure 5.30 - Single trips final SOC plotted with the trip difference in altitude

Even though there are some short blended trips where the control manage to reach the final target SOC, it's possible to note that the blended strategy sometimes presents a difficulty in reaching the final target SOC for short trips. An analogous observation can be done for Figure 5.30 where the higher blended final SOC are in the region of the lower differences in altitude.

Furthermore for both Figure 5.29 and Figure 5.30, it's possible to discern that for high trip distances and differences in altitude there is not such a wide number of CD-CS trips. That highlight the fact that in this study it was possible to select only a few CD-CS trips with the impossibility to analyse each doable case study, obtaining less reliable results.

Moreover additional aspects could be analysed to strengthen the results, for example the GPS employment and the different traction modes which the user can select from the dashboard: Hybrid, Charging level reserve and E-mode: the Hybrid and the E-mode selections correspond respectively to the blended and the CD-CS strategies. Therefore it would be relevant to analyse the vehicle behaviour in determined circumstances that can occur in a real-world context and can create not optimal blended strategy results. For example when the user select the Hybrid mode without entering the final destination on the GPS or in case of trips shorter than the vehicle all electric range or anyhow practicable with the only electric drive. Other instances could refer to the cases when the user select the Hybrid mode and the destination on the GPS, but then an alternative itinerary is chosen or the journey ends ahead of schedule.

Conclusions

In this thesis work, an analysis of some real-world trips of a Plug-in Hybrid Electric Vehicle (PHEV) with different control strategies was carried out.

A first general evaluation of the differences between type approval tests and real-world trips and some examples of the blended control strategies operation are examined.

Then some peculiar aspects of the two control strategies analysed, the blended one and the charge depleting and charge sustaining (CD-CS) one, of the selected real-world trips were compared.

At the end a fuel consumption comparison revealed quite comparable results, when instead an advantage in the blended mode performances was expected. However a discrepancy on the average final battery state of charge (SOC) of the two sets of trips was detected: 30,5% for the blended and 26,1% for the CD-CS. This means that in some blended trips the energy management system (EMS) didn't succeed in reaching the lower SOC reference value at the end of the journey, condition instead always fulfilled in the CD-CS trips. Thus it was possible that a part of the energy that should have been used in the blended trips remained stocked in the battery and was substituted by a greater usage of the ICE causing, in these cases, underestimated blended fuel economy values.

Moreover, despite the many trips available, only 18 trips could be considered as blended. From the latter, it was possible to select only 10 CD-CS similar trips. Therefore the number of trips involved in the analysis is not so broad and the CD-CS trips can't represent each feasible case study, for example the cases of long total distances and high differences in altitude. With a higher number of trips, it would be probably possible to obtain more precise results.

Furthermore there are other variables that it would be possible to examine to improve the robustness of the results or for future developments, such as the GPS usage and the different traction modes selectable by the user with a monitoring on the actual vehicle's control strategy behaviour in these circumstances.

Appendix A

The CO₂ mass emission correction coefficient K_{CO_2} , determined by driving a set of charge-sustaining tests, is defined by the following equation:

$$K_{CO_2} = \frac{\sum_{n=1}^{n_{CS}} \left((EC_{DC,CS,n} - EC_{DC,CS,avg}) \times (M_{CO_2,CS,nb,n} - M_{CO_2,CS,nb,avg}) \right)}{\sum_{n=1}^{n_{CS}} (EC_{DC,CS,n} - EC_{DC,CS,avg})^2}$$

where:

- K_{CO_2} is the CO₂ mass emission correction coefficient, (g/km)/(Wh/km);
- $EC_{DC,CS,n}$ is the charge-sustaining electric energy consumption of test n based on the REESS depletion, Wh/km;
- $EC_{DC,CS,avg}$ is the arithmetic average of the charge-sustaining electric energy consumption of n_{CS} tests based on the REESS depletion, Wh/km;
- $M_{CO_2,CS,nb,n}$ is the charge-sustaining CO₂ mass emission of test n , not corrected for the energy balance, g/km;
- $M_{CO_2,CS,nb,avg}$ is the arithmetic average of the charge-sustaining CO₂ mass emission of n_{CS} tests based on the CO₂ mass emission, not corrected for the energy balance, g/km;
- n is the index number of the considered test;
- n_{CS} is the total number of tests.

and:

$$M_{CO_2,CS,nb,avg} = \frac{1}{n_{CS}} \times \sum_{n=1}^{n_{CS}} M_{CO_2,CS,nb,n}$$

The CO₂ mass emission correction coefficient shall be rounded to four significant figures.

Appendix B

A part of the Python script, written to manage the data from the real-world trips and to carry out the analysis, is presented in this appendix as an example. This Python script section creates a dictionary which is filled with different values calculated from some data obtain from the vehicle.

```
trips={}

for i, datafile in enumerate(datafiles):
    trip_name = os.path.splitext(os.path.basename(datafile))[0]
    print("Trip %d: %s" % (i, trip_name))
    dft = pd.read_excel(datafile)
    dft["Distance [km]"] = calc_distance(dft["Time [s]"],
    dft["Vehicle Speed IDE00075 [km/h]"])
    dft["Electric driving [-]"] = np.where(dft["EngineSpeedStd
    [rpm]"] > 500, 0, 1)
    dft["Electric distance [km]"] = np.cumsum(ca
    lc_delta_distance(dft["Time [s]"], dft["Vehicle Speed IDE00075
    [km/h]"]) * dft["Electric driving [-]"])
    dft["Fuel consumption [l]"] = integrate.cumtrapz(dft["Consumo
    di carburante all'ora IDE04008 [lt/hr]"], dft["Time
    [s]"]/3600, initial=0)
    dft["Fuel consumption [kg]"] = (integrate.cumtrapz(dft["Fuel
    Rate Vehicle VO_FuelRateVeh [gr/sec]"], dft["Time [s]"],
    initial=0))/1000
    dft["Electric energy consumed [kWh]"] =
    integrate.cumtrapz(calc_electric_power(dft["Tensione della
    batteria ad alto voltaggio IDE06346 [V]"], dft["Corrente 2
    batteria del sistema ibrido ad alto voltaggio BattCurrent
    [A]"]), dft["Time [s]"], initial=0)/3600

    trips[trip_name] = dft
```

References

- [1] “European Council, Infographic - Fit for 55: how the EU will turn climate goals into law,” [Online]. Available: <https://www.consilium.europa.eu/en/infographics/fit-for-55-how-the-eu-will-turn-climate-goals-into-law/>. [Accessed April 2023].
- [2] “European Environment Agency,” [Online]. Available: <https://www.eea.europa.eu/ims/total-greenhouse-gas-emission-trends#ref-bHNbA>. [Accessed March 2023].
- [3] “News European Parliament,” [Online]. Available: <https://www.europarl.europa.eu/news/en/headlines/society/20190313STO31218/co2-emissions-from-cars-facts-and-figures-infographics>. [Accessed March 2023].
- [4] “European Environment Agency,” [Online]. Available: <https://www.eea.europa.eu/data-and-maps/daviz/ghg-emissions-by-aggregated-sector-5#tab-dashboard-02>. [Accessed March 2023].
- [5] A. Tansini, *Flexible calculation approaches to support the European CO2 emissions regulatory scheme for road vehicles*, 2020.
- [6] *CO2 EMISSION STANDARDS FOR PASSENGER CARS AND LIGHT-COMMERCIAL VEHICLES IN THE EUROPEAN UNION*, The International Council on Clean Transportation (ICCT), January 2019.
- [7] J. Pavlovic, B. Ciuffo, G. Fontaras, V. Valverde and A. Marotta, “How much difference in type-approval CO2 emissions from passenger cars in Europe can be expected from changing to the new test procedure (NEDC vs. WLTP)?,” *Transportation Research Part A*, 2018.
- [8] J. Pavlovic, G. Fontaras, M. Ktistakis, K. Anagnostopoulos, D. Komnos, B. Ciuffo, M. Clairotte and V. Valverde, “Understanding the origins and variability of fuel consumption gap: lessons learned from laboratory tests and a real-driving campaign,” *Environmental Science Europe*, 2020.
- [9] G. Fontaras, B. Ciuffo, N. Zacharof, S. Tsiakmakis, A. Marotta, J. Pavlovic and K. Anagnostopoulos, “The difference between reported and real-world CO2 emissions: How much improvement can be expected by WLTP introduction?,” *Transportation Research Procedia*, 2017.
- [10] J. Pavlovic, G. Fontaras, S. Broekaert, B. Ciuffo, M. Ktistakis and T. Grigoratos, “How accurately can we measure vehicle fuel consumption in real world operation?,” *Transportation Research Part D: Transport and Environment*, 2021.
- [11] L. Rolando, *AN INNOVATIVE METHODOLOGY FOR THE DEVELOPMENT OF HEVS ENERGY MANAGEMENT SYSTEMS*, 2012.

- [12] H. Kraus, M. Ackerl, P. Karoshi, J. Fabian and M. Hofstetter, "A New Approach to an Adaptive and Predictive Operation Strategy for PHEVs," *SAE International*, 2015.
- [13] *MILD-HYBRID VEHICLES: A NEAR TERM TECHNOLOGY TREND FOR CO2 EMISSIONS REDUCTION*, The International Council on Clean Transportation (ICCT), July 2022.
- [14] "EUR-Lex, Document 02017R1151-20200125," [Online]. Available: <https://eur-lex.europa.eu/legal-content/EN/TXT/?uri=CELEX%3A02017R1151-20200125>. [Accessed February 2023].
- [15] F. Millo, L. Rolando, L. Pulvirenti and G. Di Pierro, "A Methodology for the Reverse Engineering of the Energy Management Strategy of a Plug-In Hybrid Electric Vehicle for Virtual Test Rig Development," *SAE Int. J. Elect. Veh.*, 11(1):2022, doi: 10.4271/14-11-01-0009.
- [16] C. Cubito, L. Rolando, F. Millo, B. Ciuffo and et al., "Energy Management Analysis under Different Operating Modes for a Euro-6 Plug-in Hybrid Passenger Car," *SAE Technical Paper*, 2017-01-1160, doi: 10.4271/2017-01-1160.
- [17] B. V. Padmarajan, A. McGordon and P. A. Jennings, "Blended Rule Based Energy Management for PHEV: System Structure and Strategy," *IEEE Transactions on Vehicular Technology*, January 2015.
- [18] H. Climent, B. Pla, P. Bares and V. Pandey, "Exploiting driving history for optimising the Energy Management in plug-in Hybrid Electric Vehicles," *Energy Conversion and Management*, 2021.
- [19] J. Soldo, B. Škugor and J. Deur, "Synthesis of Optimal Battery State-of-Charge Trajectory for Blended Regime of Plug-in Hybrid Electric Vehicles in the Presence of Low-Emissions Zones and Varying Road Grades," *Energies*, 2019.
- [20] V. Larsson, L. Johannesson and B. Egardt, "Impact of trip length uncertainty on optimal discharging strategies for PHEVs," *International Federation of Automatic Control (IFAC)*, 2010.
- [21] SAE J2841, "Utility Factor Definitions for Plug-In Hybrid Electric Vehicles Using Travel Survey Data," September 2010, Hybrid - EV Committee.
- [22] J. Pavlovic, A. Tansini, G. Fontaras, B. Ciuffo and et al., "The Impact of WLTP on the Official Fuel Consumption and Electric Range of Plug-in Hybrid Electric Vehicles in Europe," *SAE Technical Paper*, 2017-24-0133, doi: 10.4271/2017-24-0133.
- [23] A. Tansini, J. Pavlovic and G. Fontaras, "Quantifying the real-world CO2 emissions and energy consumption of modern plug-in hybrid vehicles," *Journal of Cleaner Production*, 2022.

- [24] J. Suarez, A. Laverde, A. Tansini, M. Ktistakis, D. Komnos and G. Fontaras, *Observations on the Driving of Plug-in Hybrid Cars in Real-world Conditions*, European Commission, Joint Research Centre, 21027 Ispra, Italy.
- [25] M. Ktistakis, A. Tansini, A. Laverde, D. Komnos, J. Suarez and G. Fontaras, “Understanding the Fuel Consumption of Pug-In Hybrid Electric Vehicles: a Real-World Case Study,” 2022.
- [26] J. Carron, “Violin Plots 101: Visualizing Distribution and Probability Density,” [Online]. Available: <https://mode.com/blog/violin-plot-examples/>. [Accessed March 2023].

